FIBRILLAR COLLAGEN MODULATION OF EXTRACELLULAR MATRIX STRUCTURE AND ORGANIZATION FOLLOWING TENDON INJURY

Jaclyn Ashley Carlson

A DISSERTATION

in

Bioengineering

Presented to the Faculties of the University of Pennsylvania

in

Partial Fulfillment of the Requirements for the

Degree of Doctor of Philosophy

2023

Supervisor of Dissertation

Dr. Louis J. Soslowsky
Fairhill Professor, Orthopaedic Surgery, Perelman School of Medicine

Graduate Group Chairperson

Dr. Yale Cohen
Professor, Bioengineering

Dissertation Committee

Dr. Susan W. Volk (Committee Chair)
Professor, Small Animal Surgery, School of Veterinary Medicine

Dr. Kyu Sang Joeng
Assistant Professor, Orthopaedic Surgery, Perelman School of Medicine

Dr. Rebecca G. Wells
Professor, Medicine, Perelman School of Medicine

FIBRILLAR COLLAGEN MODULATION OF EXTRACELLULAR MATRIX STRUCTURE AND ORGANIZATION FOLLOWING TENDON INJURY

COPYRIGHT

2023

Jaclyn Ashley Carlson

ACKNOWLEDGEMENTS

I'd like to start by thanking my advisor, Dr. Lou Soslowsky. Lou supported and encouraged my research from the beginning, allowing me freedom to think independently, grow through challenges and gain leadership experiences, enabling me to develop as a scientist and person. I am grateful that I have been able to learn from Lou and know I will continue to use the skills I acquired throughout my next pursuit.

Dr. Susan Volk served as a second mentor of mine throughout the second half of my PhD. One of the most rewarding pieces of my PhD was developing the new Collagen 3 grant with Susan and Lou and gaining invaluable grant formulation and writing experience. Susan encouraged me throughout the process, having patience and taking time to teach, support and push me to grow scientifically. As a graduate of the VMD/PhD program, she has been an invaluable resource and champion for me, and I know will continue to be a close mentor throughout my career.

I'd also like to thank Dr. Rebecca Wells and Dr. Kyu-Sang Jeong for serving on my thesis committee and providing scientific expertise to help formulate this project and see it through to completion. Without their guidance the project scope would not have been as refined, and the questions they provided helped push my thinking to the next level and expand my knowledge significantly.

Next, I would like to thank the entire Soslowsky Lab, new and old, who helped guide and teach me along the way, enabling me to complete this dissertation. Our lab is filled with incredible colleagues, and I was also lucky to make friends along the way. Dr. Snehal Shetye, Dr. Julianne Heugel, Dr. Brittany Taylor, Stephanie Weiss and Courtney Nuss were crucial educators, mentors and teammates throughout my time in lab. My fellow graduate students, Ashley Fung, Thomas Leahy, Joseph Newton, and Drs. Ryan Leiphart and Zakary Beach, were the group of students I spent the most time with and that bond is special and lifelong. Ashley

and Thomas made going to the lab each day enjoyable, with the scientific discussions, life updates and general comradery I will be forever grateful for. Michael DiStefano and Margaret Tamburro were amazing supporters of my work, with Maggie providing many hours of histology protocol development this past year alongside me and continuing my work on the Collagen 3 grant. Lastly, Dr. Jeremy Eekhoff for this guidance during the final months of my PhD and his AFM protocol.

I am thankful for the support of the VMD/PhD program and the students for the encouragement, especially Ashley Vanderbeck, who has been on this journey alongside me since day 1. The steering committee, especially Drs Michael Atchison, Michael May and Susan Volk, have been supportive and reassuring throughout. Additionally, the Bioengineering Department and McKay community have provided valuable resources, guidance, and help.

My parents, Susan and Kurt Carlson have encouraged me, literally since day one of my life, to pursue my passions, work hard, but stay grounded and enjoy the journey. They have provided me with guidance on balance, family, and commitment. Without their support I would never be where I am today and I cannot fully express how thankful I am to have such wonderful parents. Alongside my parents are my brothers, Jon and Chris Carlson, with whom I have an amazing friendship and lifelong support system, always enjoying the time we spend together. My family now includes my two sisters-in-law, Jamie and Annie Carlson, whom I feel lucky to have in my life and add so much. Friends near and far, from childhood through Cornell, have been an amazing inspiration to be a strong woman, pursue my dreams, and stay upbeat, energetic and kind. Without this group of women, my life would be infinitely harder.

Lastly, my husband Patrick Dooley has been the ultimate rock throughout this program, from encouraging me to apply, to helping me every day to stick with it and push through the challenges. Alongside our pup, Spot, he’s been my true support system the whole time, day in and day out. Our family grew during the last year of my PhD, with the birth of our son Aidan

James, and without Pat's unwavering support I would not have been able to have the time or energy to finish my dissertation in a way that makes me proud. He pushed me daily to stay strong and finish my work, while taking amazing care of our son. Aidan, you inspire me every day to be a mom, scientist, and person that you can be proud of, and I will always be grateful for you and can't wait to see where this life takes our family.

ABSTRACT

FIBRILLAR COLLAGEN MODULATION OF EXTRACELLULAR MATRIX STRUCTURE AND ORGANIZATION FOLLOWING TENDON INJURY

Jaclyn Ashley Carlson

Louis J. Soslowsky

Tendons can withstand large forces due to a highly aligned, dense collagen matrix. However, their low cellularity and relative inability to recruit reparative cells post-injury, as well as susceptibility to excessive scarring, results in loss of tendon structure and mechanical function. Type I collagen (Col1) is the primary collagen of healthy tendon and type III collagen (Col3) is a minor constituent that increases in response to injury. In other Col1-rich tissues such as skin and bone, Col3 directs reparative cell activities by regulating early cellular infiltration to promote healing, as well as collagen deposition, architecture and crosslink formation, supporting an early critical role of Col3 in wound healing, which has not been studied in tendon. While Col3 may orchestrate cellular activities and fate that are critical for an optimal reparative response post-injury at early stages in tendon, its persistent expression in the remodeling phase may compromise the desired healing response. Therefore, the overall objective of this study was to define the critical role of fibrillar collagens, Col3 and Col5, in modulating matrix maturation and healing potential throughout tendon healing.

Overall, it is apparent that both fibrillar collagens studied play a role in tendon healing, through modulation of fibrillogenesis, matrix organization and engagement. While Col5 seems to be necessary for matrix integrity throughout the time course studied, Col3 seems to play a larger role in fibrillogenesis early on, as well as plays a large role in influencing cellular populations during the inflammatory phase.

Further elucidating the mechanistic roles of fibrillar collagens in tendon healing will allow for potential modulation of matrix deposition post-injury to optimize the regenerative environment and result in better functional outcomes.

TABLE OF CONTENTS

ACKNOWLEDGEMENTS ..... **III**

ABSTRACT ..... **VI**

LIST OF TABLES ..... **XII**

LIST OF FIGURES ..... **XIII**

CHAPTER 1: INTRODUCTION **1**

1.1 – Background **1**
1.1.1 Tendon Matrix Structure-Function and Cell-Matrix Organization 1
1.1.2 Tendon Injury Response and Tissue Pathology 4
1.1.3 Collagen III in Tendon Injury Response 5
1.1.4 Collagen V in Tendon Injury Response 6

1.2 – Significance of Studies **7**
1.2.1 Clinical Need for Improving Tendon Repair 7
1.2.2 Ehlers-Danlos Syndrome 7
1.2.3 Translational Implications 8
1.2.4 Overall Significance 9

1.3 – Approach **9**
1.3.1 Overall Strategy and Study Design 9
1.3.2 Specific Aims 10

1.4 - Chapter Overview **12**

1.5 - References **13**

CHAPTER 2: COLLAGEN V HAPLOINSUFFICIENCY RESULTS IN ALTERED MATRIX ARCHITECTURE, REALIGNMENT AND CELLULARITY THROUGHOUT TENDON HEALING, DEMONSTRATING DECREASED HEALING COMPARED TO WILD-TYPE TENDONS **17**

2.1 – Introduction **17**

2.2 – Methods **18**
2.2.1 Animal Model and Study Design 18
2.2.2 Patellar Tendon Defect Surgery 19
2.2.3 Immuno-blot Analysis 19
2.2.4 Real-time PCR of Col5a1 Expression 20
2.2.5 Mechanical Testing 20
2.2.6 Histological Analysis 21
2.2.7 Statistics 22

2.3 – Results **22**

2.3.1 Col5a1 gene expression was not increased post-injury in Col5-deficient mice 22
2.3.2 Type V Collagen Content was decreased in Col5-deficient mice compared to wild-type 22
2.3.3 Col5-deficient tendons had an altered healing response compared to wild-type tendons 23
2.3.4 Tendon cellularity and cell shape differed between genotypes 29

2.4 – Discussion 29

2.5 – References 35

CHAPTER 3: COLLAGEN III DEFICIENCY FOLLOWING INJURY IN FEMALE MURINE TENDONS ALTERS MATRIX COMPOSITION, ALIGNMENT AND MECHANICAL PROPERTIES 38

3.1 – Introduction 38

3.2 – Methods 41
3.2.1 Animal Model and Study Design 41
3.2.2 Surgical Induction of Patellar Tendon Injury 41
3.2.3 Gene Expression 42
3.2.4 Matrix Functional Analyses 43
3.2.5 Collagen Localization, Cell Infiltration and Phenotype 45
3.2.6 Statistics 47

3.3 - Results 47
3.3.1 Gene expression changed from baseline levels differently in Col3a1$^{+/-}$ tendons compared to WT tendons in key categories. 47
3.3.2 Collagen III immunolabelling was decreased in Col3a1$^{+/-}$ tendons post-injury 50
3.3.3 Collagen III deficiency resulted in increased αSMA activity post-injury at 3- and 6-weeks 51
3.3.4 Collagen III deficiency resulted in reduced iNOS positive signal at 1-week post-injury and an increase in CD206 positive signal at 6-weeks post-injury when evaluated qualitatively 51
3.3.5 Collagen fiber alignment was increased in Col3a1$^{+/-}$ tendons compared to WT post-injury 54
3.3.6 Quasistatic mechanical properties were increased in Col3-deficient tendons compared to WT, with no decreases from uninjured levels post-injury 58
3.7 Viscoelastic mechanical properties were unaffected by injury in Col3-deficient tendons 59
3.3.8 Col3-deficient tendons had faster and more drastic collagen fiber realignment in response to load than WT tendons 62

3.4 – Discussion 63

3.5 – References 73

CHAPTER 4: COLLAGEN III DEFICIENCY FOLLOWING INJURY IN FEMALE MURINE TENDONS AFFECTS FIBRIL STRUCTURAL AND MECHANICAL PROPERTIES 77

4.1 – Introduction 77

4.2 – Methods 79
4.2.1 Animal Model and Study Design 79
4.2.2 Surgical Induction of Patellar Tendon Defect 80
4.2.3 Matrix Structural Analyses 80
4.2.4 Matrix Functional Analyses 82

4.2.5 Statistics 82

4.3 – Results 83
4.3.1 Fibril diameter distributions differed between genotypes and across injury time-points 83
4.3.2 Fibril sliding is increased in Col3a1$^{+/-}$ tendons at 1% strain compared to WT tendons, with sliding decreasing with increased strain. 85

4.4 – Discussion 86

4.5 – References 90

CHAPTER 5: COLLAGEN III DEFICIENCY ALTERS MECHANICAL PROPERTIES AND DECREASES REGULATION OF FIBRILLOGENESIS FOLLOWING INJURY IN FEMALE ADOLESCENT MURINE TENDONS 93

5.1 – Introduction 93

5.2 – Methods 95
5.2.1 Animal Model and Study Design 95
5.2.2 Surgical Induction of Patellar Tendon Defect 95
5.2.3 Real-time PCR of Col3a1 Expression 95
5.2.4 Matrix Functional Analyses 96
5.2.5 Matrix Structural Analyses 96
5.2.6 Statistics 97

5.3 – Results 97
5.3.1 Col3a1 expression was increased post-injury in both genotypes, and increased in both uninjured and injured WT compared to Col3-deficient tendons 97
5.3.2 Fibril diameter distributions were altered in uninjured and 1-week injured Col3-deficient tendons 98
5.3.3 Failure load and stiffness were increased in Col3-deficient tendons compared to WT post-injury 99

5.4 – Discussion 100

5.5 – References 104

CHAPTER 6: OVERALL CONCLUSIONS AND FUTURE DIRECTIONS 106

6.1 – Chapter Conclusions 106
6.1.1 Chapter 2 Conclusions 106
6.1.2 Chapter 3 Conclusions 107
6.1.3 Chapter 4 Conclusions 109
6.1.4 Chapter 5 Conclusions 112
6.1.5 Overall Conclusions 113

6.2 – Future Directions 116
6.2.1 Examine matrix cross-linking and additional interfibrillar interactions in the conventional mouse model 116
6.2.2 Evaluate the temporal response of Col3 throughout tendon healing 116
6.2.3 Col3 knockdown impacts on aged tendon 121
6.2.4 Sex differences in Col3 knockdown 121
6.2.5 Developmental effects of Col3 knockdown 122

6.3 – References **123**

APPENDIX A: PROTOCOLS **126**

LIST OF TABLES

Table 2.1 Primer Sequences of RNA…….20
Table 3.1 Gene panel for 96.96 microfluidic qPCR array……..…..……..…..……....43

LIST OF FIGURES

Figure 1.1: Structural Hierarchy of Tendon 1
Figure 1.2: Spatial distribution of cellular and matrix components in tendons 2
Figure 1.3: Cell-matrix dynamic reciprocity in the tumor microenvironment 3
Figure 1.4: Tendon heals in 3 phases 4
Figure 1.5: Aim 1 Study Design 10
Figure 1.6: Aim 2 Study Design 11
Figure 1.7: Aim 3 Study Design 11

Figure 2.1: Collagen V Content and *Col5a1* Gene Expression Following Injury 23
Figure 2.2: Tendon Cross-Sectional Area and Gauge Length Following Injury 24
Figure 2.3: Dynamic Modulus 25
Figure 2.4: Tangent Delta 26
Figure 2.5: Collagen Fiber Realignment During Loading 27
Figure 2.6: Quasistatic Mechanical Properties 28
Figure 2.7: Histological Analysis 29

Figure 3.1: *Col3a1* Gene Expression 47
Figure 3.2: Gene Expression Heatmaps by Category 49
Figure 3.3: Col3 Immunofluorescence 50
Figure 3.4: αSMA Immunofluorescence 52
Figure 3.5: Representative images evaluating macrophage staining 53
Figure 3.6: Uninjured SHG Representative Image 54
Figure 3.7: SHG Representative Images in injured Wild-type and Col3-deficient tendons 55
Figure 3.8: Alignment Measurements 56
Figure 3.9: CT Fire Analysis 57
Figure 3.10: Tendon Cross-Sectional Area and Gauge Length 58
Figure 3.11: Tendon Material and Structural Properties 59
Figure 3.12: Stress Relaxation 60
Figure 3.13: Dynamic Modulus and Tan Delta 61
Figure 3.14: Collagen Fiber Realignment 62

Figure 4.1: Molecular and fibrillar structure of collagen 77
Figure 4.2: TEM Embedding 81
Figure 4.3: Representative Images of Tendon in Cross-section 83
Figure 4.4: Fibril Diameter Distributions 84
Figure 4.5: Sample scan of collagen fibrils using Atomic Force Microscopy 85
Figure 4.6: AFM Imaging Results 85

Figure 5.1: *Col3a1* Gene Expression 97
Figure 5.2: Representative Images of Collagen Fibrils from Tendon in Cross-Section 98
Figure 5.3: Fibril Diameter Distributions 99
Figure 5.4. Tendon gauge length and cross-sectional area 100
Figure 5.5. Quasistatic Mechanical Properties 101

Figure 6.1: Structural and functional changes related to alterations in fibrillar collagen 114
Figure 6.2: Efficient knockout of the floxed Col3 allele in the ERT2 conditional *Col3a1* knockout model 117
Figure 6.3: Aim 1 expected outcomes of Col3 loss at the time of injury 119
Figure 6.4: Aim 2 expected outcomes of Col3 loss at 1w post-injury 120
Figure 6.5: Aim 3 expected healing outcomes after Col3 loss at 3w post-injury 120
Figure 6.6: Col3 levels throughout physiologic tendon healing, the impact of age and proposed strategy to optimize healing through temporal Col3 regulation 121

CHAPTER 1: Introduction

1.1 – Background

1.1.1 Tendon Matrix Structure-Function and Cell-Matrix Organization

Tendons play a critical role attaching muscle to bone and are crucial in mobility and joint stabilization. Tendon is composed of highly aligned and dense extracellular matrix (ECM) composed predominantly of type I collagen (Col1). The unique hierarchical structure (**Fig.1.1**)[1] allows for withstanding of large loads, repetitive use and resisting deformation. Cross-linked matrix architecture contributes to tendon's hierarchical connectivity and resistance to stresses[2], and tendon cells (tenocytes) are organized along collagen fibrils in a relatively low-density manner but contribute to overall functional properties through interactions with ECM. Although Col1 comprises 80-90% of tendon ECM, lower abundance fibrillar collagen molecules, such as type III collagen (Col3) and type V collagen (Col5), modulate tendon healing capacity.

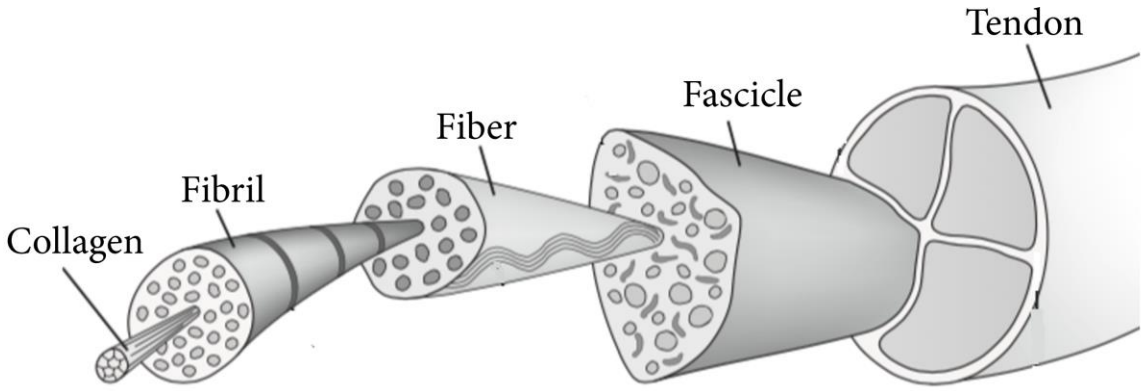

Figure 1.1: Structural Hierarchy of Tendon. Unique hierarchical organization of tendon allows for high tensile properties and characteristic function. Reprinted with permission from Alshomer *et al*. 2018.

Fibrillar collagens constitute a major part of tendon matrix and influence its characteristic structure.[3] Extracellular matrix makes up the load bearing structure of tendon, with its composition dictating tissue integrity and mechanical resilience.[4] Specifically, Col3 is found in the endotenon and epitenon layers surrounding Col1, mediating tendon response to injury, while Col5 is located at the center of the collagen fibrils and modulates fibril development and growth **(Fig.1.2)**.[4]

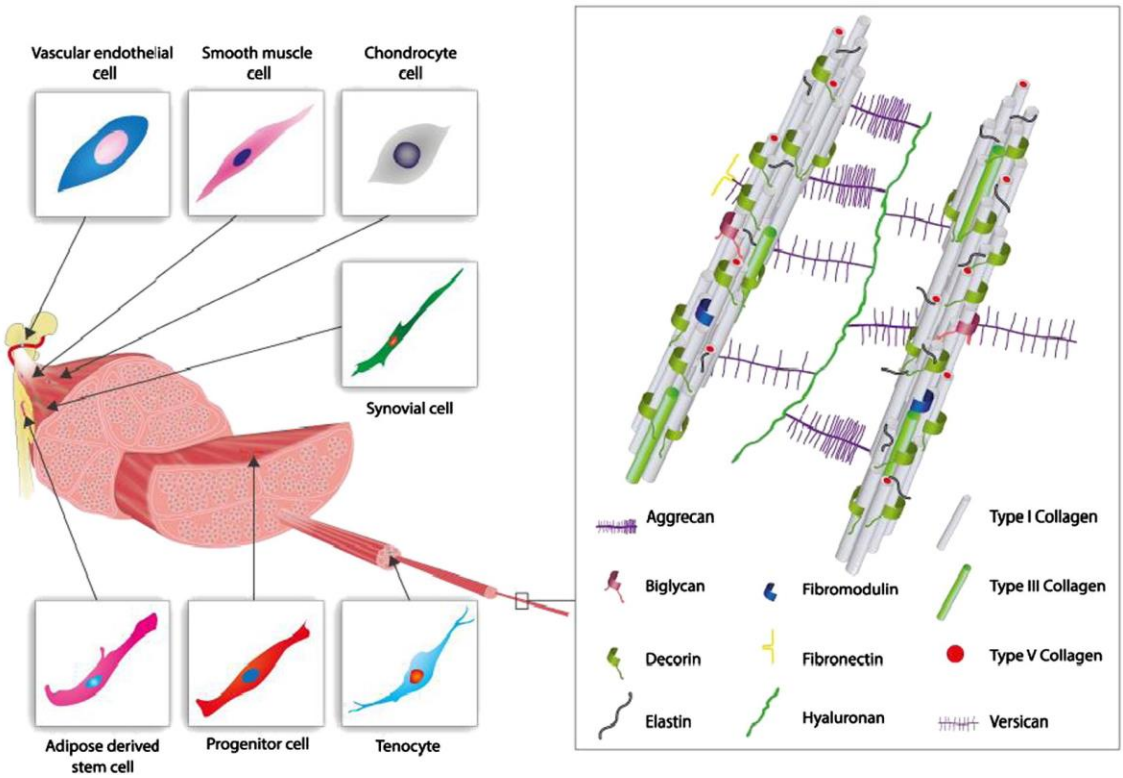

Figure 1.2: Spatial distribution of cellular and matrix components in tendons. Reprinted with permission from Lomas *et al.* 2018.

Although Col3 constitutes a relatively minor component (<10% in healthy, uninjured tendon) of tendon, it plays a regulatory role modulating fibril surface interactions with other matrix components and cells, while also resisting multiaxial stress and forming crucial cross-links.[2] Deficiency of Col3 results in extreme phenotypes in other soft tissues of the body, indicating a role in proper development of tissue. Its role in matrix microarchitecture in other

tissues (e.g., skin[5], meniscus[6], articular cartilage[6], and bone[7–9]) suggest that Col3 plays an important, yet ill-defined role in tendon structural integrity, potentially due to formation of triple-helices with Col1[10]. ECM architecture, organization, and stiffness regulate cell differentiation, proliferation, and migration, indicating that a Col3-rich matrix may influence tendon development and its healing environment.[11,12] A fibrillar collagen study showed that an aligned Col1 matrix has crosslinks important for hierarchical connectivity and resisting axial stress, while Col3-rich matrix is directionally disorganized, leading to resistance of multiaxial stress.[2] Cell-matrix dynamic reciprocity between fibroblasts and collagen fibrils in the tumor microenvironment further highlight the importance of cell-ECM cross-talk in matrix deposition, reorganization and remodeling (**Fig. 1.3**).[13] Therefore, the abundance of Col3 in matrix will ultimately affect the structural and functional properties, due to the physical differences in cross-linking, stiffness, and density of the matrix, as well as the influence on the cellular environment, activity, and progenitor migration. Further understanding these interactions will allow us to modulate the effects of Col3 on the matrix and cellular environment to optimize tendon healing and recovery post-injury.

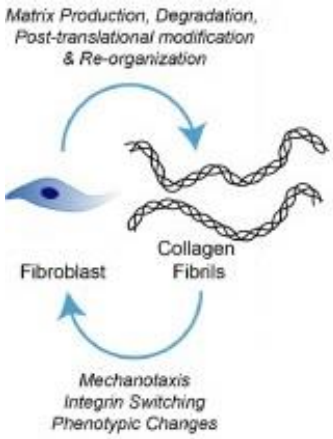

Figure 1.3: Cell-matrix dynamic reciprocity in the tumor microenvironment. Reprinted with permission from Brisson *et al.* 2022.

Additionally, while Col5 comprises only ~2% of the total collagen, important regulatory roles during fibrillogenesis have been firmly established.[14] *Col5a1* haploinsufficiency leads to abnormal tissue development caused by altered collagen assembly and has been linked to altered matrix architecture and mechanical properties.[15] Via heterotypic interactions with Col1, Col5 regulates fibril nucleation.[16,17] This regulatory interaction determines the number of fibrils assembled, the location of deposition in the developing matrix, as well as the initial diameter.[18]

Due to this crucial role in fibrillogenesis, it is expected that Col5 plays a crucial role in tendon healing and influencing matrix deposition and the resultant healing environment.

1.1.2 Tendon Injury Response and Tissue Pathology

Tissue response to injury is a complex, series of orchestrated events that results in the removal of damaged tissue and its replacement through the dynamic and reciprocal interactions of reparative and progenitor cells, soluble factors and ECM proteins. Healing typically occurs in three stages (**Fig. 1.4**), beginning with the inflammatory phase during week one post-injury, the proliferative phase through day 21, and ending with the remodeling phase. Poor healing following tendon injury is attributed to innate low vascularity and cellularity compared to other tissues and the prolonged presence of fibrotic scarring.[19,20] While the mechanism behind persistent scar tissue formation in tendon healing is unknown, it is believed to be due to ineffective remodeling of the provisional Col3-rich matrix into an aligned Col1-rich matrix seen in uninjured tendons, and results in an abundance of disorganized Col3 in the fibrotic scar.

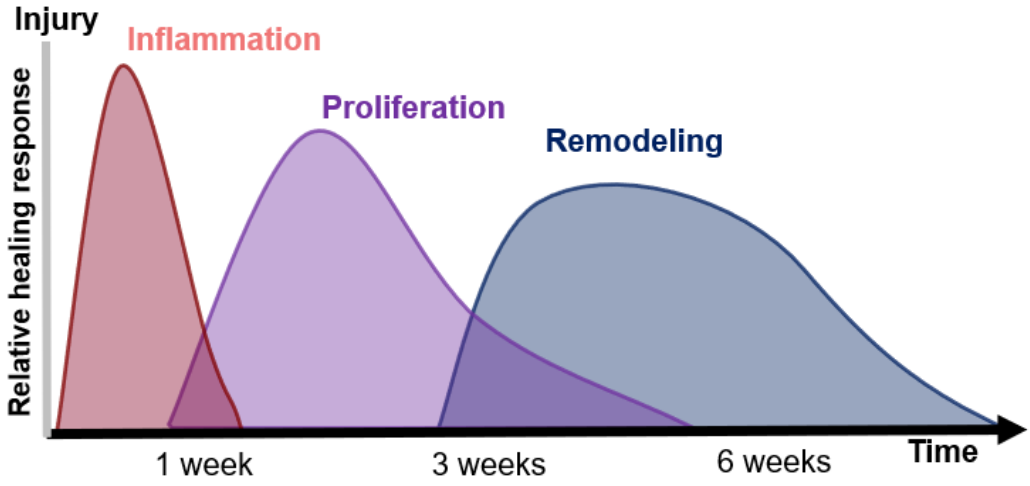

Figure 1.4: Tendon heals in 3 phases. The inflammatory phase, is followed by the proliferative phase, ending with the remodeling phase.

An initial inflammatory phase results in microdebridement of damaged tissue and importantly, influences the next phase of repair through recruitment of additional reparative cells and subsequent modulation of their activities and fate. The skin's dermal layer and tendon, in their unwounded state, are both comprised primarily of Col1, however, Col1 organization is basket-weave in skin and uniaxially aligned in tendon, due to key functional differences.

1.1.3 Collagen III in Tendon Injury Response

Following injury of young, healthy tendons, Col1:Col3 content rises from an initial ~ 9:1 to 1:1.[21,22] In skin, data has shown that a Col3-deficient early healing niche fails to support formation of healthy cellular infiltration, initial collagen deposition in granulation tissue and repair of the overlying epidermis.[5] Given the role of Col3 in regulating cell differentiation, proliferation, and migration in early tissue repair,[5,7] it is likely that Col3 is required in early tendon healing to recruit and direct reparative cells, which are necessary to produce sufficient fibrillar collagen for future remodeling and return to function. Additionally, data suggests that Col3 directs cellular responses by attenuating matrix alignment, collagen cross-linking and stiffness.[21] In later stages of healing, a reparative response in tendon likely requires downregulation of Col3 to achieve a highly aligned matrix, as Col3 levels impact collagen fiber microarchitecture[23] and cross-linking[6], introducing an interesting temporal role in tendon healing. We hypothesize that continued expression of Col3 during tendon remodeling prevents optimal deposition of Col1 and matrix remodeling, leading to disorganized scar tissue and inferior functional properties. In skin wounds[5], Col3 directs reparative cell activities by regulating early cellular infiltration and proliferation to promote healing, and in later healing Col3 protects against scar formation[5] by directing an open weave matrix microarchitecture. However, and importantly, preferred collagen remodeling in tendon repair diverges from skin wounds, relying on formation of a highly aligned matrix at later stages, supporting the innovative concept that Col3 plays unique, temporal roles

throughout tendon healing. Further, while ECM organization and stiffness affected by Col3 content likely influence cell behavior,[11–13] the impact of Col3 expression on fibroblast matrix production and immune cell activity has not been studied in tendon.

Lastly, healing wounds that are comparatively enriched in Col3, such as those of the African spiny mouse and midgestational fetus, are distinct in their ability to heal in a scarless manner.[24] These, and additional studies in other tissues[5,25,26] elucidate how changes in Col3 impact both cells and their surrounding ECM in the healing niche and importantly, suggest a premise for Col3 to play an essential role in tendon repair. Understanding the mechanistic roles of Col3 in each phase of tendon healing is critical to develop therapeutic strategies that optimize tendon repair (by decreased scar formation) and improve long-term structure-function.

1.1.4 Collagen V in Tendon Injury Response

Col5 is known to play a critical role in wound healing and scarring in tendons and other connective tissues. Following injury in wild-type (WT) tendons, Col5 is significantly upregulated,[14,27] while diminished expression of Col5 is associated with abnormal wound healing.[14,28] During development, Col5 plays an important regulatory role in fibrillogenesis, modulating the deposition of Col1 fibrils into the developing matrix,[14] indicating that following injury, Col5 is critical to proper provisional matrix deposition and long-term fibril growth and remodeling. *Col5a1* haploinsufficiency leads to abnormal tissue development caused by altered collagen assembly and has been linked to altered matrix architecture and mechanical properties.[15] Additionally, studies suggest that differences in hormone physiology between sexes may influence tendon health and result in differing healing paradigms.[29–31] Female estrogen expression may be associated with decreased collagen synthesis[32,33] and altered gene expression during repair.[34].The physiologic environment may exacerbate changes present in pathological tendons. Previous work in a male model of Col5-deficiency has shown that

decreased *Col5a1* expression results in fibril morphology, fibril diameter distributions and decreased mechanical integrity of healing matrix,[35] however, the role of Col5-deficiency in female murine uninjured and healing tendons has not yet been investigated.

1.2 – Significance of Studies

1.2.1 Clinical Need for Improving Tendon Repair

Tendinopathies, including tendon rupture and chronic degeneration, account for >30% of musculoskeletal consultations.[36,37] Unsatisfactory tendon healing has an enormous impact on patient quality of life due to pain and disability and significant socioeconomic burden. Insufficient healing is attributed to tendon's innate low vascularity and cellularity compared to many other tissues, concomitant with increased decreased function and high risk of recurrent re-injury.[19,20] Elucidation of the pathophysiology and healing response in these injuries will improve treatment of those affected and improve long-term functional outcomes.

1.2.2 Ehlers-Danlos Syndrome

1.2.2a Vascular Ehlers-Danlos Syndrome

Insight into the critical impact of Col3 on tissue homeostasis and repair is evidenced by the severe clinical complications and early death of patients with vascular Ehlers-Danlos syndrome (vEDS), a rare genetic disease caused by reduction in *Col3a1*, due to catastrophic tissue failure of the vasculature, bowel and uterus.[38].Tendon rupture and dysfunction exist in up to 20% of patients,[38–40] supporting a critical role of Col3 in tendon homeostasis and maintenance. Despite the rarity of vEDS, Col3 expression may be negatively impacted by aging, menopause, smoking and other factors,[41–44] and therefore, relative Col3 deficiency in subpopulations of the general population is not to be underestimated. Understanding the critical

role of Col3 in ECM deposition and fibrosis will provide further insight into management of patient groups.

1.2.2b Classic Ehlers-Danlos Syndrome

Classic EDS (*c*EDS*)* is defined by haploinsufficiency for COL5A1 present in ~67% of affected individuals.[45,46] Patients with *c*EDS present with hyperextensible skin, joint hypermobility and instability, connective tissue fragility, as well as abnormal wound healing and scarring.[28,47] Therefore, understanding critical role of collagen V during the tendon response to injury will improve treatment of this subset of the population.

Additionally, clinical studies have shown that the incidence of *c*EDS is higher in female populations.[27,48] Given the joint laxity and connective tissue hyperelasticity in *c*EDS patients, sex-specific changes in hormone levels could further exacerbate the detrimental changes present in pathological tendons. This may significantly alter the healing response and warrants further examination.

1.2.3 Translational Implications

Extracellular matrix is a critical component of tendon, and clinically is implicated in increased scar formation and re-tear rates. Through understanding the critical role of Col3 and Col5 in tendon healing, we can provide insight into a possible therapeutic, to modulate the amount of collagen expression and activity throughout healing. This could improve the infiltration of healing cells, better regulate fibrillogenesis, increase vascularization early and promote scarless healing.

Additionally, Col3 is known to be expressed at different levels throughout development and aging. Adolescent and adult tendons exhibit key differences in their local environment and the differential effects of Col3 on cell behavior during healing in each population is unknown.

Understanding the role of Col3 is necessary for future clinical application where both patient age populations are affected by tendon injury and understanding its temporal role throughout healing will elucidate specific mechanisms that can be targeted to improve healing outcomes.

1.2.4 Overall Significance

ECM organization, architecture and composition are known to influence tendon mechanics, function and cellular activity following injury. Healing potential of the tissue directly relies on the deposited matrix, with both Col3 and Col5 playing important roles post-injury in fibrillogenesis, matrix deposition and organization. The specific roles of fibrillar collagens remain unelucidated and this is critical for defining the coordinated cell-cell and cell-matrix interactions required for establishing tendon structure-function during healing. Evaluating these findings in a tendon model is crucial for advancement of the tendon field.

Previous work in skin, as well as other soft tissues, supports the role of Col3 in both matrix formation and remodeling, as well as reducing pathologic scar formation. However, persistent increases in Col3 expression in long-term remodeling leads to increased fibrosis, indicating a temporal role of Col3 throughout healing. Additionally, Col5 deficiency has been shown to negatively impact healing in a male murine model, making female mice very important to study due to the potential impacts of hormones on Col5 expression.

1.3 – Approach

1.3.1 Overall Strategy and Study Design

The overall objective of this study is to define the critical role of fibrillar collagens, Col3 and Col5, in modulating matrix maturation and healing potential throughout tendon healing. Due to the critical regulatory roles of fibrillar collagens in matrix development, maturation and remodeling, the goal of this study was to utilize conventional knockdown models

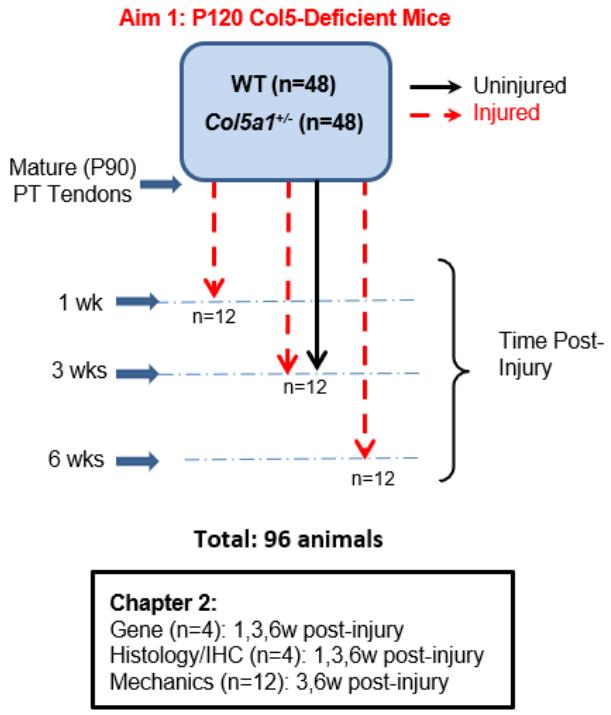

Figure 1.5: Aim 1 Study Design.

to evaluate the role of Col3 and Col5 in tendon healing. Aim 1 utilized a Haploinsufficient model of *Col5a1* knockdown[49] in order to evaluate Col5 importance in tendon healing in female mice and expand upon previous work in male mice (**Fig. 1.5**). Aims 2 (**Fig. 1.6**) and 3 (**Fig. 1.7**) utilized a Haploinsufficient model of *Col3a1* knockdown[38] to elucidate the role of Col3 in regulating cell behavior during tendon healing and differences between adolescent and adult tendons.

1.3.2 Specific Aims

This study was composed of 3 specific aims and is a comprehensive approach to evaluating the role of fibrillar collagens in tendon healing. Innovation approaches were used, including collagen fiber realignment analysis, matrix response to strain at the fiber level, and evaluating, for the first time, a knockdown model of *Col3a1* in tendon.

Aim 1: Evaluate the effect of Col5 on the cellular and structural composition, as well as functional properties in tendon healing. *We hypothesized that the reduction in Col5a1 expression would result in an abnormal wound matrix during the injury response, resulting in reduced mechanical properties of healing tendons compared to normal tendons. Due to the regulatory role of Col5 during the remodeling phase during healing[50], we anticipate a decreased healing response in the Col5a1$^{+/-}$ mice when compared to WT controls.*

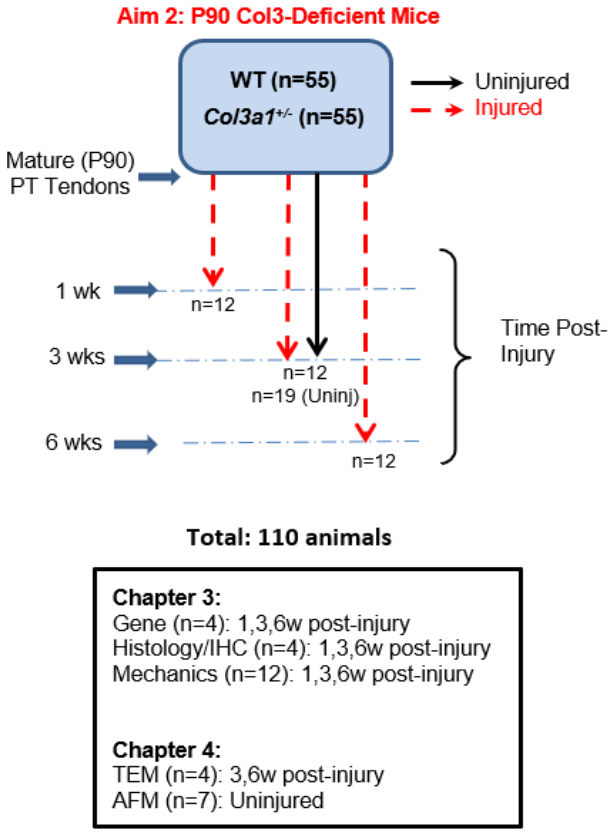

Figure 1.6: Aim 2 Study Design.

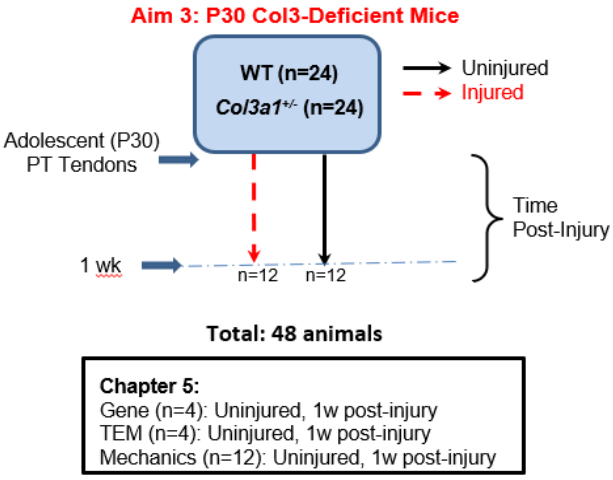

Figure 1.7: Aim 3 Study Design.

Aim 2: Elucidate the mechanistic roles of Col3 in tendon healing and resultant alterations to matrix structure, organization and function. Col3-rich matrix is critical for efficient recruitment, proliferation, migration, and vulnerary activity of reparative cells during early healing, however, also has been shown to contribute to long-term scar tissue in tendon healing. *We hypothesized that reduced Col3 expression will impair the early, provisional Col3-rich matrix necessary for cellular activity, due to increased stiffness and alignment in the early matrix. Col3-deficiency will increase cell-matrix engagement and fibril-fibril interactions due to the unique structure and organization of the deposited matrix.*

Aim 3: Assess differences in adolescent animals compared to adult mice in tendon healing in a Col3-deficient tendon. *We hypothesized that adolescent mice would have less of an effect during early healing, due to their ability to compensate for a reduction in Col3.*

1.4 - Chapter Overview

Chapter II will describe how Col5 affects cellular and structural composition, as well as mechanical properties throughout tendon healing. Chapter III will describe the role of Col3 in influencing cellular populations and activity, matrix organization and response to load. Chapter IV will describe the role of Col3 in influencing matrix structure and response to load at the fibril level. Chapter V will describe the role of Col3 in fibrillogenesis and alterations in mechanical properties during tendon healing in an adolescent model. Chapter VI will summarize the conclusions of these chapters and present future directions.

1.5 - References

1 Alshomer F, Chaves C, Kalaskar DM. Advances in Tendon and Ligament Tissue Engineering: Materials Perspective. *J Mater* 2018;**2018**:1–17. https://doi.org/10.1155/2018/9868151.

2 Wess TJ. Collagen fibril form and function. *Adv Protein Chem* 2005;**70**:341–74. https://doi.org/10.1016/S0065-3233(05)70010-3.

3 Yang G, Rothrauff BB, Tuan RS. Tendon and ligament regeneration and repair: Clinical relevance and developmental paradigm. *Birth Defects Res Part C - Embryo Today Rev* 2013:203–22. https://doi.org/10.1002/bdrc.21041.

4 Lomas AJ, Ryan CNM, Sorushanova A, Shologu N, Sideri AI, Tsioli V, *et al.* The past, present and future in scaffold-based tendon treatments. *Adv Drug Deliv Rev* 2015:257–77. https://doi.org/10.1016/j.addr.2014.11.022.

5 Volk SW, Wang Y, Mauldin EA, Liechty KW, Adams SL. Diminished type III collagen promotes myofibroblast differentiation and increases scar deposition in cutaneous wound healing. *Cells Tissues Organs* 2011;**194**:25–37. https://doi.org/10.1159/000322399.

6 Wang C, Brisson BK, Terajima M, Li Q, Hoxha K, Han B, *et al.* Type III collagen is a key regulator of the collagen fibrillar structure and biomechanics of articular cartilage and meniscus. *Matrix Biol* 2020;**85**–**86**:47–67. https://doi.org/10.1016/j.matbio.2019.10.001.

7 Miedel EL, Brisson BK, Hamilton T, Gleason H, Swain GP, Lopas L, *et al.* Type III collagen modulates fracture callus bone formation and early remodeling. *J Orthop Res* 2015;**33**:675–84. https://doi.org/10.1002/jor.22838.

8 Liu SH, Yang R-S A-SR. Collagen in tendon, ligament, and bone healing. A current review 1995:265–278.

9 Volk SW, Shah SR, Cohen AJ, Wang Y, Brisson BK, Vogel LK, *et al.* Type III collagen regulates osteoblastogenesis and the quantity of trabecular bone. *Calcif Tissue Int* 2014;**94**:621–31. https://doi.org/10.1007/s00223-014-9843-x.

10 Xue M, Jackson CJ. Extracellular Matrix Reorganization During Wound Healing and Its Impact on Abnormal Scarring. *Adv Wound Care* 2015;**4**:119–36. https://doi.org/10.1089/wound.2013.0485.

11 Kanta J. Collagen matrix as a tool in studying fibroblastic cell behavior. *Cell Adhes Migr* 2015;**9**:308–16. https://doi.org/10.1080/19336918.2015.1005469.

12 Juneja SC, Schwarz EM, O'Keefe RJ, Awad HA. Cellular and molecular factors in flexor tendon repair and adhesions: A histological and gene expression analysis. *Connect Tissue Res* 2013;**54**:218–26. https://doi.org/10.3109/03008207.2013.787418.

13 Brisson BK, Stewart DC, Burgwin C, Chenoweth D, Wells RG, Adams SL, *et al.* Cysteine-rich domain of type III collagen N-propeptide inhibits fibroblast activation by attenuating TGFβ signaling. *Matrix Biol* 2022;**109**:19–33. https://doi.org/10.1016/j.matbio.2022.03.004.

14 Wenstrup RJ, Florer JB, Brunskill EW, Bell SM, Chervoneva I, Birk DE. Type V collagen controls the initiation of collagen fibril assembly. *J Biol Chem* 2004;**279**:53331–7. https://doi.org/10.1074/jbc.M409622200.

15 Collins M, Posthumus M. Type V collagen genotype and exercise-related phenotype relationships: A novel hypothesis. *Exerc Sport Sci Rev* 2011;**39**:191–8. https://doi.org/10.1097/JES.0b013e318224e853.

16 Wenstrup RJ, Smith SM, Florer JB, Zhang G, Beason DP, Seegmiller RE, *et al.* Regulation of collagen fibril nucleation and initial fibril assembly involves coordinate interactions with collagens V and XI in developing tendon. *J Biol Chem* 2011;**286**:20455–65. https://doi.org/10.1074/jbc.M111.223693.

17 Birk DE. Type V collagen: Heterotypic type I/V collagen interactions in the regulation of fibril assembly. *Micron* 2001:223–37. https://doi.org/10.1016/S0968-4328(00)00043-3.

18 Wenstrup RJ, Smith SM, Florer JB, Zhang G, Beason DP, Seegmiller RE, *et al.* Regulation of collagen fibril nucleation and initial fibril assembly involves coordinate interactions with collagens V and XI in developing tendon. *J Biol Chem* 2011;**286**:20455–65. https://doi.org/10.1074/jbc.M111.223693.

19 Shimokobe H, Gotoh M, Honda H, Nakamura H, Mitsui Y, Kakuma T, *et al.* Risk factors for retear of large/massive rotator cuff tears after arthroscopic surgery: An analysis of tearing patterns. *J Orthop Surg Res* 2017;**12**:140. https://doi.org/10.1186/s13018-017-0643-7.

20 Galatz LM, Ball CM, Teefey SA, Middleton WD, Yamaguchi K. The outcome and repair integrity of completely arthroscopically repaired large and massive rotator cuff tears. *J Bone Joint Surg Am* 2004;**86**:219–24. https://doi.org/10.2106/00004623-200402000-00002.

21 Dyment NA, Liu CF, Kazemi N, Aschbacher-Smith LE, Kenter K, Breidenbach AP, *et al.* The Paratenon Contributes to Scleraxis-Expressing Cells during Patellar Tendon Healing. *PLoS One* 2013;**8**:. https://doi.org/10.1371/journal.pone.0059944.

22 Freedman BR, Gordon JA, Bhatt PR, Pardes AM, Thomas SJ, Sarver JJ, *et al.* Nonsurgical treatment and early return to activity leads to improved Achilles tendon fatigue mechanics and functional outcomes during early healing in an animal model. *J Orthop Res* 2016;**34**:2172–80. https://doi.org/10.1002/jor.23253.

23 Brisson BK, Mauldin EA, Lei W, Vogel LK, Power AM, Lo A, *et al.* Type III collagen directs stromal organization and limits metastasis in a murine model of breast cancer. *Am J Pathol* 2015;**185**:1471–86. https://doi.org/10.1016/j.ajpath.2015.01.029.

24 Seifert AW, Kiama SG, Seifert MG, Goheen JR, Palmer TM, Maden M. Skin shedding and tissue regeneration in African spiny mice (Acomys). *Nature* 2012;**489**:561–5. https://doi.org/10.1038/nature11499.

25 D'hondt S, Guillemyn B, Syx D, Symoens S, De Rycke R, Vanhoutte L, *et al.* Type III collagen affects dermal and vascular collagen fibrillogenesis and tissue integrity in a mutant Col3a1 transgenic mouse model. *Matrix Biol* 2018;**70**:72–83. https://doi.org/10.1016/j.matbio.2018.03.008.

26 Liu X, Wu H, Byrne M, Krane S, Jaenisch R. Type III collagen is crucial for collagen I fibrillogenesis and for normal cardiovascular development. *Proc Natl Acad Sci U S A* 1997;**94**:1852–6. https://doi.org/10.1073/pnas.94.5.1852.

27 Ainsworth, SR, Aulicino P. A survey of patients with Ehlers-Danlos syndrome - PubMed. *Clin Orthop Relat Res* 1993:286:250-256.

28 Steinmann B, Royce PM, Superti-Furga A. The Ehlers-Danlos Syndrome. *Connect. Tissue Its Heritable Disord.* Hoboken, NJ, USA: John Wiley & Sons, Inc.; n.d. p. 431–523.

29 Bridgeman JT, Zhang Y, Donahue H, Wade AM, Juliano PJ. Estrogen receptor expression in posterior tibial tendon dysfunction: A pilot study. *Foot Ankle Int* 2010;**31**:1081–4. https://doi.org/10.3113/FAI.2010.1081.

30 Liu SH, Al-Shaikh R, Panossian V, Yang RS, Nelson SD, Soleiman N, *et al.* Primary immunolocalization of estrogen and progesterone target cells in the human anterior cruciate ligament. *J Orthop Res* 1996;**14**:526–33. https://doi.org/10.1002/jor.1100140405.

31 Romani WA, Russ DW. Acute effects of sex-specific sex hormones on heat shock proteins in fast muscle of male and female rats. *Eur J Appl Physiol* 2013;**113**:2503–10. https://doi.org/10.1007/s00421-013-2686-8.

32 Yu WD, Panossian V, Hatch JD, Liu SH, Finerman GAM. Combined effects of estrogen and progesterone on the anterior cruciate ligament. *Clin Orthop Relat Res* 2001:268–81. https://doi.org/10.1097/00003086-200102000-00031.

33 Kjaer M, Magnusson P, Krogsgaard M, Moller JB, Olesen J, Heinemeier K, *et al.* Extracellular matrix adaptation of tendon and skeletal muscle to exercise. *J Anat* 2006;**208**:445–50. https://doi.org/10.1111/j.1469-7580.2006.00549.x.

34 Hart DA , Archambault JM, Kydd A, Reno C, Frank CB HW. Gender and neurogenic variables in tendon biology and repetitive motion disorders. *Clin Orthop Relat Res* 1998;**351**:44–56.

35 Johnston JM, Connizzo BK, Shetye SS, Robinson KA, Huegel J, Rodriguez AB, *et al.* Collagen V haploinsufficiency in a murine model of classic Ehlers–Danlos syndrome is associated with deficient structural and mechanical healing in tendons. *J Orthop Res* 2017;**35**:2707–15. https://doi.org/10.1002/jor.23571.

36 Thampatty BP, Wang JH-C. Mechanobiology of young and aging tendons: In vivo studies with treadmill running. *J Orthop Res* 2017;**36**:557–65. https://doi.org/10.1002/jor.23761.

37 McCormick A, Charlton J, Fleming D. Assessing health needs in primary care. *BMJ* 1995;**310**:1534–1534. https://doi.org/10.1136/bmj.310.6993.1534d.

38 Cooper TK, Zhong Q, Krawczyk M, Tae HJ, Müller GA, Schubert R, *et al.* The Haploinsufficient Col3a1 Mouse as a Model for Vascular Ehlers-Danlos Syndrome. *Vet Pathol* 2010;**47**:1028–39. https://doi.org/10.1177/0300985810374842.

39 Maffulli N, Moller HD, Evans CH. Tendon healing: Can it be optimised? *Br J Sports Med* 2002:315–6. https://doi.org/10.1136/bjsm.36.5.315.

40 Ong KT, Perdu J, De Backer J, Bozec E, Collignon P, Emmerich J, *et al.* Effect of

celiprolol on prevention of cardiovascular events in vascular Ehlers-Danlos syndrome: A prospective randomised, open, blinded-endpoints trial. *Lancet* 2010;**376**:1476–84. https://doi.org/10.1016/S0140-6736(10)60960-9.

41 Knuutinen A, Kokkonen N, Risteli J, Vähäkangas K, Kallioinen M, Salo T, *et al.* Smoking affects collagen synthesis and extracellular matrix turnover in human skin. *Br J Dermatol* 2002;**146**:588–94. https://doi.org/10.1046/j.1365-2133.2002.04694.x.

42 Varani J, Dame MK, Rittie L, Fligiel SEG, Kang S, Fisher GJ, *et al.* Decreased collagen production in chronologically aged skin: Roles of age-dependent alteration in fibroblast function and defective mechanical stimulation. *Am J Pathol* 2006;**168**:1861–8. https://doi.org/10.2353/ajpath.2006.051302.

43 Oishi Y, Fu ZW, Ohnuki Y, Kato H, Noguchi T. Molecular basis of the alteration in skin collagen metabolism in response to in vivo dexamethasone treatment: Effects on the synthesis of collagen type I and III, collagenase, and tissue inhibitors of metalloproteinases. *Br J Dermatol* 2002;**147**:859–68. https://doi.org/10.1046/j.1365-2133.2002.04949.x.

44 Stevenson S, Thornton J. Effect of estrogens on skin aging and the potential role of SERMs. *Clin Interv Aging* 2007:283–97. https://doi.org/10.2147/cia.s798.

45 Symoens S, Syx D, Malfait F, Callewaert B, De Backer J, Vanakker O, *et al.* Comprehensive molecular analysis demonstrates type V collagen mutations in over 90% of patients with classic EDS and allows to refine diagnostic criteria. *Hum Mutat* 2012;**33**:1485–93. https://doi.org/10.1002/humu.22137.

46 Malfait F, Coucke P, Symoens S, Loeys B, Nuytinck L, De Paepe A. The molecular basis of classic Ehlers-Danlos syndrome: A comprehensive study of biochemical and molecular findings in 48 unrelated patients. *Hum Mutat* 2005;**25**:28–37. https://doi.org/10.1002/humu.20107.

47 Malfait F, Wenstrup RJ, De Paepe A. Clinical and genetic aspects of Ehlers-Danlos syndrome, classic type. *Genet Med* 2010:597–605. https://doi.org/10.1097/GIM.0b013e3181eed412.

48 Stanitski DF, Nadjarian R, Stanitski CL, Bawle E, Tsipouras P. Orthopaedic manifestations of Ehlers-Danlos syndrome. *Clin Orthop Relat Res* 2000:213–21. https://doi.org/10.1097/00003086-200007000-00029.

49 Wenstrup RJ, Florer JB, Davidson JM, Phillips CL, Pfeiffer BJ, Menezes DW, *et al.* Murine model of the Ehlers-Danlos syndrome: col5a1 haploinsufficiency disrupts collagen fibril assembly at multiple stages. *J Biol Chem* 2006;**281**:12888–95. https://doi.org/10.1074/jbc.M511528200.

50 Sun M, Chen S, Adams SM, Florer JB, Liu H, Kao WWY, *et al.* Collagen V is a dominant regulator of collagen fibrillogenesis: Dysfunctional regulation of structure and function in a corneal-stroma-specific Col5a1-null mouse model. *J Cell Sci* 2011;**124**:4096–105. https://doi.org/10.1242/jcs.091363.

CHAPTER 2: Collagen V haploinsufficiency results in altered matrix architecture, realignment and cellularity throughout tendon healing, demonstrating decreased healing compared to wild-type tendons

2.1 – Introduction

Classic Ehlers-Danlos syndrome (*c*EDS) is most commonly characterized by haploinsufficiency in COL5a1 with patients suffering from hyperextensible skin, joint instability, and connective tissue hyperelasticity.[1] It is estimated that 1:20,000 people are afflicted with *c*EDS,[2] with patients suffering multiple orthopedic complications throughout life including joint disease, tendon and ligament injury and abnormal wound healing.[3]

While collagen V (Col5) comprises only ~2% of the total collagen in tendon, important regulatory roles of Col5 during fibrillogenesis have been firmly established.[4] Col5 haploinsufficiency leads to abnormal tissue development caused by altered collagen assembly and has been linked to altered matrix architecture and mechanical properties.[2,4] In addition, Col5 is also known to play a critical role in wound healing and scarring in tendons and other connective tissues. Following injury in wild-type tendons, Col5 is significantly upregulated,[4,6] while diminished expression of Col5 is associated with abnormal wound healing.[3,4]

Clinical studies have shown that *c*EDS is heavily skewed to the female population[6,8] and recent basic science studies suggest that differences in hormone physiology between sexes may be a factor influencing tendon health.[9–11] Estrogen in females is suggested to be associated with decreased collagen synthesis[12,13] and altered gene expression during repair,[14] potentially exacerbating the detrimental changes present in pathological tendons. Given the joint laxity and connective tissue hyperelasticity in classic EDS patients, sex-specific changes in hormone levels could further exacerbate the detrimental changes present in pathological

tendons, and significantly alter the injury response. A previous murine study[7] utilizing male mice indicated that Col5-deficient tendons demonstrated a diminished healing response when compared to WT tendons; however, the role of Col5 in female murine uninjured and healing tendons has not yet been investigated. Our approach coupled mechanical and organizational properties, together with compositional profiles, to derive a mechanistic understanding of how sex influences Col5 mediated establishment and repair of functional tendons.

Given the sex differences observed in clinical populations it is important to include studies of female mice in addition to the previously described male mice. Therefore, utilizing wild-type and a *Col5a1*$^{+/-}$ classic EDS mouse model (*c*EDS),[4,15] the objective of this study is to determine the effect of Col5 on tendon cell morphology, cell density, tissue composition, and mechanical properties throughout healing. We hypothesized that the reduction in Col5 expression would result in an abnormal wound matrix during the injury response, resulting in reduced mechanical properties of healing tendons compared to normal tendons. Due to the regulatory role of Col5 during the remodeling phase during healing,[16] we anticipate a decreased healing response in the *Col5a1*$^{+/-}$ mice when compared to WT controls.

2.2 – Methods

2.2.1 Animal Model and Study Design

This study was approved by the University of Pennsylvania and the University of South Florida Institutional Animal Care and Use Committees. Adult (120 days) female wild-type (WT) C57BL/6 (Source, Charles River) littermates and heterozygous *Col5a1*$^{+/-}$ mice in the same background, an established model for *c*EDS[4,15] (n=96) were used. Mice were randomly divided into uninjured (n=24) and injured (n=72) groups, with injured mice undergoing bilateral patellar tendon defect injury surgery, as described below. Injured mice were euthanized at 1-, 3-, or 6-weeks post-injury using carbon dioxide inhalation. Right limbs were utilized for histology

(n=4/group/timepoint) and *Col5a1* expression (n=10/group/timepoint) at all post-injury time points. Left limbs were utilized for mechanical testing (n=15/group/timepoint) at 3- and 6-weeks post-injury. Uninjured age-matched (150 days of age) mice were sacrificed using the same method and underwent the same assays.

2.2.2 Patellar Tendon Defect Surgery

All mice in the injured group underwent bilateral patellar tendon injury as previously described.[17] Using aseptic technique, the patellar tendon was initially exposed through a medial incision on the flexed knee, and then isolated with longitudinal incisions following the medial and lateral edge of the tendon. A 0.75 mm biopsy punch was used to create a full-thickness, partial width defect (~60%) in the midsubstance of the patellar tendon. A rubber-coated backing was used during this procedure to protect the joint under the tendon. Mice were returned to cage activity following skin closure with sutures and were administered Buprenorphine (0.1mg/kg) prior to surgery and then 2x daily for 3 days following surgery.

2.2.3 Immuno-blot Analysis

Immuno-blots were performed as previously described.[18,19] Col5 content was analyzed immuno-chemically using a Wes™ automated western blotting system (ProteinSimple, San Jose, CA). Patellar tendon samples were dissected from female WT and *Col5a1*$^{+/-}$ mice at post-natal day 120. Individual mice (n=3–8) were used for each genotype. Two patellar tendons from each mouse were cut into small pieces and protein was extracted using an extraction buffer composed of 50 mM Tris-HCl, pH 6.8, 1% SDS with proteinase inhibitor cocktail (ThermoFisher Scientific). Equal amounts (1.5 mg) of denatured protein samples were loaded into single designated wells of Wes Separation 12–230 kDa 25 Capillary Cartridges, 1:100 diluted rabbit anti-mouse Col V antibody and the Wes anti-rabbit detection module was used for Col5 detection. Quantification by densitometry was performed using the area of the targeted protein

(α1(V)) and normalized to total protein (β-actin, 1:200 dilution of anti-β-actin antibodies (Millipore, Billerica, MA)). All Wes reagents (separation module and detection modules) were purchased from ProteinSimple and the Wes assay was carried out following the manufacturer's instructions. Data analyses were performed using the Compass Software (ProteinSimple).

2.2.4 Real-time PCR of Col5a1 Expression

Real-time PCR was performed as previously described.[18,19] Briefly, patellar tendons were dissected, cut into small pieces, and total RNA was extracted using the RNeasy Micro Kit (QIAGEN, Germantown, MD). Total RNA (3 ng per well) was subjected to reverse transcription using a High Capacity cDNA Reverse Transcription Kit (Thermo Fisher Scientific) and real-time PCR was performed with SYBR Green PCR master mix (Thermo Fisher Scientific) on a StepOnePlus Real Time PCR system (Thermo Fisher Scientific) utilizing the primer sequences in Table 1.

Col5a1 forward primer	AAGCGTGGGAAACTGCTCTCCTAT
Col5a1 reverse primer	AGCAGTTGTAGGTGACGTTCTGGT
β-actin forward primer	AGATGACCCAGATCATGTTTGAGA
β-actin reverse primer	CACAGCCTGGATGGCTACGT

Table 2.1: Primer sequences for real-time PCR.

Each sample (n= 4 patellar tendons/group/time point) was run in duplicate and data were analyzed using StepOne software v2.0. β-actin was used as an internal control to standardize the amount of sample total RNA.

2.2.5 Mechanical Testing

Patella-patellar tendon-tibia complexes were dissected and prepared for mechanical testing, as previously described.[20] Excess soft tissue was removed such that the tendon surface was clearly exposed. Tendon cross-sectional area was measured using a custom laser

device.[21] The tendon was stamped into a dog bone shape using a custom stamping device, such that the injury site was within the narrowest part of the tendon (0.75 mm wide). Following stamping, cross-sectional area was measured again for use in stress calculations. Four Verhoeff stain lines were equally spaced and placed from tibial insertion to patella for fiber alignment analysis. The tibia was embedded into a fixture using PMMA and the tendon was loaded into custom grips for testing.

Tendons were submerged in a temperature regulated 37°C PBS bath throughout testing. Tendon length was measured prior to mechanical testing using imaging. Utilizing an Instron 5848, tendons were subjected to a viscoelastic testing protocol[17,20] consisting of: 1) preconditioning, 2) stress relaxation at 2, 3 and 4% strain, 3) a sinusoidal frequency sweep (10 cycles at 0.1, 1, 5 and 10 Hz) at each strain level, 4) return to initial gauge length, and 5) ramp to failure at a rate of 0.1%/s. Tendon length was measured at nominal load (.005N) prior to test initiation. The dynamic modulus $|E^*|$ (stress amplitude divided by the strain amplitude) and the phase angle δ (used to calculate the dissipation factor, $\tan(\delta)$) are computed at each frequency and strain level using Matlab (Natick, MA). A polarized light imaging system was used to quantify fiber realignment throughout the ramp to failure.[22,23]

2.2.6 Histological Analysis

Following sacrifice, skin was removed from the lower limb and the femur and tibia were cut to remove the entire knee. The knee was positioned at a 90° angle and fixed in formalin, decalcified with Immunocal, and then processed using a standard paraffin protocol. Sagittal 7 µm sections were collected and stained with an aqueous preparation of Hematoxylin & Eosin. Masked graders assessed cellularity and cell shape using a semi-quantitative method,[23] with increased cellularity and rounded cell shape corresponding to values >1 on a 1-4 and 1-3 scale, respectively.

2.2.7 Statistics

Two-way ANOVAs with post-hoc Bonferroni tests were used to assess the effects of genotype (Col5 expression), injury time-point, and their interaction on viscoelastic and quasi-static mechanical properties, as well as gene expression. Kruskal-Wallis non-parametric one-way ANOVA followed by post-hoc Dunn's test for multiple comparisons were used for histologic data. Two-way repeated measures ANOVAs with post-hoc Bonferroni tests were used to assess the differences in realignment between genotypes over increasing strain levels. Significance was set at $p \leq 0.05$ and trends at $p \leq 0.1$.

2.3 – Results

2.3.1 Col5a1 gene expression was not increased post-injury in Col5-deficient mice

Col5a1 mRNA expression was significantly decreased in *Col5a1*$^{+/-}$ tendons at 1- and 3-weeks post-injury, when compared to WT tendons; however, no significant differences were seen in *Col5a1* expression between genotypes in uninjured or 6-week post-injury tendons (**Fig. 2.1A**). Following injury, *Col5a1* expression was significantly increased in WT tendons at 1- and 3-weeks post-injury compared to uninjured controls (**Fig. 2.1A**). No significant changes in *Col5a1* expression were seen following injury in *Col5a1*$^{+/-}$ tendons (**Fig. 2.1A**).

2.3.2 Type V Collagen Content was decreased in Col5-deficient mice compared to wild-type

Col5 content was significantly decreased in uninjured *Col5a1*$^{+/-}$ patellar tendons compared to WT (**Fig. 2.1B**). This decrease was also significant 3-weeks post-injury; however, no significant differences were found between genotypes at 1- or 6-weeks post-injury (**Fig. 2.1B**). Following injury, Col5 content was significantly increased at 3- and 6-weeks post-injury in both WT and *Col5a1*$^{+/-}$ tendons when compared to respective uninjured controls (**Fig. 2.1B**).

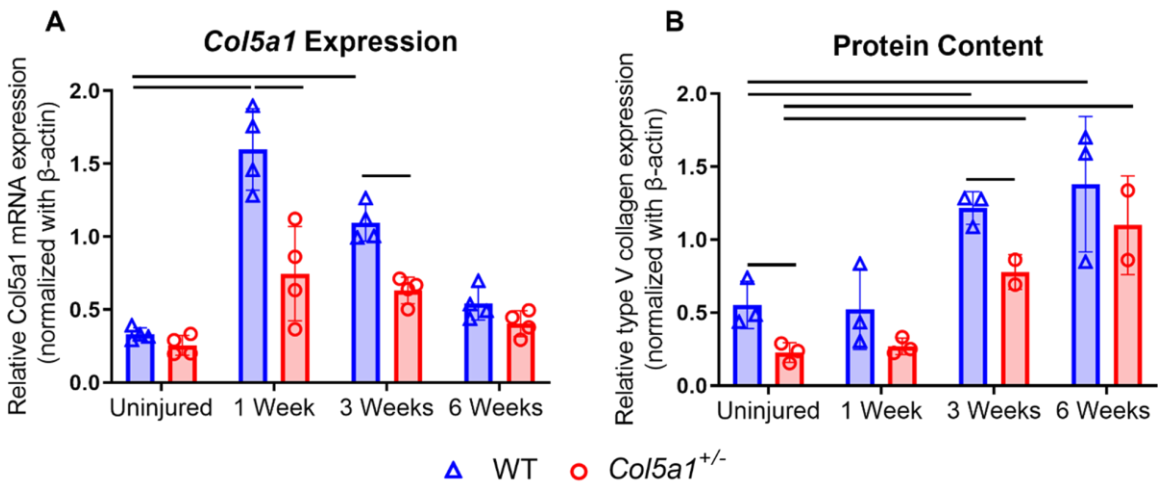

Figure 2.1: Col5a1 Gene Expression and Col5 Protein Content Following Injury. (A) Gene expression was increased from uninjured levels in WT mice 1- and 3-weeks post-injury, as well as between genotypes at both timepoints. **(B)** Col5 content was decreased in uninjured and 3-weeks post-injury Col5-deficient tendons compared to WT. Col5 content was increased 3- and 6-weeks post-injury in both genotypes. Solid lines denote statistical significance of $p \leq 0.05$. n=4 samples/genotype/timepoint.

2.3.3 Col5-deficient tendons had an altered healing response compared to wild-type tendons

There were no significant differences in tendon cross-sectional area between genotypes or over the healing time course (**Fig. 2.2A**). There were no differences in tendon length at any time point between genotypes (**Fig. 2.2B**). However, WT tendons significantly decreased in length at 3- and 6-weeks post-injury compared to uninjured controls (**Fig. 2.2B**). *Col5a1*$^{+/-}$ tendons also decreased in length 3-weeks post-injury compared to uninjured controls, with no differences seen 6-weeks post-injury (**Fig. 2.2B**).

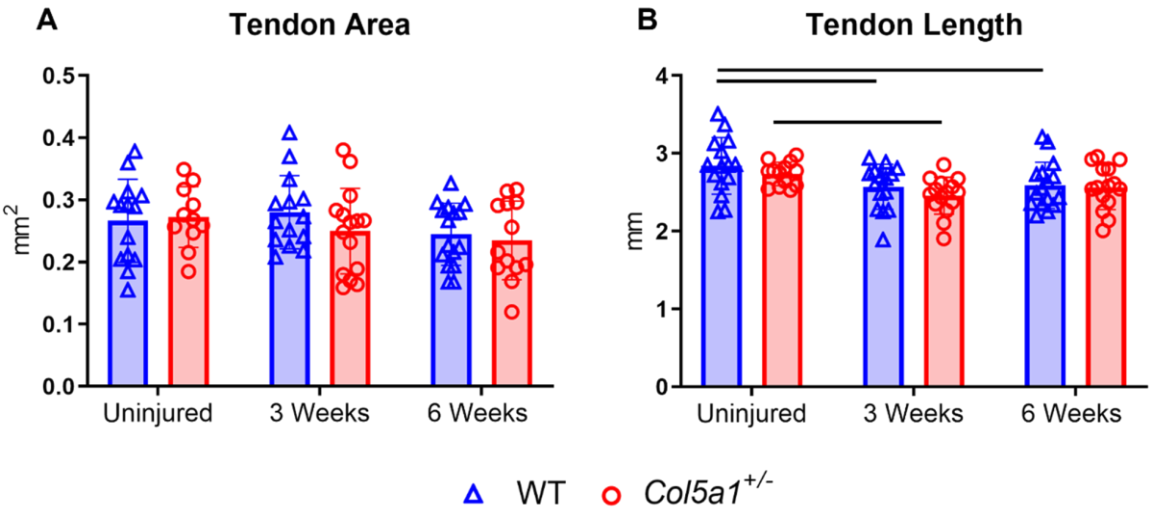

Figure 2.2: Tendon Cross-Sectional Area and Gauge Length. (A) No changes in cross-sectional area were seen between genotypes or across injury time-points. **(B)** Tendon length decreased post-injury at 3-weeks (both genotypes) and 6-weeks (WT). Solid lines denote statistical significance of $p \leq 0.05$. n=11-14 samples/genotype/timepoint.

There were no differences in dynamic modulus between genotypes (**Fig. 2.3**). Following initial preconditioning, tendons underwent stress relaxation at 2, 3, and 4% strain, followed by a sinusoidal frequency sweep at each strain level. After injury, the dynamic modulus of WT tendons was significantly increased at 3- and 6-weeks post-injury across all frequencies at each strain level when compared to uninjured tendons (**Fig. 2.3**). No significant differences were seen following injury in *Col5a1*$^{+/-}$ tendons, however a significant interaction of genotype*time point was seen at 2 and 3% strain, indicating healing differences between WT and *Col5a1*$^{+/-}$ tendons.

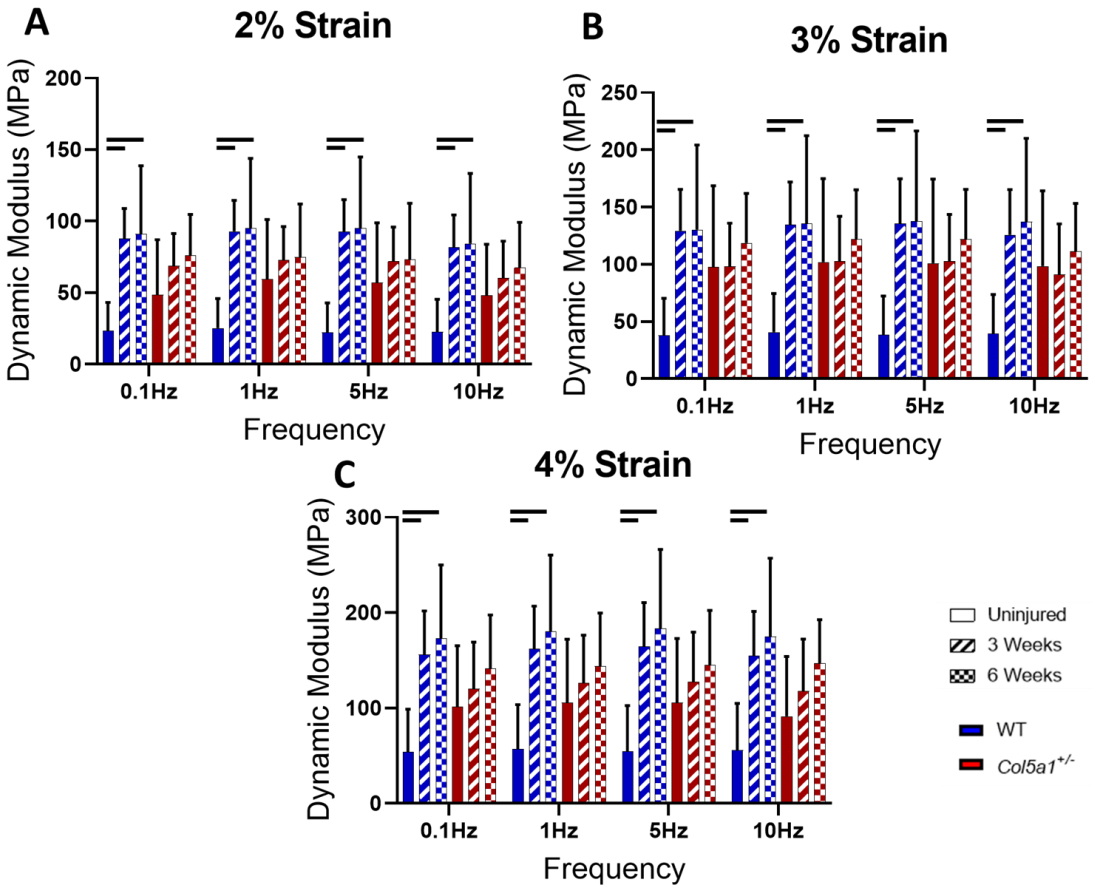

Figure 2.3: Dynamic Modulus. Dynamic modulus of WT tendons increased at 3- and 6-weeks post-injury across all frequencies at each strain level when compared to uninjured tendons. Solid lines denote statistical significance of $p \leq 0.05$. n=11-14 samples/genotype/timepoint.

When comparing between genotypes, uninjured WT tendons had increased tangent delta, indicative of greater viscous contributions, compared to uninjured *Col5a1*$^{+/-}$ tendons at 4% strain, 0.1 and 1 Hz (**Fig. 2.4C**). However, no significant genotypic differences were seen following injury (**Fig. 2.4C**). Similar to dynamic modulus, tangent delta was decreased 3- and 6-weeks post-injury across all strains at 0.1 and 1 Hz in WT tendons compared to uninjured controls (**Fig. 2.4A-C**).

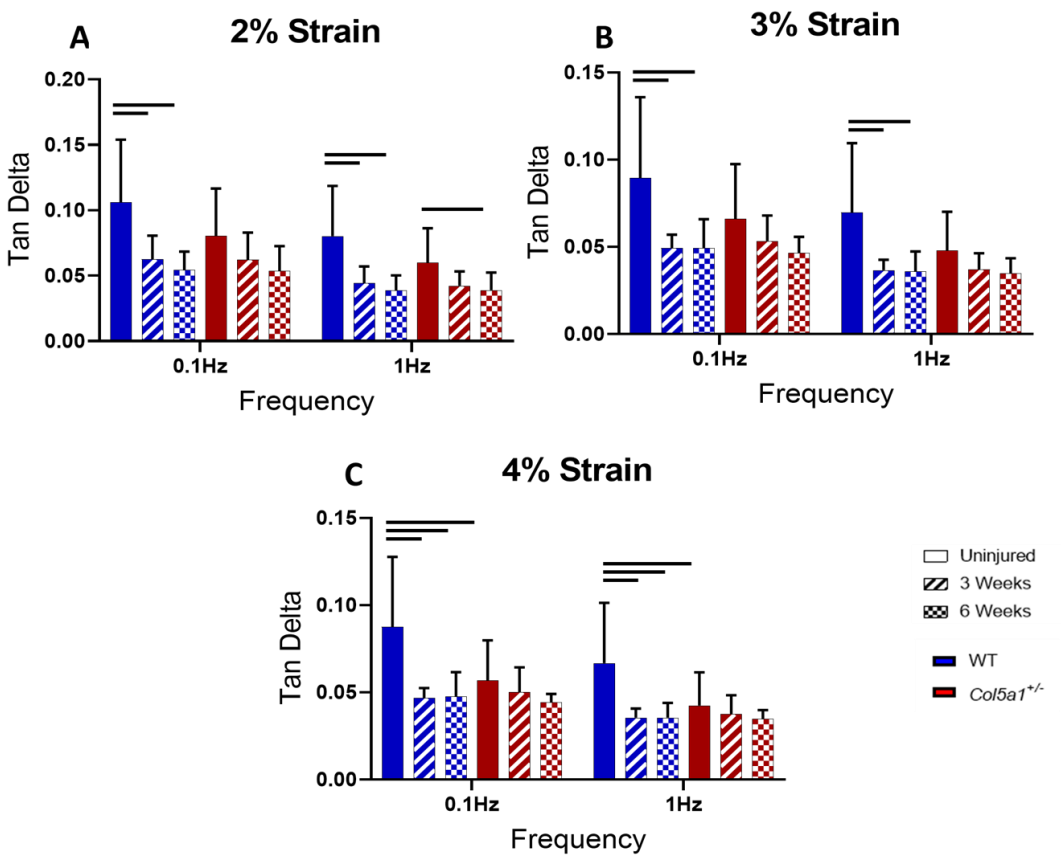

Figure 2.4: Tangent Delta. (A-C) Tangent delta was decreased 3- and 6-weeks post-injury across all strains at 0.1 and 1 Hz in WT tendons compared to uninjured controls. **(C)** Uninjured WT tendons had increased tangent delta values compared to Col5-deficient tendons at 4% strain, 0.1 and 1 Hz. Solid lines denote statistical significance of $p \leq 0.05$. n=11-14 samples/genotype/timepoint.

Polarized light was used to analyze the regional realignment patterns of fibers in both the tendon insertion and midsubstance during the ramp to failure. Similar patterns of realignment were seen in the insertion of uninjured and injured WT and *Col5a1*$^{+/-}$ tendons (**Fig. 2.5A-C**). In the midsubstance, no changes in realignment were seen from 5-6% strain in uninjured or 3-week post-injury WT tendons, although a trending change was seen at 6-weeks (**Fig. 2.5F**). However, *Col5a1*$^{+/-}$ tendons continue to show significant changes in fiber realignment through 6% strain, with greater changes in alignment following injury (**Fig. 2.5D-F**), indicating that *Col5a1*$^{+/-}$ tendons continue to increase collagen alignment at higher strains where WT tendons have reached an equilibrium alignment.

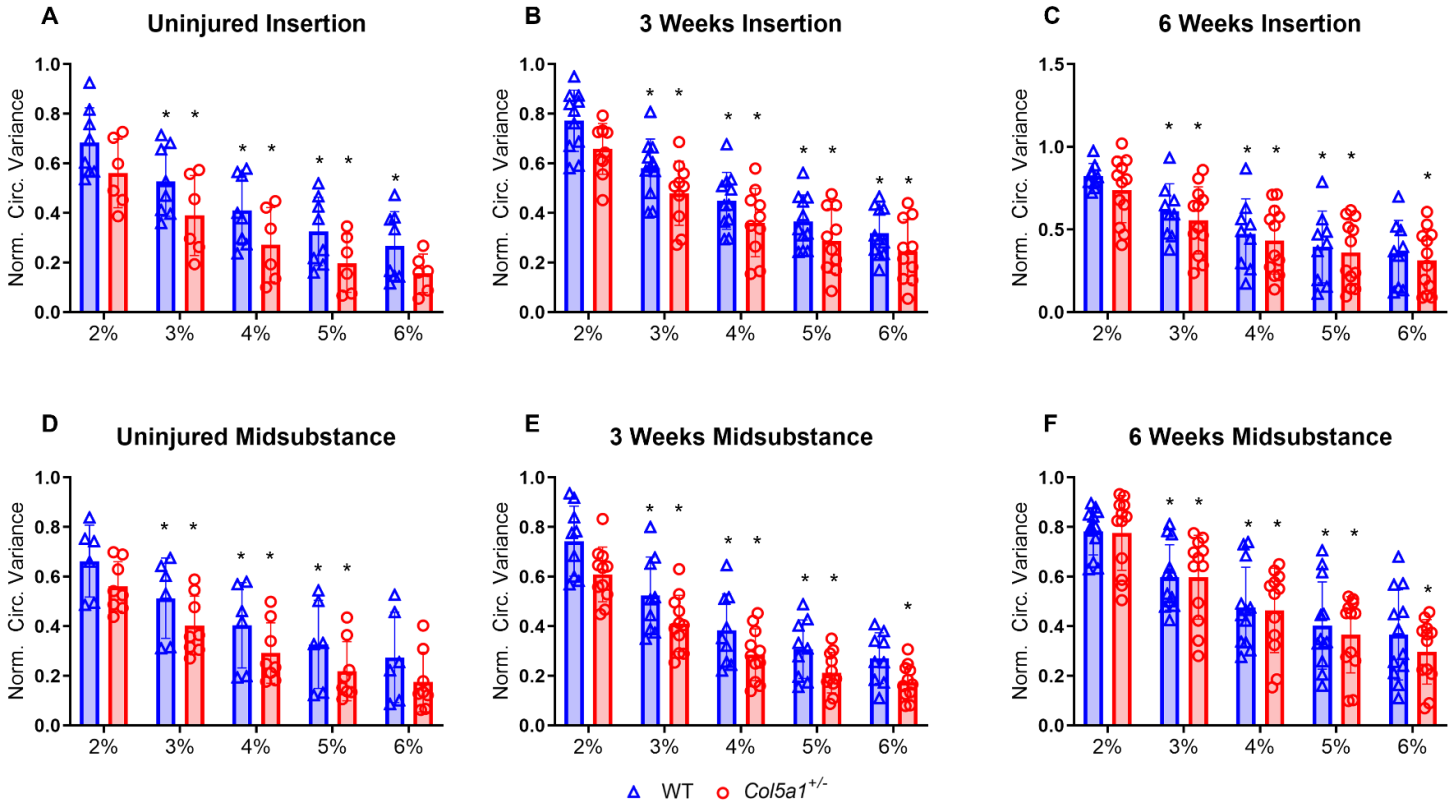

Figure 2.5: Collagen Fiber Realignment During Loading. (A-C) Similar patterns of realignment were seen in the insertion of uninjured and injured WT and Col5-deficient tendons. **(D-F)** In the midsubstance, Col5-deficient tendons continue to show changes in fiber realignment through 6% strain with greater changes in alignment following injury. No changes were seen from 5-6% strain in uninjured and 3-week post-injury WT tendons **(A,B)**. *Indicates significance from previous strain level within the same genotype. Solid lines denote statistical significance of $p \leq 0.05$. n=11-14 samples/genotype/timepoint.

Additionally, failure properties were calculated from the ramp to failure. There were no differences seen between genotypes in failure properties. A trending increase in modulus was seen 3-weeks following injury in WT tendons compared to uninjured controls, but no other changes were seen in the structural properties of the tendons post-injury or between genotypes (**Fig. 2.6A,B**). WT tendons were stiffer 3- (trend) and 6-weeks post-injury, with no changes in *Col5a1*$^{+/-}$ tendon stiffness after injury (**Fig. 2.6C**), indicating that a reduction in Col5 results in an altered healing process. No changes in maximum load to failure were evident following injury or between genotypes (**Fig. 2.6D**).

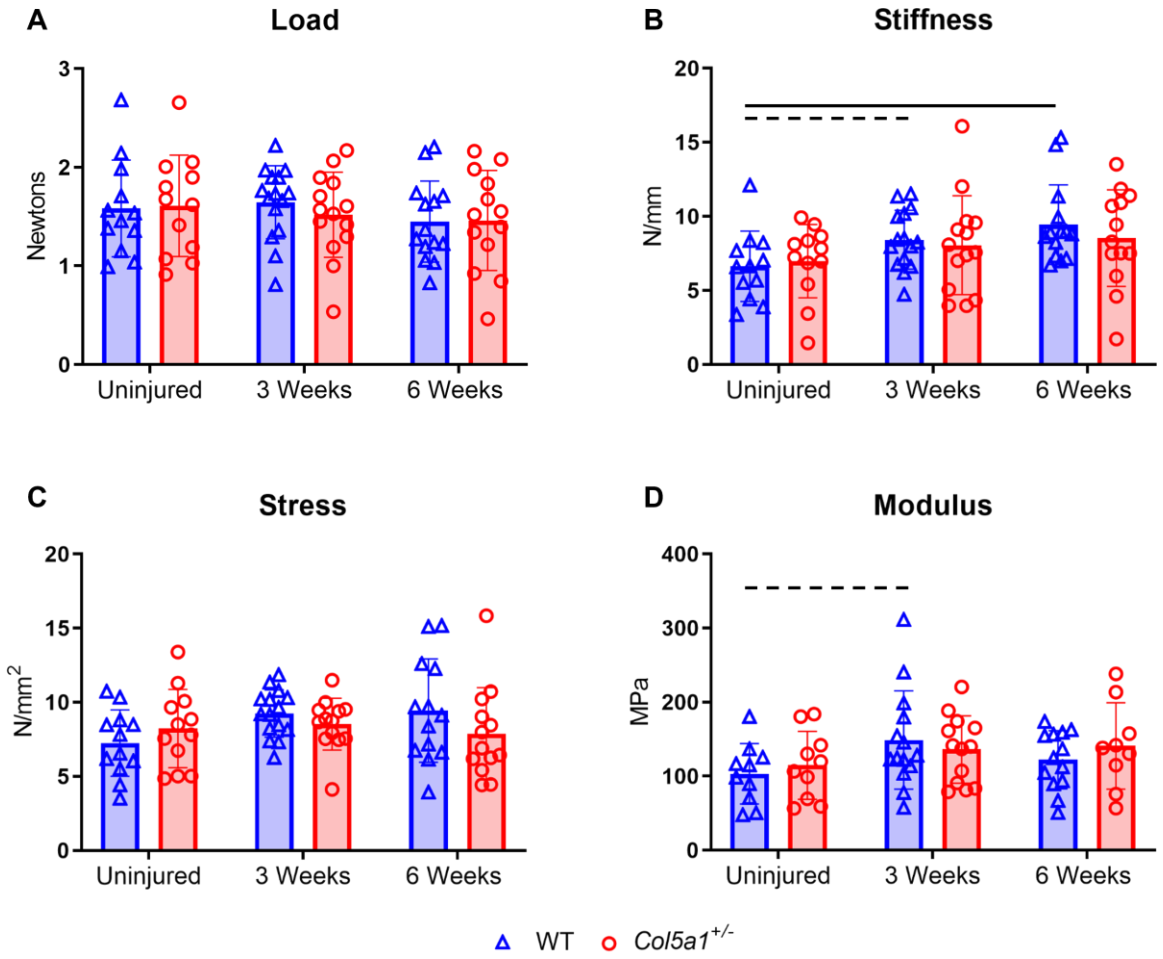

Figure 2.6: Quasistatic Mechanical Properties. (A-D) There were no differences between genotypes in failure properties. WT tendons were stiffer **(B)** 3- (trend) and 6-weeks post-injury, and had an increased modulus **(D)** 3-weeks (trend) post-injury. Solid lines denote statistical significance of $p \leq 0.05$. n=11-14 samples/genotype/timepoint.

2.3.4 Tendon cellularity and cell shape differed between genotypes

Significant differences in cellularity and cell shape (**Fig. 2.7**) were seen between uninjured and both 1- and 3-week samples in both genotypes, and between 1- and both 3- and 6-week samples, with no difference between genotypes at any time-point. *Col5a1*$^{+/-}$ tendons had a significant increase in cellularity persisting to 6-weeks post-injury when compared to uninjured tendons (**Fig. 2.7**).

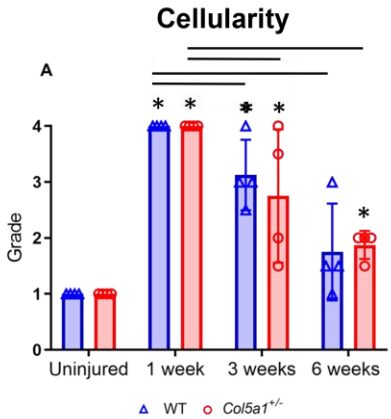

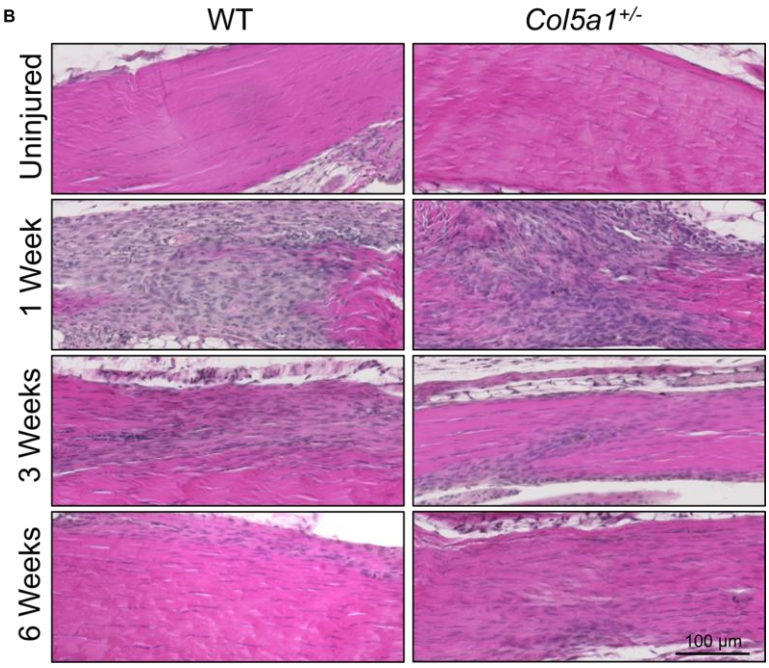

Figure 2.7: Histological Analysis. (A) Col5-deficient tendons had a significant increase in cellularity persisting to 6-weeks post-injury when compared to uninjured tendons. * indicates significantly different from respective uninjured control, p≤0.05. **(B)** H&E representative images. n=4 samples/genotype/timepoint.

2.4 – Discussion

This study indicates that increased *Col5a1* expression post-injury is necessary to re-establish matrix architecture, alignment and cellularity throughout tendon healing in female mice. Utilizing our well establish mouse patellar tendon injury model,[1,2] we were able to examine Col5-deficient tendons throughout healing to determine healing alterations when compared to WT mice.

Col5 plays a key role regulating fibrillogenesis, including early fibril initiation, fibril structure and resulting matrix organization.[4,24] Additionally, studies have shown that following matrix disruption and injury, Col5 impacts matrix remodeling, affecting the structure and function of the healing tendon.[7,25] Previous clinical studies have shown that *c*EDS is heavily skewed to the female population[6,8] and basic science studies suggest that differences in hormone physiology between sexes may be a factor influencing tendon health.[9–11] Given the previous data implicating Col5 in recovery post injury in a male mouse model[7], and the implication of sex on overall tendon health and recovery, this study investigated a Col5 Haploinsufficient female mouse model[4,15] to further understand sex impacts on the role of Col5 in tendon healing.

Uninjured differences in Col5 protein levels initially validated this model for investigation into the role of Col5 in post-injury tendon healing. Additionally, previous studies have shown that Col5 is upregulated following tendon injury, affecting healing and highlighting the potential of downstream effects from alteration in early expression, which was supported by our findings. This study found that *Col5a1* gene expression increased in WT tendons 1- and 3-weeks following injury, but this increase was lacking in *Col5a1*$^{+/-}$ tendons, resulting in decreased protein content 3-weeks following injury in *Col5a1*$^{+/-}$ tendons compared to WT. This lack of an early increase in *Col5a1* gene expression likely affected all stages of later healing and indicates a reduction in regulation of fibrillogenesis throughout healing. WT *Col5a1* expression returns to uninjured and *Col5a1*$^{+/-}$ levels by 6-weeks post-injury, indicating that the early increase plays an important role in reestablishing the mechanical properties and cellularity throughout healing, as differences post-injury and between genotypes are seen. Alterations in Col5 content and gene expression in both uninjured and injured tendons emphasize that this is a valid approach to studying the role of Col5 in the healing process.

Following injury, WT tendons underwent a period of increased stiffness and contraction. This likely corresponds to initial wound scaffold deposition early in healing, and before

remodeling of initial scar tissue is complete. Stiffness did not change between uninjured and injured *Col5a1*$^{+/-}$ tendons, indicating that reduced Col5 in the healing matrix may dampen the injury response and scar formation, due to reduced cell-matrix engagement and a reduction in collagen deposition. This finding is supported by decreased cutaneous wound contraction and closure shown in *Col5a1*$^{+/-}$ mice.[26] Interestingly, in a previous study examining *Col5a1*$^{+/-}$ male mice[7], stiffness was decreased in *Col5a1*$^{+/-}$ mice at uninjured and 6-weeks post-injury when compared to WT controls. This finding was accompanied by decreased contraction of *Col5a1*$^{+/-}$ tendons, seen by gauge length differences, when compared to WT mice. This finding supports our work examining genotypic differences in healing, and taken together with the female data, indicates that structural properties of *Col5a1*$^{+/-}$ male tendons were affected by the reduction of Col5 to a greater degree than the structural properties of *Col5a1*$^{+/-}$ female tendons. In male *Col5a1*$^{+/-}$ tendons, *Col5a1* expression was decreased compared to WT through 6-weeks post-injury[7], while in female Col5-deficient tendons *Col5a1* expression returned to WT levels by 6-weeks post-injury. This may explain the continued decreases in structural properties in male tendons, which were not seen in female tendons. Further examination of gene expression is necessary to understand compensation of other gene targets, especially as gene expression may also be affected by sex.

Col5 plays an important role in tissue laxity, stiffness and maintaining the hierarchical structure of the tendon. This may be attributed to dysregulated matrix deposition immediately post-injury, when *Col5a1* fails to increase in expression and therefore a lack of fibril nucleation and resulting matrix deposition. Additionally, Col5 may play a direct role in fibroblast activity, as well as a regulatory role in the migration of healing cells to the wound site, further explaining the different healing potential in a Haploinsufficient *c*EDS model.[3] When examining viscoelastic properties, WT tendons showed an increase in dynamic modulus and decrease in tangent delta following injury. Tendons heal with a disorganized wound matrix initially, with our findings

supporting increased stiffness and more elastic behavior throughout healing. Lack of an increase in stiffness of *Col5a1*$^{+/-}$ tendons following injury supports disruption in the early deposition of scar tissue and further supports altered fibrillogenesis regulation and a lack of an increase in the rigidity of the matrix, resulting in dynamic modulus values that are unchanged from uninjured levels. This was also indicated by the *Col5a1*$^{+/-}$ tendon tangent delta results, which showed inconsistent decreases following injury, indicating the lack of a robust healing response.

Decreased elasticity has been explained by increased fibril diameters[20] and altered fibrillogenesis regulation has been shown to result in a broader distribution of larger fibrils following injury in male *Col5a1*$^{+/-}$ tendons.[7] Our realignment data supports altered fiber structure, elongating the realignment period in *Col5a1*$^{+/-}$ tendons due to inferior response to loading, which is supported by previous work.[19] Previous studies have shown that WT tendons can more efficiently utilize collagen fibers through aligning fibers faster when load is applied.[19] Extended realignment in *Col5a1*$^{+/-}$ tendons indicates a lack of efficiency in load transfer and engagement of the fibers throughout loading, and higher strain needed to increase the organization of the tissue. This further implicates Col5 in fibril growth, interfibrillar interactions and overall matrix organization.

Histological results support the mechanical testing findings, as the persistent increased cellularity seen in *Col5a1*$^{+/-}$ tendons could alter the matrix alignment and architecture, thereby weakening the tissue and affecting mechanical properties. This persistence of increased cellularity in *Col5a1*$^{+/-}$ tendons to 6-weeks post-injury is consistent with viscoelastic findings which indicate a reduced healing response in *Col5a1*$^{+/-}$ tendons. Qualitative comparisons to male data[7] show *Col5a1*$^{+/-}$ cellularity returned to uninjured levels by 6-weeks post-injury, unlike the data shown, indicating that sex affects outcomes of reduction in Col5.[11] Increased cellularity is likely due to prolonged presence of healing cells in the wound region, leading to delayed

inflammation resolution and resulting reduced healing. A previous study[26] showed delayed wound healing in *Col5a1*$^{+/-}$ mice, with decreased proliferation and migration of dermal fibroblasts *in vitro*, supporting these findings and further explaining the mechanical results in this study.

This study is not without its limitations. We examined the patellar tendon as it is a reproducible injury model with mechanical testing showing low variance compared to other tendons,[17] making a smaller sample size sufficient. However, we understand that behavior differs between tendons with various functional requirements, and therefore Col5 may have different effects on the healing response of other tendons. Additionally, it is difficult to separate alterations throughout healing that are due to an abnormal matrix resulting from a reduction in Col5 throughout development and changes in properties following injury that are due to a direct effect of Col5 during the healing process in this conventional mouse model. However, results from this model are still valuable due to the clinical incidence of a Col5 deficiency in *c*EDS patients where the effects of Col5 reduction during development and healing are similarly affected.

Overall, this study indicates that the lack of an early increase in *Col5a1* expression post-injury in *Col5a1*$^{+/-}$ tendons influences matrix architecture, alignment, and cellularity throughout tendon healing, demonstrating altered and decreased healing compared to WT tendons. Increased cellularity at 6-weeks in *Col5a1*$^{+/-}$ tendons indicates delayed healing compared to WT, and parallels the findings seen in mechanical properties. Mechanical properties also exhibited delayed healing compared to WT tendons, as was seen in the extended realignment in *Col5a1*$^{+/-}$ tendons indicating a lack of efficiency in fiber engagement. Lastly, this study indicates that structural and viscoelastic properties of *Col5a1*$^{+/-}$ male tendons were affected by the reduction of Col5 to a greater degree than those of *Col5a1*$^{+/-}$ female tendons, however, histologically female tendons are more affected by genotype than male. Prolonged inflammation could be a potential mechanism for poor healing in Col5-deficient tendons, especially female. Hormones

have been shown to influence the inflammatory environment directly, as well as indirectly through altered gene expression, influencing long-term remodeling and healing potential of tendon. In our study, increased cellularity was seen in *Col5a1*$^{+/-}$ tendons, and this corresponded with delayed realignment throughout loading, potentially indicating that optimal cell-matrix engagement is affected by the presence of immune cells. This likely will affect the overall quality of the tissue long-term.

Future directions may include examining fibril diameter distribution in this mouse model to understand if a reduction in Col5 alters the diameter distribution and if this can explain the mechanical alterations and support the histological findings from this study. Additionally, we will examine the response to fatigue loading of these tendons to further understand how the dampened healing response of *Col5a1*$^{+/-}$ tendons responds to cyclic loading, as preservation of mechanical properties throughout repetitive loading is a characteristic quality of healthy tendon function. Lastly, proteomic analysis would allow further understanding of the effect of Col5 expression on protein content post-injury and could help explain sex-differences in tendon healing to a greater degree. In conclusion, the lack of an early increase in *Col5a1* expression post-injury in Col5-deficient tendons influences matrix mechanical properties post-injury, cell-matrix engagement and fiber realignment, and inflammation resolution throughout tendon healing, demonstrating altered and delayed healing compared to WT tendons. Increased *Col5a1* expression post-injury is necessary to re-establish matrix architecture, alignment and cellularity throughout tendon healing.

2.5 – References

1 Malfait F, Wenstrup RJ, De Paepe A. Clinical and genetic aspects of Ehlers-Danlos syndrome, classic type. Genet Med 2010:597–605. https://doi.org/10.1097/GIM.0b013e3181eed412.

2 Byers PH. Disorders of Collagen Biosynthesis and Structure. The Online Metabolic and Molecular Bases of Inherited Disease. McGraw Hill; 2019.

3 Steinmann B, Royce PM, Superti-Furga A. The Ehlers-Danlos Syndrome. Connect. Tissue Its Heritable Disord. Hoboken, NJ, USA: John Wiley & Sons, Inc.; n.d. p. 431–523.

4 Wenstrup RJ, Florer JB, Brunskill EW, Bell SM, Chervoneva I, Birk DE. Type V collagen controls the initiation of collagen fibril assembly. J Biol Chem 2004;279:53331–7. https://doi.org/10.1074/jbc.M409622200.

5 Collins M, Posthumus M. Type V collagen genotype and exercise-related phenotype relationships: A novel hypothesis. Exerc Sport Sci Rev 2011;39:191–8. https://doi.org/10.1097/JES.0b013e318224e853.

6 Ainsworth, SR, Aulicino P. A survey of patients with Ehlers-Danlos syndrome - PubMed. Clin Orthop Relat Res 1993:286:250-256.

7 Johnston JM, Connizzo BK, Shetye SS, Robinson KA, Huegel J, Rodriguez AB, et al. Collagen V haploinsufficiency in a murine model of classic Ehlers–Danlos syndrome is associated with deficient structural and mechanical healing in tendons. J Orthop Res 2017;35:2707–15. https://doi.org/10.1002/jor.23571.

8 Stanitski DF, Nadjarian R, Stanitski CL, Bawle E, Tsipouras P. Orthopaedic manifestations of Ehlers-Danlos syndrome. Clin Orthop Relat Res 2000:213–21. https://doi.org/10.1097/00003086-200007000-00029.

9 Bridgeman JT, Zhang Y, Donahue H, Wade AM, Juliano PJ. Estrogen receptor expression in posterior tibial tendon dysfunction: A pilot study. Foot Ankle Int 2010;31:1081–4. https://doi.org/10.3113/FAI.2010.1081.

10 Liu SH, Al-Shaikh R, Panossian V, Yang RS, Nelson SD, Soleiman N, et al. Primary immunolocalization of estrogen and progesterone target cells in the human anterior cruciate ligament. J Orthop Res 1996;14:526–33. https://doi.org/10.1002/jor.1100140405.

11 Romani WA, Russ DW. Acute effects of sex-specific sex hormones on heat shock proteins in fast muscle of male and female rats. Eur J Appl Physiol 2013;113:2503–10. https://doi.org/10.1007/s00421-013-2686-8.

12 Yu WD, Panossian V, Hatch JD, Liu SH, Finerman GAM. Combined effects of estrogen and progesterone on the anterior cruciate ligament. Clin Orthop Relat Res 2001:268–81. https://doi.org/10.1097/00003086-200102000-00031.

13 Kjaer M, Magnusson P, Krogsgaard M, Moller JB, Olesen J, Heinemeier K, et al. Extracellular matrix adaptation of tendon and skeletal muscle to exercise. J Anat 2006;208:445–50. https://doi.org/10.1111/j.1469-7580.2006.00549.x.

14 Hart DA , Archambault JM, Kydd A, Reno C, Frank CB HW. Gender and neurogenic variables in tendon biology and repetitive motion disorders. Clin Orthop Relat Res 1998;351:44–56.

15 Wenstrup RJ, Florer JB, Davidson JM, Phillips CL, Pfeiffer BJ, Menezes DW, et al. Murine model of the Ehlers-Danlos syndrome: col5a1 haploinsufficiency disrupts collagen fibril assembly at multiple stages. J Biol Chem 2006;281:12888–95. https://doi.org/10.1074/jbc.M511528200.

16 Sun M, Chen S, Adams SM, Florer JB, Liu H, Kao WWY, et al. Collagen V is a dominant regulator of collagen fibrillogenesis: Dysfunctional regulation of structure and function in a corneal-stroma-specific Col5a1-null mouse model. J Cell Sci 2011;124:4096–105. https://doi.org/10.1242/jcs.091363.

17 Beason DP, Kuntz AF, Hsu JE, Miller KS, Soslowsky LJ. Development and evaluation of multiple tendon injury models in the mouse. J Biomech 2012;45:1550–3. https://doi.org/10.1016/j.jbiomech.2012.02.022.

18 Sun M, Luo EY, Adams SM, Adams T, Ye Y, Shetye SS, et al. Collagen XI regulates the acquisition of collagen fibril structure, organization and functional properties in tendon. Matrix Biol 2020;94:77–94. https://doi.org/10.1016/j.matbio.2020.09.001.

19 Robinson KA, Sun M, Barnum CE, Weiss SN, Huegel J, Shetye SS, et al. Decorin and biglycan are necessary for maintaining collagen fibril structure, fiber realignment, and mechanical properties of mature tendons. Matrix Biol 2017;64:81–93. https://doi.org/10.1016/j.matbio.2017.08.004.

20 Dunkman AA, Buckley MR, Mienaltowski MJ, Adams SM, Thomas SJ, Satchell L, et al. Decorin expression is important for age-related changes in tendon structure and mechanical properties. Matrix Biol 2013;32:3–13. https://doi.org/10.1016/j.matbio.2012.11.005.

21 Favata M. Bioengineering PhD Thesis. University of Pennsylvania; 2006; 2006.

22 Lake SP, Miller KS, Elliott DM, Soslowsky LJ. Tensile properties and fiber alignment of human supraspinatus tendon in the transverse direction demonstrate inhomogeneity, nonlinearity, and regional isotropy. J Biomech 2010;43:727–32. https://doi.org/10.1016/j.jbiomech.2009.10.017.

23 Lake SP, Miller KS, Elliott DM, Soslowsky LJ. Effect of fiber distribution and realignment on the nonlinear and inhomogeneous mechanical properties of human supraspinatus

tendon under longitudinal tensile loading. J Orthop Res 2009;27:1596–602. https://doi.org/10.1002/jor.20938.

24 Sun M, Connizzo BK, Adams SM, Freedman BR, Wenstrup RJ, Soslowsky LJ, et al. Targeted deletion of collagen V in tendons and ligaments results in a classic Ehlers-Danlos syndrome joint phenotype. Am J Pathol 2015;185:1436–47. https://doi.org/10.1016/j.ajpath.2015.01.031.

25 Niyibizi C, Kavalkovich K, Yamaji T, Woo SLY. Type V collagen is increased during rabbit medial collateral ligament healing. Knee Surgery, Sport Traumatol Arthrosc 2000;8:281–5. https://doi.org/10.1007/s001670000134.

26 DeNigris J, Yao Q, Birk EK, Birk DE. Altered dermal fibroblast behavior in a collagen V haploinsufficient murine model of classic Ehlers-Danlos syndrome. Connect Tissue Res 2016;57:1. https://doi.org/10.3109/03008207.2015.1081901.

CHAPTER 3: Collagen III Deficiency Following Injury in Female Murine Tendons Alters Matrix Composition, Alignment and Mechanical Properties

3.1 – Introduction

Tendon is composed of a highly aligned Col1-rich matrix, resulting in its ability to withstand large loads. Following injury, matrix disruption results in a shift to a Col3-rich matrix and susceptibility to excessive scarring and loss of structure and mechanical function. Innate low vascularity and cellularity contribute to poor healing following tendon injury and the prolonged presence of fibrotic scarring. While the mechanism behind persistent scar tissue formation in tendon healing is unknown, it is believed to be due to ineffective remodeling of the provisional Col3-rich matrix into aligned Col1 matrix seen in uninjured tendons, resulting in abundance of disorganized collagen in the fibrotic scar.

Col3 is essential in homeostasis and healing of other Col1-rich tissues (e.g., skin,[1] meniscus,[2] and bone[3,4]) due to its role regulating fibrillogenesis, ECM organization and remodeling, and the formation of cross-links and scar tissue.[1,2] In skin wounds,[1] Col3 directs reparative cell activities by regulating early cellular infiltration and proliferation to promote healing, and in later healing Col3 protects against scar formation by directing an open weave matrix microarchitecture. However, and importantly, preferred collagen remodeling in tendon repair diverges from skin wounds, relying on formation of a highly aligned matrix at later stages, supporting the innovative concept that Col3 plays unique, temporal roles throughout tendon healing. Further, while ECM organization and stiffness affected by Col3 content likely influence cell behavior, the impact of Col3 expression on fibroblast matrix production and immune cell activity has not been studied in tendon.

Following tendon injury, Col3 is deposited to fill the wound void[5] and comprises a large proportion of the provisional matrix that lays the groundwork for future healing. Col3 expression increases by 3 days following tendon injury,[5] suggesting a crucial role in early tendon healing. The matrix production associated with efficient cellular infiltration is key to support rebuilding of the tendon. In both skin and tendon, macrophages and mesenchymal cells are recruited, proliferate and lay down a provisional wound matrix.[2,6,7] These cell types modulate the dynamic reciprocity between the cells and their matrix that shifts from poor healing toward an optimal healing response. In previous work, Col3-deficient mice have significant impairment in the formation of granulation tissue at 7 days post-injury,[1] indicating the importance of Col3 in the provisional matrix. Col3 is critical for efficient recruitment of reparative cells and to promote their vulnerary activities, additionally influencing myofibroblast activity and proliferation. Early healing mechanisms have been shown to contribute to long-term scar tissue and provide the foundation that will eventually be remodeled and replaced with tissue more closely resembling naïve tendon tissue. By examining healing in a Col3-deficient mouse, we evaluated the altered microarchitecture, structure and organization of the provisional matrix early in healing, changes in cellular populations, and resultant changes in matrix remodeling, scar tissue deposition, and mechanical properties throughout healing.

We propose that Col3 alters the biophysical and biomechanical features of the collagen fibrous network to optimize the efficiency and quality of tendon repair. In this study, we defined the importance of Col3 in early provisional matrix and showed that reduced Col3 affected downstream healing by increasing fibroblast activation and fiber alignment, resulting in increased mechanical properties. Evaluation of the role of Col3 in regulating qualitative differences in tissue immune cell populations provides a previously unrecognized mechanism by which the Col3-enriched provisional matrix directs immune cell activity and highlight the importance of modulating matrix structure throughout healing. Our comprehensive study allows

us to relate Col3-dependent cellular activities to functional properties and remodeling capability of the tendon throughout healing.

Questions regarding the relationship between matrix architecture, composition, and cell-ECM interactions have arisen, with recent interest in the dynamic collagen-cellular interactions dictating tendon healing. This relationship likely shifts overtime throughout the different phases of tendon healing. Early in tendon healing, a disorganized, basket weave matrix will allow for proper cellular infiltration and a robust healing environment. This unique structure allows for a well-regulated inflammatory phase, that is dampened with a reduction of Col3 in the early provisional matrix.[8–10] Following this early phase of healing, proper cell-ECM interactions are then required to engage the fibrils and lead to remodeling and alignment. Without proper interactions, alignment is suboptimal, scar tissue remains and fibrosis progresses. In tendon healing, elevated Col3 in later stages of healing indicates increased scar tissue and reduced function. Through this study, we evaluated how Col3-deficiency affected early and later stage matrix alignment, myofibroblast activation, immune cell populations, and matrix deposition. We were able to evaluate tendon mechanical properties in relation to matrix architecture and cellular activity to better understand structure-function relationships throughout tendon healing.

The overall objective of this study was to define the critical role of Col3 in modulating matrix deposition and organization throughout tendon healing, its influence on specific cell populations and resultant functional changes. *We hypothesized that a reduction in Col3 would result in a more highly aligned, stiffer provisional matrix early in healing, and altering fibroblast and macrophage activity. Utilizing a conventional Col3 heterozygous (Col3a1$^{+/-}$) mouse model,[11] we examined the role of Col3 in driving alterations in in gene expression, cellular populations, matrix organization and alignment, and the effect on mechanical properties to elucidate the structure-function relationship throughout healing.*

3.2 – Methods

3.2.1 Animal Model and Study Design

The Institutional Animal Care and Use Committee (IACUC) at the University of Pennsylvania approved all use and care of the animals used in this study. A breeding pair of *Col3a1* heterozygous (*Col3a1*$^{+/-}$) mice in the BALB/c strain (originally obtained from Jackson Laboratories, Bar Harbor, ME) was transferred from the Volk Laboratory at the University of Pennsylvania School of Veterinary Medicine to begin our colony, and this colony was used for all experiments outlined in Chapters 3-5. These mice have been widely used and the model well characterized.[11] All the animals were genotyped for *Col3a1* by PCR of DNA extracted from tail biopsy specimens and processed in our lab.

Female wild-type (WT) BALB/c littermates and heterozygous *Col3a1*$^{+/-}$ mice at 90 days of age (n=96) were used. Uninjured (n=24) and injured (n=72) groups were randomly assigned, with injured mice undergoing bilateral patellar tendon defect injury surgery, described below. Injured animals at 1-, 3-, or 6 weeks post-injury, and uninjured age-matched (110 days of age) animals were euthanized using carbon dioxide. Left limbs were utilized for mechanical testing (n=12) and right limbs for histology or gene expression (n=4).

3.2.2 Surgical Induction of Patellar Tendon Injury

Our reproducible bilateral patellar tendon (PT) defect model[20] was used as it has several critical and fundamental advantages for our studies over other mouse injury models that we and others have used. PT loading is low during healing due to adjacent tendon struts, thus minimizing the effects of post-injury loading and allowing bilateral surgery to utilize both hindlimbs. Further, this model does not require suture repair, which avoids confounding suture induced (e.g., inflammatory) effects. Using aseptic technique, the patellar tendon was initially exposed through a medial incision on the flexed knee, and then isolated with longitudinal incisions following the medial and lateral edge of the tendon. A 0.75 mm biopsy punch was used

to create a full-thickness, partial width defect (~60%) in the midsubstance of the patellar tendon. A rubber-coated backing was used during this procedure to protect the joint under the tendon. Mice were administered Buprenorphine SR (0.1mg/kg) prior to surgery and returned to cage activity following skin closure with 2 sutures. Mice were monitored for 5 days post-surgery with no adverse effects seen.

3.2.3 Gene Expression

To define changes in gene expression induced by Col3 loss during healing, a microfluidic qPCR array (Fluidigm 96.96 Dynamic IFCs) was used to quantify expression of 96 genes from 40 independent samples (9,216 C_T reactions) as described. We analyzed gene expression (**Table 3.1**) within the following categories: i) collagens, ii) non-collagenous matrix, iii) matrix remodeling, iv) cell-ECM interactions markers, v) cell signaling, vi) cell markers, vii) inflammation, and viii) cell cycle genes. The use of arrays allowed expansion of a traditional candidate analysis to include candidates less obviously involved and minimize bias. The non-collagenous matrix genes included proteoglycans and glycoproteins differentially expressed in the pericellular matrix (PCM) and ECM, given the predominant PCM localization of Col3 in cartilage,[2] these are of particular interest. Matrix remodeling genes included enzymes involved in matrix degradation (MMPs) or matrix cross-linking, as well as cross-linking cofactors and modifiers.[8] The communication between the ECM and cell, in addition to cell-cell communication, is critical to normal tendon function. Therefore, we measured expression of integrins, connexins, and cadherins that are expressed in tendons. Additionally, genes from major signaling pathways active in tendon were measured. We examined inflammatory cell populations, tenocyte markers, and fibroblast activation with various cell markers, and finally, genes that are active during cell cycle were measured to monitor proliferative and apoptotic state of cells.

For heatmap analysis ΔCt was calculated by subtracting the gene Ct from the average housekeeper value (*Abl1 and Rps17*) Ct and depicted as change post-injury from uninjured levels of WT tendons. To calculate *Col3a1* fold change, the ΔCt value was first calculated. The ΔCt values for the WT uninjured group were averaged and then this average was subtracted from each ΔCt value across genotypes and injury timepoint (ΔΔCt). Finally, fold change was calculated using the formula: fold change = $2^{-\Delta\Delta Ct}$. 3-4 tendons were assessed per genotype and time-point.

Collagens	Non-Collagenous Matrix	Matrix (Re)modeling & Modification	Cell-ECM Interactions	Signaling Pathways	Cell Markers	Inflammation	Cell Cycle	Housekeeping
Col1a1, Col1a2, Col2a1, Col3a1, Col5a1, Col6a1, Col6a2, Col11a1, Col12a1, Col14a1	Acan, Aspn, Bgn, Dcn, Fap, Fbn1, Fmod, Fn1, Hspg2, Kera, Lum, Postn, Prg4, Sparc, Thbs2, Thbs4 Tnc, Tnmd, Vcan	Adamts1, Adamts15, Loxl1, Loxl2, Mmp2, Mmp3, Mmp7, Mmp8, Mmp9, Mmp13, Mmp14, Timp1, Timp3	Cdh11, Gja1, Itgb1, Itga1, Itga2, Itga5, Itgb5, Itga11, Itgav, Plod2, Plod3	Bmp4, Ctgf, Egr1, Ltbp1, Ltbp4, Mstn, Taz, Tgfb1, Tgfb2, Tgfb3, Tgfbr2, Yap1	Acta2, Adgre1, Cd3e, Cd31, Cd38, Cd68, Cd163, Mkx, Mpo, Scx, Sox9, Vim	IL1B, IL6, IL10, IL12, IL13, IL33,TLR2, TLR4, TNFa	Axin2, Casp3, H2AFX, Pcna	18S, Abl1, Rps17

Table 3.1: Gene panel for 96.96 microfluidic qPCR array.

3.2.4 Matrix Functional Analyses

Biomechanical Testing*.** Evaluating tendon biomechanics is crucial to understanding structure-function relationships throughout healing. We will use a sophisticated testing protocol to assess the viscoelastic tissue response over a range of strain levels and loading frequencies. Measurement of viscoelastic parameters is necessary to define and predict the response of tendons to physiological loading regimens. Significant and consistent changes in these parameters were seen in previous studies where quasi-static parameters remained unaltered. Dynamic collagen fiber realignment will be quantified throughout loading using our sensitive fiber-alignment assay to elucidate changes in tendon architecture throughout. 8-11 tendons were assessed per genotype and time-point. ***Sample Preparation. Patella-PT-tibia complex,

will be dissected and prepared as described. Excess soft tissue is removed, and cross-sectional area was measured using a custom laser device.[9]

Tendons were stamped into a dog-boned shape, with a minimum width surrounding the injury site to evaluate the mechanical properties of the injury site. The tibia was potted using PMMA in a custom 3D-printed pot, which holds the bone at a 35° angle, to test the tendon at a physiologically relevant angle. ***Viscoelastic testing***. Specimens will be tested utilizing the following protocol on an Instron 5848, as described[20]: 1) preload to 0.05 N, 2) 10 cycles of preconditioning to 1.5% strain at 0.25 Hz, 3) stress relaxation to 3% strain at 5%/s, 4) sinusoidal frequency sweep, 5) stress relaxation to 6% strain at 5%/s, 6) sinusoidal frequency sweep, 9) return to gauge length and 10) ramp to failure at 0.05%/s. Each frequency sweep consists of 10 cycles of 0.125% amplitude sinusoidal strain at frequencies of 0.01, 0.1, 1, 5 and 10 Hz. The dynamic modulus $|E^*|$ (stress amplitude divided by the strain amplitude) and the phase angle, δ (between the stress and strain) are computed at each frequency and strain level using a custom Matlab program. $|E^*|$ represents how difficult the material is to deform under dynamic loading, while δ is a measure of viscous dissipation in the tendon. ***Fiber re-alignment measurement.*** Collagen fiber re-alignment was quantified.[11,12] During the ramp to failure test, images were acquired every 5 seconds for strain analysis. In addition, sets of polarized images are acquired every 20 seconds as the polarizers rotate through 45-135º for fiber alignment analysis which is calculated throughout testing from the images.[11] Circular variance (VAR), a measure of the distribution of fiber alignment,[11,13] will determine if significant re-alignment occurred during each portion of the mechanical test.

3.2.5 Collagen Localization, Cell Infiltration and Phenotype

Histology.

Whole joints were harvested and fixed for 24 hours in 4% PFA, then switched to 30% sucrose for 24 hours. Knee joints were embedded in OCT and submerged in methyl butane chilled with dry ice. Cryosections were collected at 7µm utilizing cryofilm, and then glued onto slides using chitosan. Slides dried for 48 hours before staining. Following immunofluorescence (IF) staining (see below), a standard Hematoxylin & Eosin Aqueous protocol was used to obtain images for histomorphometric analysis as has been previously described.[14,15] Slides were imaged using a Zeiss Axioscan.Z1 with a 10X Brightfield objective. Two masked reviewers performed semi-quantitative grading for cell shape and cellularity and their scores were averaged.

Immunofluorescence.

Standard IF protocols were optimized for our targets, which included collagen III, myofibroblasts (α-SMA), M1/M2 macrophages (anti-iNOS/CD206) and general macrophages (anti-F480). Each protocol began with an antigen retrieval method, pepsin (Col3, α-SMA) or proteinase K (iNOS, CD206, F480), followed by blocking in the host serum and primary antibody incubation overnight at 4°C. Finally on day two, sections were incubated with fluorescently conjugated secondary antibodies for 1 hour and coverslips were applied with a mixture of glycerol and PBS including a nuclear stain. Slides stained for macrophages were imaged using a Zeiss Axioscan.Z1 with a 40X objective, with appropriate excitation wavelengths and exposure times. Multiplexed staining protocol for Col3 and α-SMA was followed with multiphoton imaging, discussed below.

Multiphoton and Second Harmonic Generation Imaging.

Sequential scans of sections stained for Col3 and α-SMA were imaged on an upright Leica SP8 confocal/multiphoton microscope (Leica Microsystems, Mannheim, Germany. Nuclei fluorescence was captured using 488nm wavelength laser, followed by α-SMA with a 555nm wavelength laser and collagen III with a 647 nm wavelength laser (PMT detectors). Imaging of fibrillar collagen was performed by tuning the Coherent Chameleon Ultra II Ti:Sapphire laser (Coherent Inc., Santa Clara, CA) to 910 nm and collecting transmitted and reflected second harmonic generation (SHG) signal on PMT-RLD and HYD-RLD detectors. Z-stacks were taken at 1 μm intervals to capture the depth of the tendon in uninjured midsubstance or through the injury site.

Quantification.

Sections were chosen to be stained when they included a full-thickness or mostly full-thickness injury region. ROIs surrounding the injured tissue were drawn on Col3, αSMA and SHG images in order to evaluate the same area for each of the three measures. For uninjured sections, a representative ROI was drawn around an uninterrupted area of uninjured tissue. ImageJ was used to measure integrated density within the region, and then divided by area to be able to compare between each group. Injury size differed between groups and therefore this standardized measurement was necessary. Additionally, ImageJ was utilized to determine collagen fiber organization by generating fast Fourier Transform powerplots (FFT-pp) of the fibrillar collagen signal. An ellipse was fit around the processed FFT-pp and the FFT Aspect Ratio was calculated by dividing the major axis by the minor axis of the ellipse.

Orientation of collagen fibers was calculated utilizing an ImageJ plug-in, OrientationJ, following a well-established protocol.[16] Images were first transformed to 8-bit images and then ROIs were selected for analysis. Distributions of fiber orientation were analyzed and the number of fibers within ±15° of the modal angle per group was used for statistical analysis.

Lastly, CT Fire analysis[17] was utilized to analyze width, length, and straightness of collagen fibers. This is a MATLAB program that can be downloaded from The Eliceiri Lab at the University of Wisconsin-Madison. After denoting individual ROIs surrounding the injury site, the program s individual collagen fibers and measures structural properties. 4 tendons were assessed per genotype and time-point

3.2.6 Statistics

Two-way ANOVAs with post-hoc Bonferroni tests were used to assess the effects of genotype, injury time-point, and their interaction on gene expression, fiber alignment measures, integrated density, and viscoelastic and quasistatic mechanical properties. Two-way repeated measures ANOVAs with post-hoc Bonferroni tests were used to assess the differences in realignment between genotypes over increasing strain levels. Significance was set at $p \leq 0.05$ and trends at $p \leq 0.1$.

3.3 - Results

3.3.1 Gene expression changed from baseline levels differently in Col3a1$^{+/-}$ tendons compared to WT tendons in key categories.

Col3 expression increased post-injury in both WT and *Col3a1*$^{+/-}$ tendons. Increased Col3 expression extended through 3-weeks post-

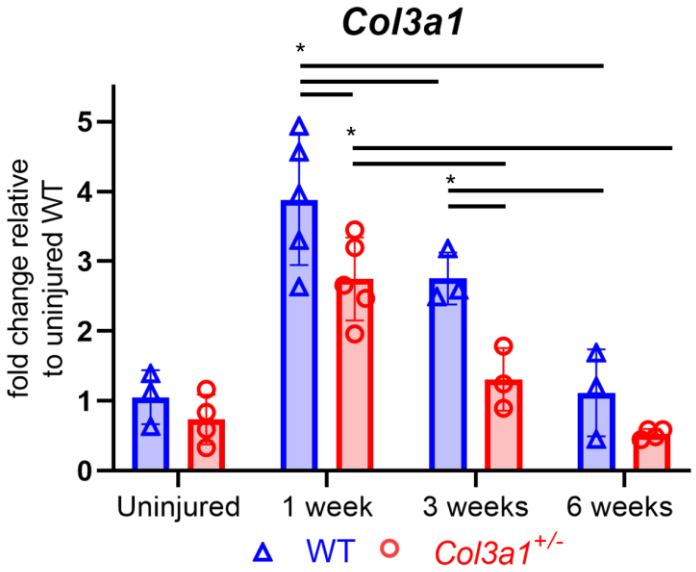

Figure 3.1: *Col3a1* Gene Expression
Col3a1 was decreased in Col3a1$^{+/-}$ tendons at all time-points following injury and increased post-injury in both genotypes. Solid lines denote statistical significance of $p \leq 0.05$. * denotes significant increase from corresponding uninjured group. n=3-4 samples/genotype/timepoint.

injury in WT tendons, with a return to uninjured levels by 3-weeks in *Col3a1*$^{+/-}$ tendons (**Fig. 3.1**). Overall trends in gene expression by category were examined (**Fig. 3.2**). Directional changes from baseline uninjured WT expression levels were evaluated. In general collagen expression (**Fig. 3.2A**) was decreased from uninjured levels to a greater extent at 6-weeks in *Col3a1*$^{+/-}$ animals. Expression of a greater number of genes associated with non-collagenous matrix decreased from 1- to 6-weeks in *Col3a1*$^{+/-}$ tendons, while WT had lesser extent of changes between 1- and 6-weeks (**Fig 3.2A**). Overall, a subset of non-collagenous matrix genes (**Fig. 3.2A**) were decreased in *Col3a1*$^{+/-}$ tendons compared to WT at 6-weeks, with 1- and 3-week expression being similar. Directional changes from uninjured at 1- and 3-weeks were similar for both genotypes.

Markers of cell-ECM interactions followed similar patterns of expression in WT and Col3-deficient tendons, with the exception of GJA1, which is increased in expression in Col3-deficient tendons (**Fig. 3.2B**). Additionally, cell cycle markers showed alterations across time-points and within genotype. AXIN2 was back to uninjured levels by 6-weeks, and significantly upregulated from 1-week (**Fig. 3.2B**). This gene was continually decreased in *Col3a1*$^{+/-}$ tendons to 6-weeks. Additionally, PCNA was continually elevated at 3-weeks post-injury in Col3-deficient tendons, while WT tendon expression dropped from 1-week. Cell signaling genes were not different in expression patterns between WT and Col3-deficient tendons (**Fig. 3.2B**).

Evaluating markers of inflammation indicates an altered response in Col3-deficient tendons. Pro-inflammatory cytokines, IL-1β and IL-6, return to baseline in Col3-deficient tendons by 3-weeks post-injury but are continually upregulated in WT tendons (**Fig. 3.2C**). Anti-inflammatory cytokines, IL-10 and IL-13, are upregulated at 3-weeks in Col3-deficient tendons however are downregulated in WT through 6-weeks. Lastly, IL-33 downregulated in Col3-deficient tendons at 3-weeks post-injury compared to uninjured and WT expression.

Lastly, evaluating cell markers, Scleraxis (Scx) expression was decreased in 3- and 6-weeks *Col3a1*$^{+/-}$ tendons compared to WT and MPO was increased at 3-weeks in Col3-deficient tendons (**Fig. 3.2C**).

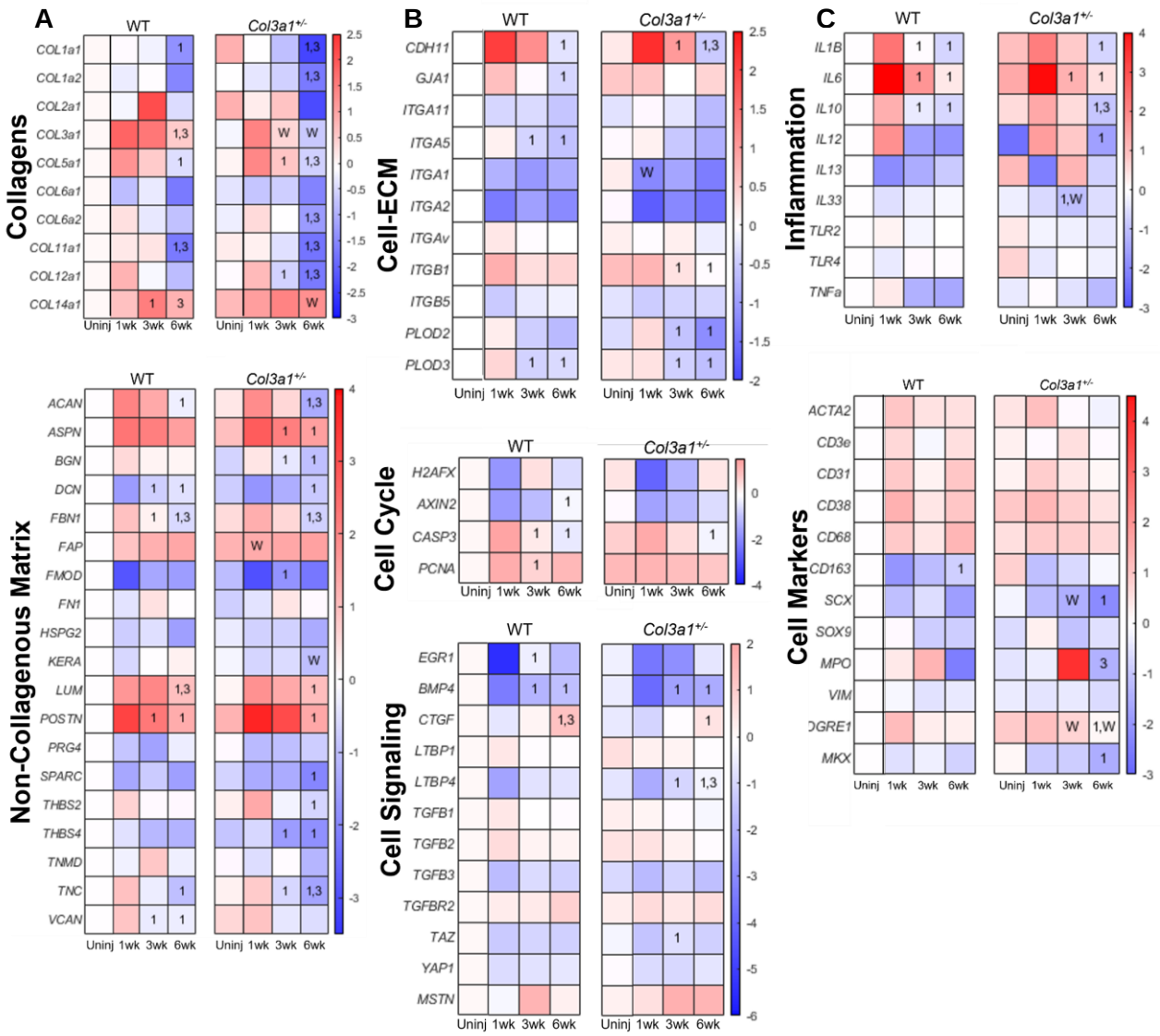

Figure 3.2: Gene Expression Heatmaps by Category
Heatmaps for each category were prepared using WT uninjured gene expression as the baseline level. 'W' indicates a significant difference from WT expression in Col3-deficient tendons. '1, 3' indicates a difference at 6-weeks from 1- and 3-week expression respectively, within genotype with significance set at p≤.05. n=3-4 samples/genotype/timepoint. **(A)** Collagens; Non-collagenous Matrix; **(B)** Cell-ECM; Cell Cycle; Cell Signaling **(C)** Inflammation; Cell Markers.

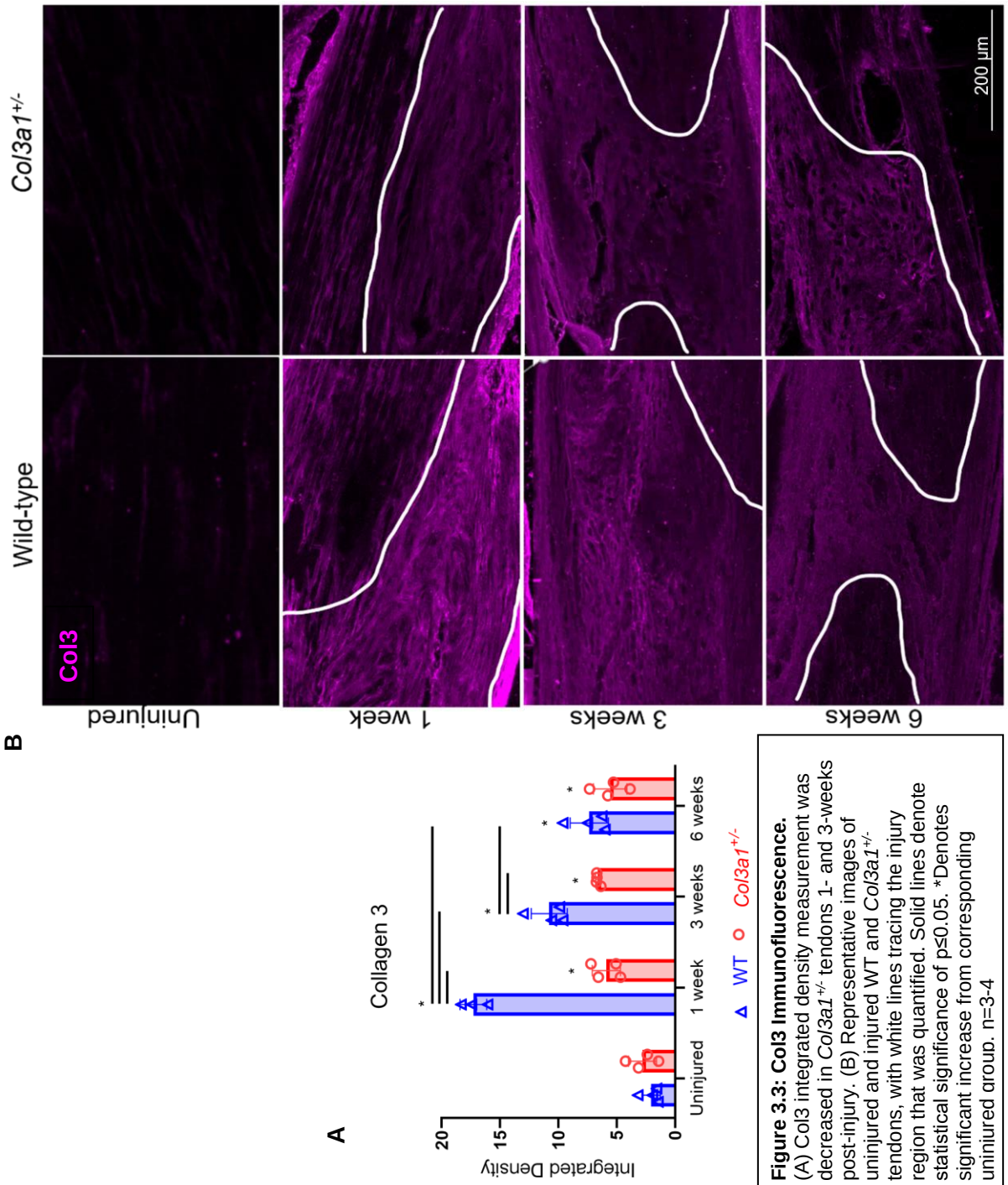

Figure 3.3: Col3 Immunofluorescence. (A) Col3 integrated density measurement was decreased in *Col3a1*$^{+/-}$ tendons 1- and 3-weeks post-injury. (B) Representative images of uninjured and injured WT and *Col3a1*$^{+/-}$ tendons, with white lines tracing the injury region that was quantified. Solid lines denote statistical significance of p≤0.05. *Denotes significant increase from corresponding uninjured group. n=3-4

3.3.2 Collagen III immunolabelling was decreased in Col3a1$^{+/-}$ tendons post-injury

Col3 integrated density increased at all timepoints post-injury in both genotypes (**Fig. 3.3**). In WT tendons, Col3 staining increased in the injury site of 1-week post-injury tendons compared to 3- and 6-weeks post-injury, and between 3- and 6-weeks post-injury separately. As

anticipated, Col3 immunolabelling was decreased at 1- and 3-weeks post-injury in Col3-deficient tendons compared to WT.

3.3.3 Collagen III deficiency resulted in increased αSMA activity post-injury at 3- and 6-weeks

Increased αSMA staining was seen post-injury at all time-points, in both genotypes when compared to uninjured tendons (**Fig. 3.4**). WT tendons did not differ between 1- and 3-weeks but were decreased closer to uninjured levels by 6-weeks post-injury. *Col3a1*$^{+/-}$ tendons had increasing integrated density measurements from 1- to 3-weeks post-injury, with a peak at 3-weeks. *Col3a1*$^{+/-}$ values were increased from WT values at both 3- and 6-weeks (trend).

3.3.4 Collagen III deficiency resulted in reduced iNOS positive signal at 1-week post-injury and an increase in CD206 positive signal at 6-weeks post-injury when evaluated qualitatively

Representative images (**Fig. 3.5**) staining for F4/80 (green), CD206 (red) and iNOS (magenta) indicate differing populations of macrophages within the injury site across genotypes. Qualitatively it appears that there is a larger population of iNOS positive cells within the injury site at 1-week post-injury in WT compared to *Col3a1*$^{+/-}$ tendons. Additionally, at 6-weeks post-injury there is increased CD206 staining in the injury site in *Col3a1*$^{+/-}$ tendons compared to WT.

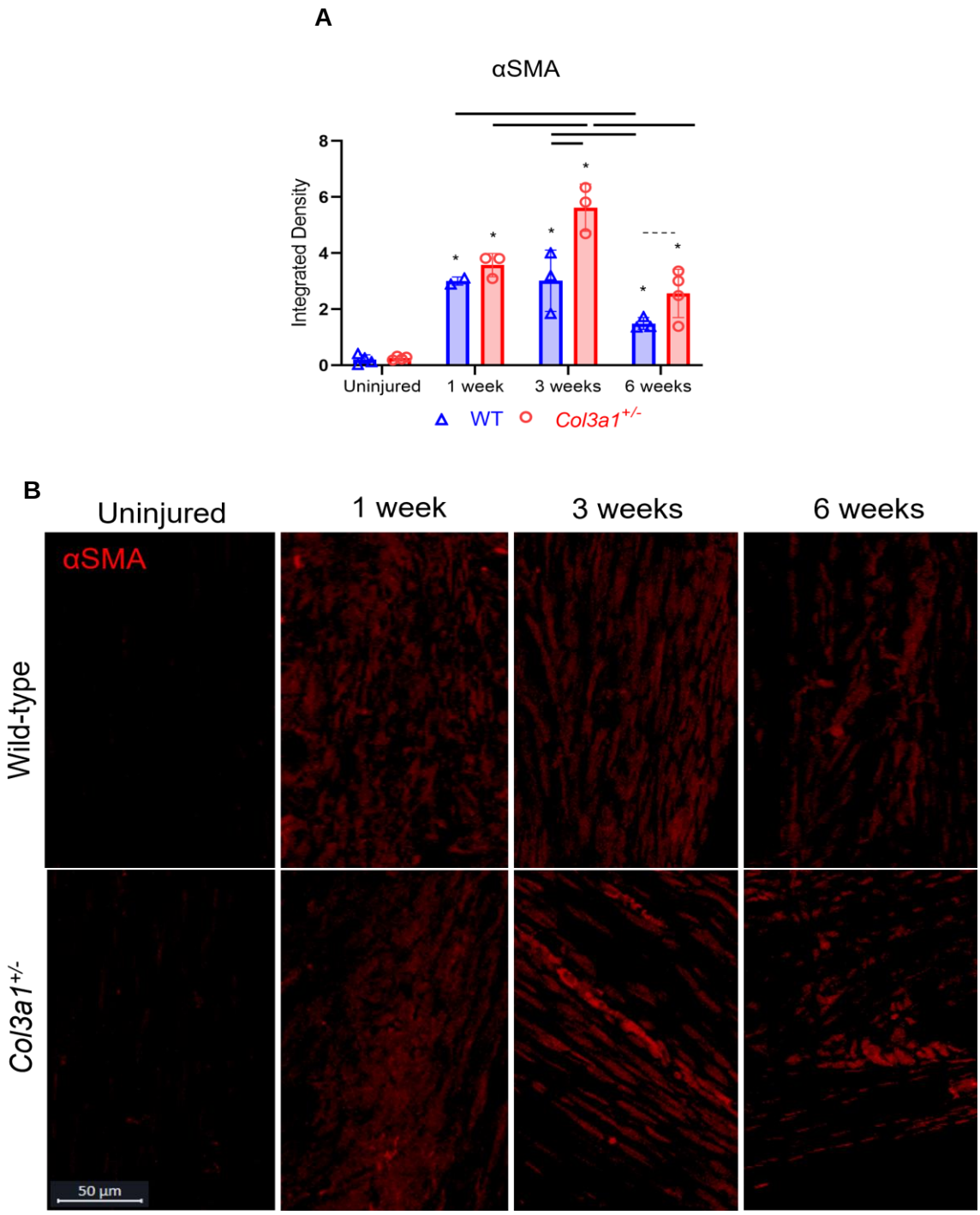

Figure 3.4: αSMA Immunofluorescence.
(A) αSMA integrated density measurement was increased in *Col3a1*$^{+/-}$ tendons 3- and 6-weeks (trend) post-injury compared to WT. (B) Representative images of uninjured and injured WT and *Col3a1*$^{+/-}$ tendons. Solid lines denote statistical significance of $p \leq 0.05$. *Denotes significant increase from corresponding uninjured group. n=3-4 samples/genotype/timepoint.

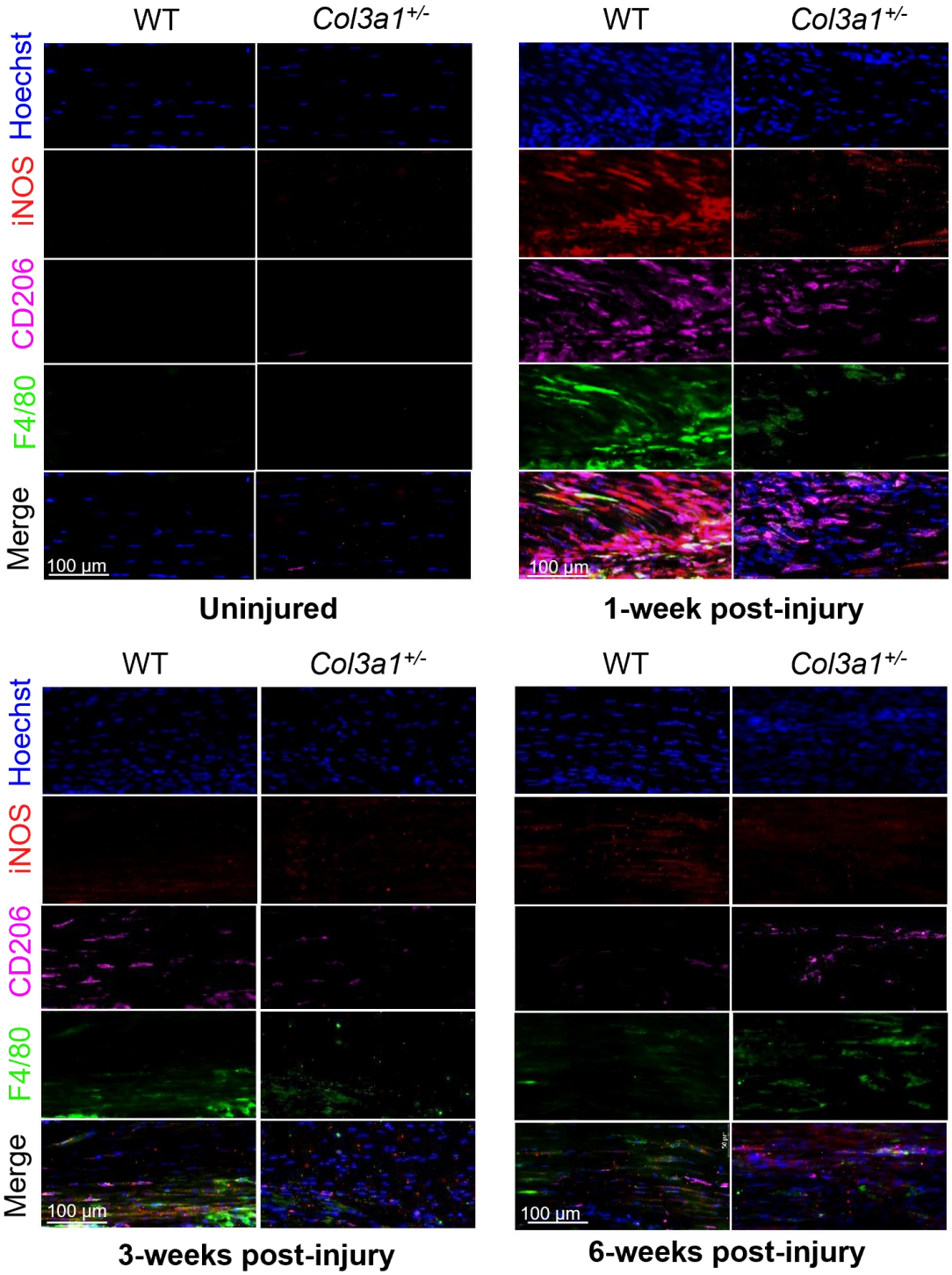

Figure 3.5: Representative images evaluating macrophage staining in the injury region or midsubstance (uninjured). iNOS (red) was evaluated as a marker of a pro-inflammatory phenotype, CD206 (pink) was considered an anti-inflammatory phenotype, and F4/80 (green) evaluated as a general macrophage marker. Col3-deficiency resulted in reduced iNOS positive staining at 1-week post-injury (B) and increased CD206 and F4/80 positive staining at 6-weeks post-injury (D) when evaluated qualitatively.

3.3.5 Collagen fiber alignment was increased in Col3a1$^{+/-}$ tendons compared to WT post-injury

An uninjured SHG image is shown separately as a lower laser power was needed avoid over exposure of the innately densely packed, highly aligned collagen fibers (**Fig. 3.6**). Utilizing SHG imaging (**Fig. 3.7**) we were able to quantify collagen fiber alignment post-injury.

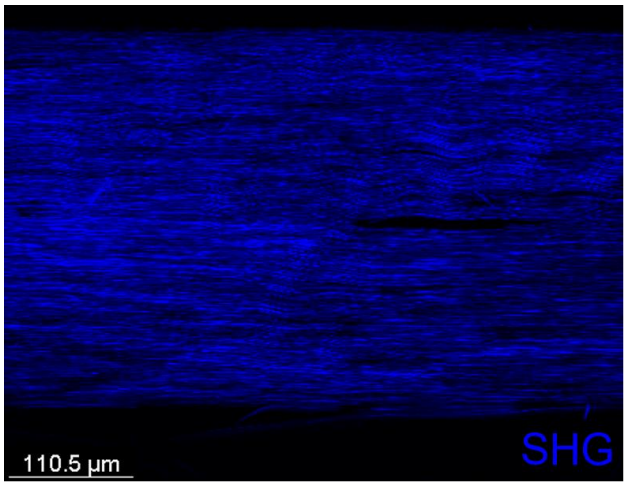

Figure 3.6: Uninjured SHG Representative Image.

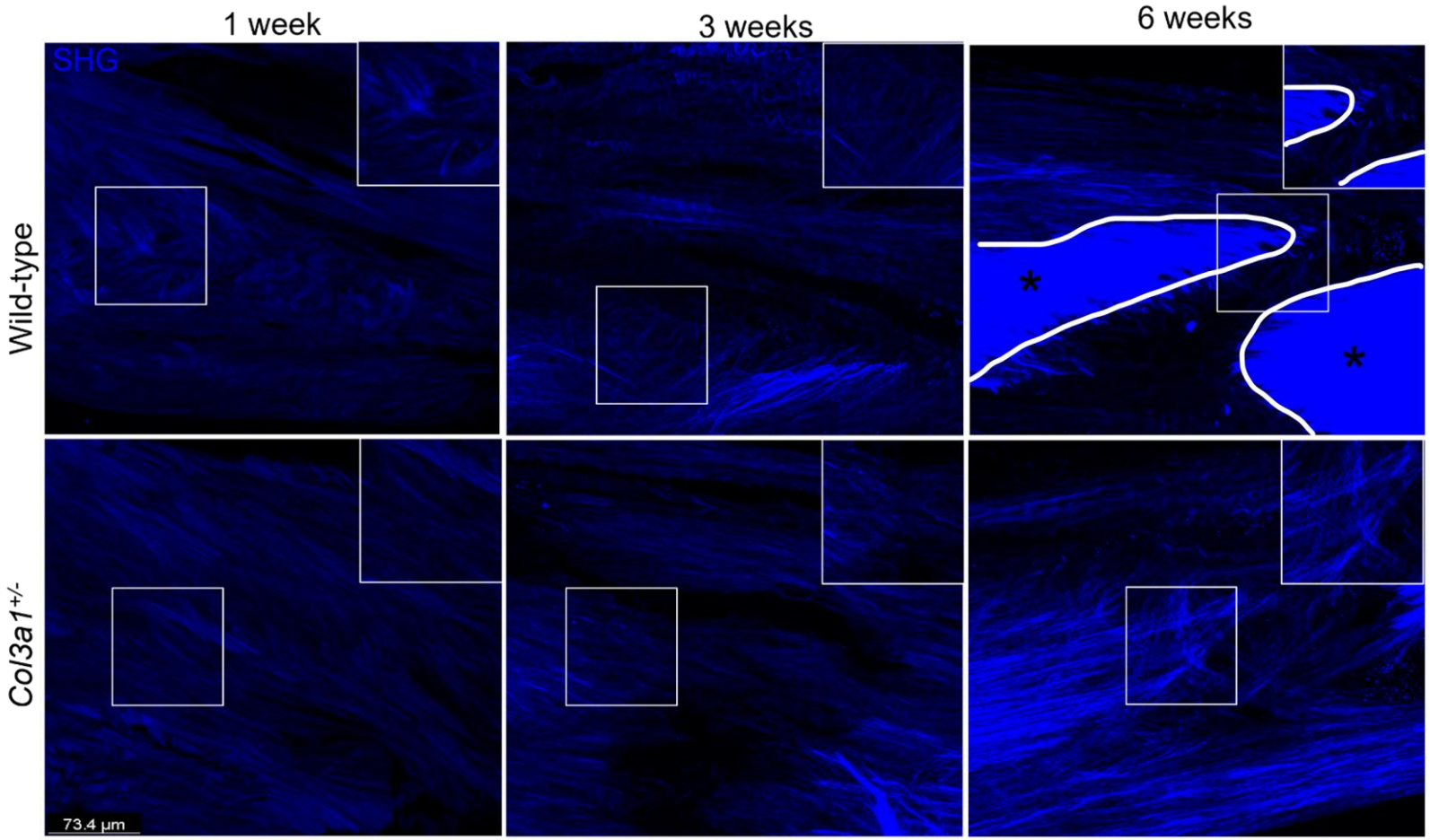

Figure 3.7: SHG Representative Images in injured Wild-type and Col3-deficient tendons. Alignment was increased in Col3-deficient tendons following injury. Entire images (except WT 6-week) were quantified, with insets to show higher magnification of representative areas. White lines and * denote excluded area in the WT 6-week image.

Utilizing Fast Fourier Transform analysis, we saw that alignment decreased at all timepoints post-injury in both genotypes (**Fig. 3.8A**). In WT tendons, alignment increased from 1- to 3- and 6- weeks, however *Col3a1*$^{+/-}$ tendons only increased in alignment at 6w post-injury. Additionally, by 6w post-injury *Col3a1*$^{+/-}$ tendons were more highly aligned. Another measure of alignment was calculated using OrientationJ (ImageJ) to calculate the fiber angle distribution and evaluate the number of fibers within 15° of the modal angle. Both genotypes had less fibers within 15° of the modal angle at all timepoints following injury (**Fig. 3.8B**). *Col3a1*$^{+/-}$ tendons had a greater number of aligned fibers at 1- and 6-weeks post-injury when compared to WT (p=.127 at 3-weeks). Despite alignment changes, no other structural changes were seen. Fiber width, length and straightness were not affected across injury timepoints or between genotypes (**Fig. 3.9**).

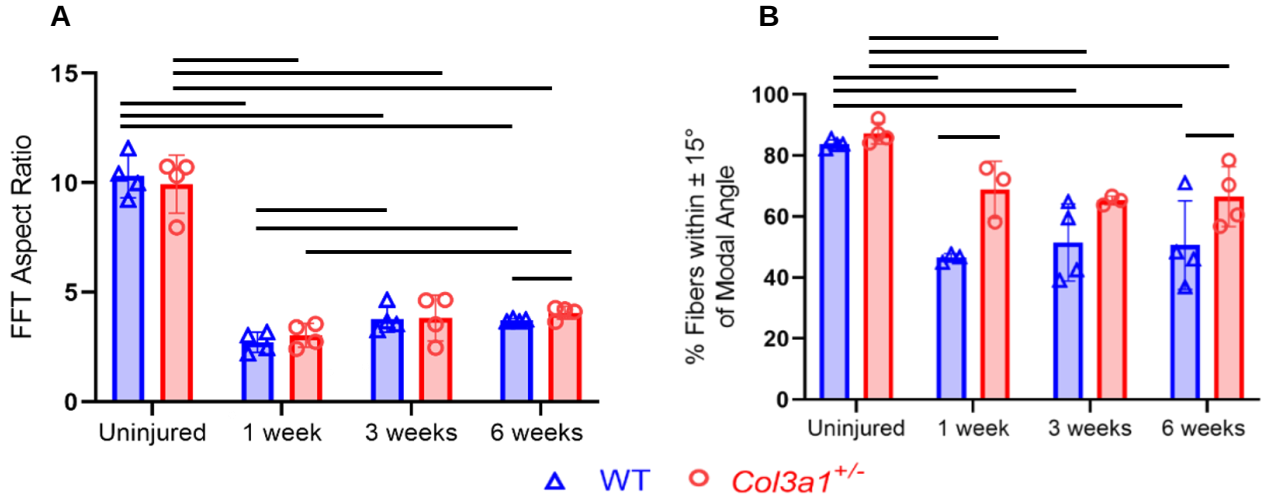

Figure 3.8: Alignment Measurements
(A) FFT aspect ratio was increased at 6w post-injury in *Col3a1*$^{+/-}$ tendons. (B) A greater number of fibers were within 15°of the modal angle at 1- and 6w in *Col3a1*$^{+/-}$ tendons. Solid lines denote statistical significance of p≤0.05. n=3-4 samples/genotype/timepoint.

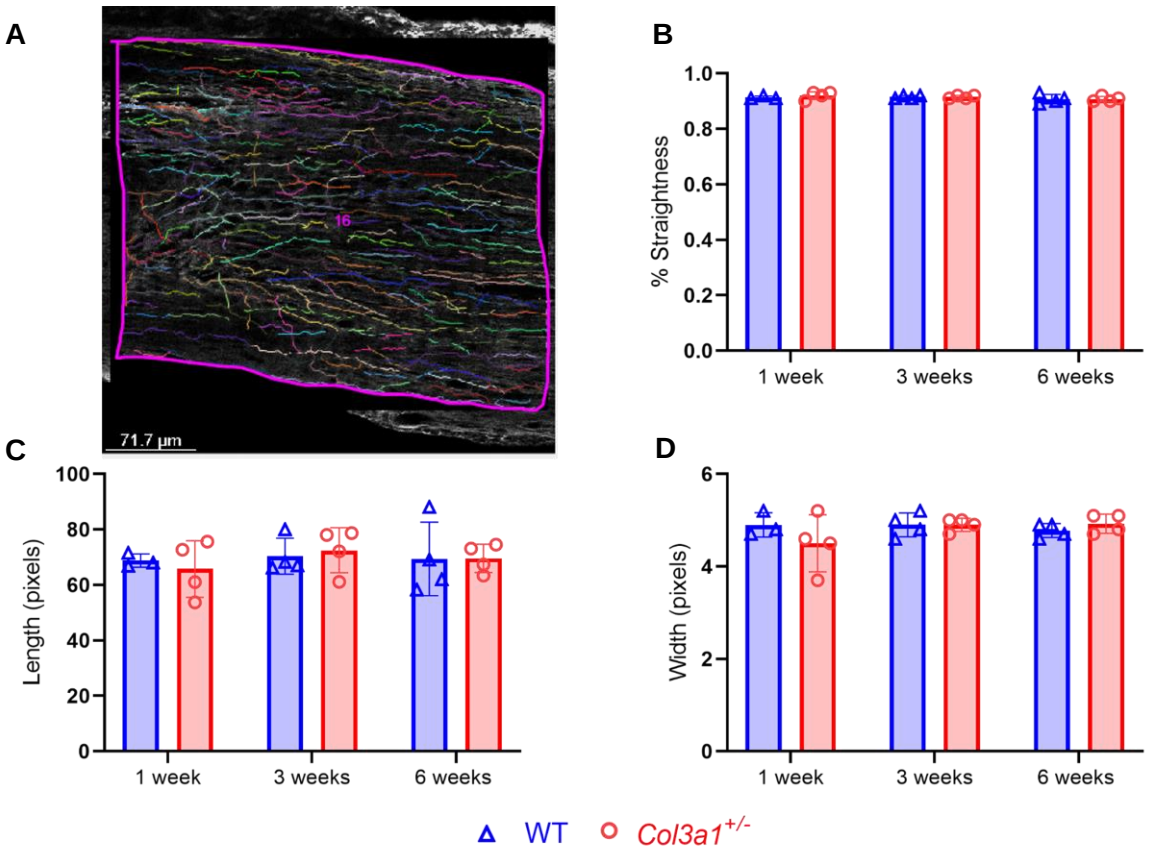

Figure 3.9: CT Fire Analysis
(A) CT Fire example analysis with overlaid analyzed fibers on an image acquired from SHG imaging. (B-D) Fiber straightness, width and length were not different between genotypes or across injury time-points. Significance was set at p≤0.05. n=3-4 samples/genotype/timepoint.

3.3.6 Quasistatic mechanical properties were increased in Col3-deficient tendons compared to WT, with no decreases from uninjured levels post-injury

Structural and material properties of *Col3a1*$^{+/-}$ tendons were increased from WT tendons post-injury. WT tendons cross-sectional area increased from uninjured and a trending increase from 1- to 3-weeks post-injury (**Fig. 3.10A**) with return to uninjured measurement by 6-weeks post-injury. No elongation was seen in either genotype post-injury (**Fig. 3.10B**).

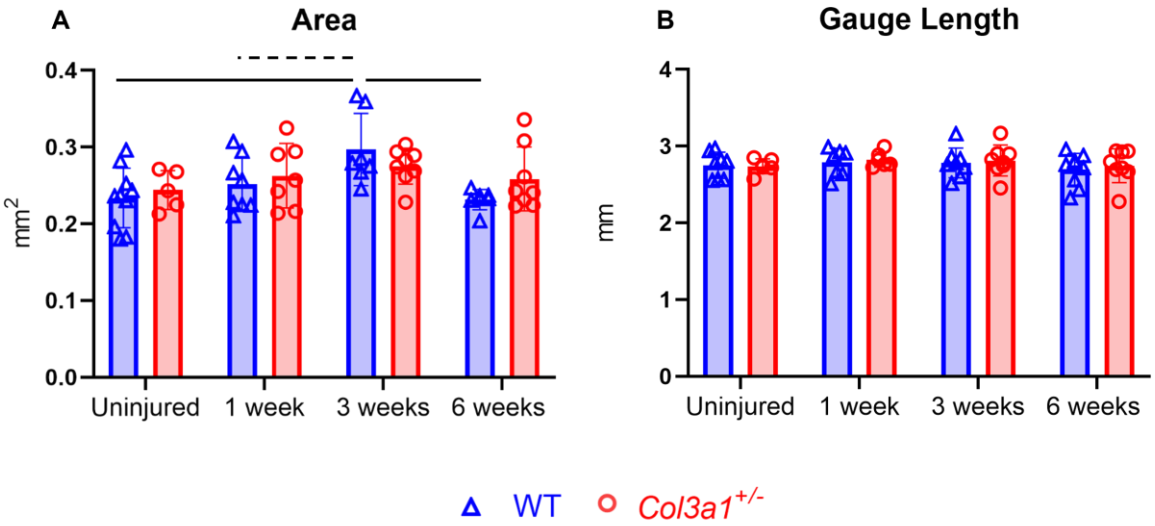

Figure 3.10: Tendon Cross-Sectional Area and Gauge Length
(A) Area increased post-injury in WT tendons with no changes in *Col3a1*$^{+/-}$ tendons. (B) Gauge length did not change post-injury in either genotype. Solid line denotes significance of p≤0.05 and dotted line denotes a trend of p≤0.10. n=7-10 tendons/genotype/timepoint.

Uninjured WT tendons had increased failure stress and modulus compared to *Col3a1*$^{+/-}$ tendons, with no changes in load or stiffness (**Fig. 3.11**). Following injury, failure load was decreased in *Col3a1*$^{+/-}$ tendons 3-weeks post-injury (**Fig. 3.11A**), and *Col3a1*$^{+/-}$ tendons had increased stiffness, failure stress and modulus at both 1- and 3-weeks (**Fig. 3.11B-D**). WT tendon stress, stiffness and modulus decreased 1-week post-injury, with continued decrease from uninjured levels at 3-weeks post-injury in stress and modulus (**Fig. 3.11B-D**). Load, stress, stiffness and modulus all increased from 1- and 3-weeks to 6-weeks post-injury back to

uninjured levels in WT tendons. *Col3a1*$^{+/-}$ tendons did not change post-injury in quasistatic properties.

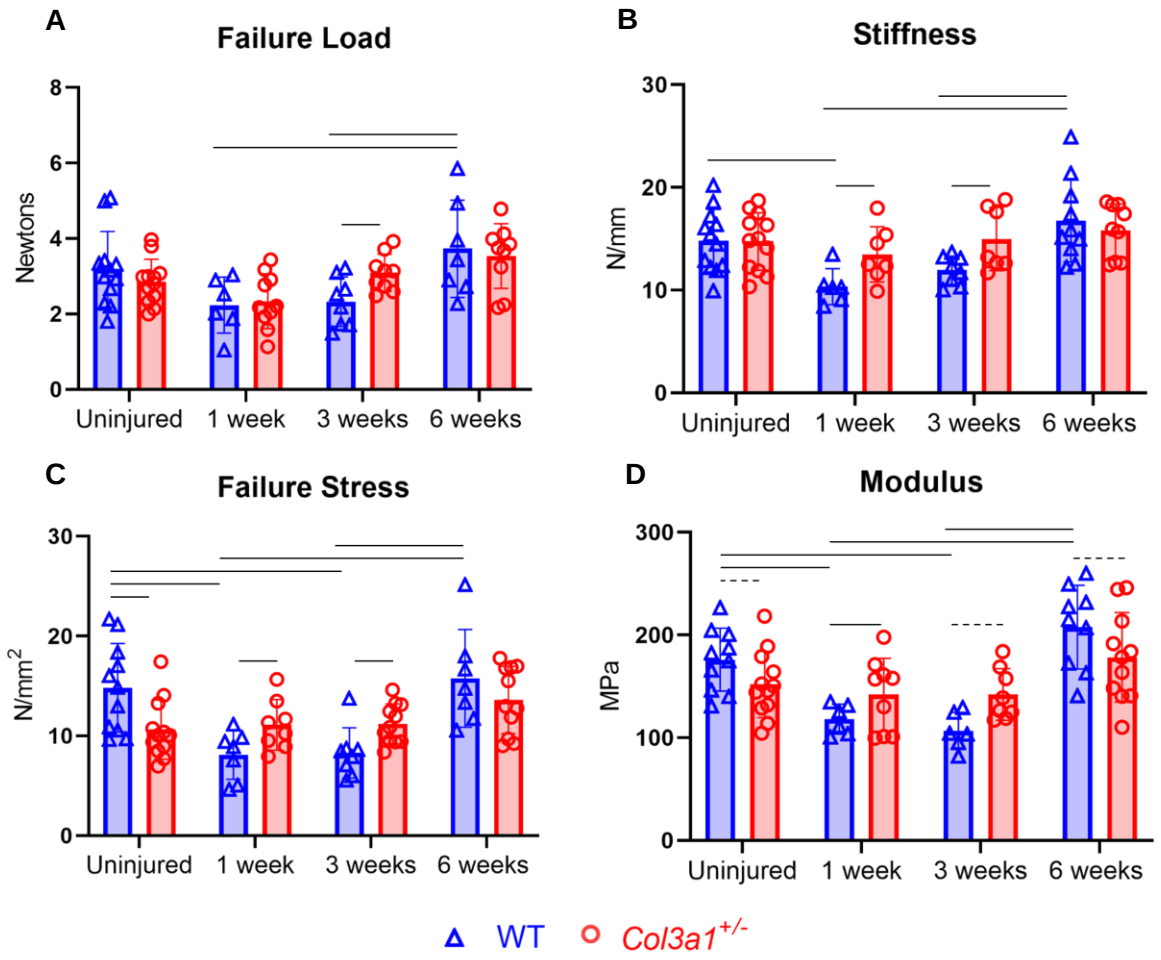

Figure 3.11: Tendon Material and Structural Properties
Changes in quasistatic mechanical properties differ post-injury between genotypes. (A) Failure load was increased at 3-weeks post-injury in Col3-deficient tendons. (B-D) Stiffness, stress and modulus were increased post-injury in Col3-deficient tendons at both 1- and 3-weeks post-injury (trend at 3-weeks in modulus). (A-D) WT properties decreased post-injury but returned to uninjured levels by 6-weeks, while Col3-deficient tendon mechanical properties were unaffected by injury. Solid line denotes significance of $p \leq 0.05$ and dotted line denotes a trend of $p \leq 0.10$. n=7-10 tendons/genotype/timepoint.

3.7 Viscoelastic mechanical properties were unaffected by injury in Col3-deficient tendons

Tendons did not differ between genotypes or across injury timepoints in viscoelastic properties at 3% strain (**Fig. 3.12A; 3.13A,C**). Percent relaxation did not differ between

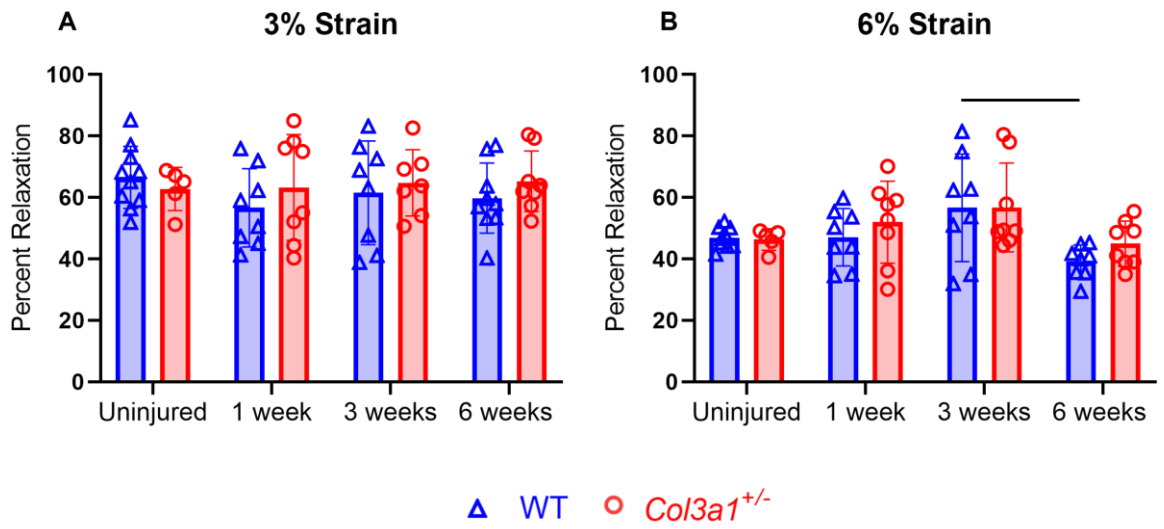

Figure 3.12: Stress Relaxation
Stress relaxation did not differ between genotypes at 3% or 6% strain levels.(B) Stress relaxation decreases between 3- and 6-w in WT tendons. Solid line denotes significance of p≤0.05. n=7-10 tendons/genotype/timepoint.

genotypes in uninjured or injured tendons (**Fig. 3.12**). Overall, differences post-injury were not seen, except a decrease from 3- to 6-weeks in percent relaxation of WT tendons at 6% strain.

When evaluating dynamic modulus, WT values decreased at 6% strain at 1w and further at 3-weeks, before rebounding by 6-weeks to uninjured levels (**Fig. 3.13B**). *Col3a1*$^{+/-}$ animals had less of an effect following injury than WT in dynamic modulus at 6% strain. *Col3a1*$^{+/-}$ values did also decrease following injury, before increasing at 6-weeks post-injury. However, while the pattern was similar to WT, the decreases were not significantly different from uninjured levels.

Lastly, no differences were seen in tanδ except a decrease from 3- to 6-weeks post-injury in *Col3a1*$^{+/-}$ tendons at 0.1Hz (**Fig. 3.13D**).

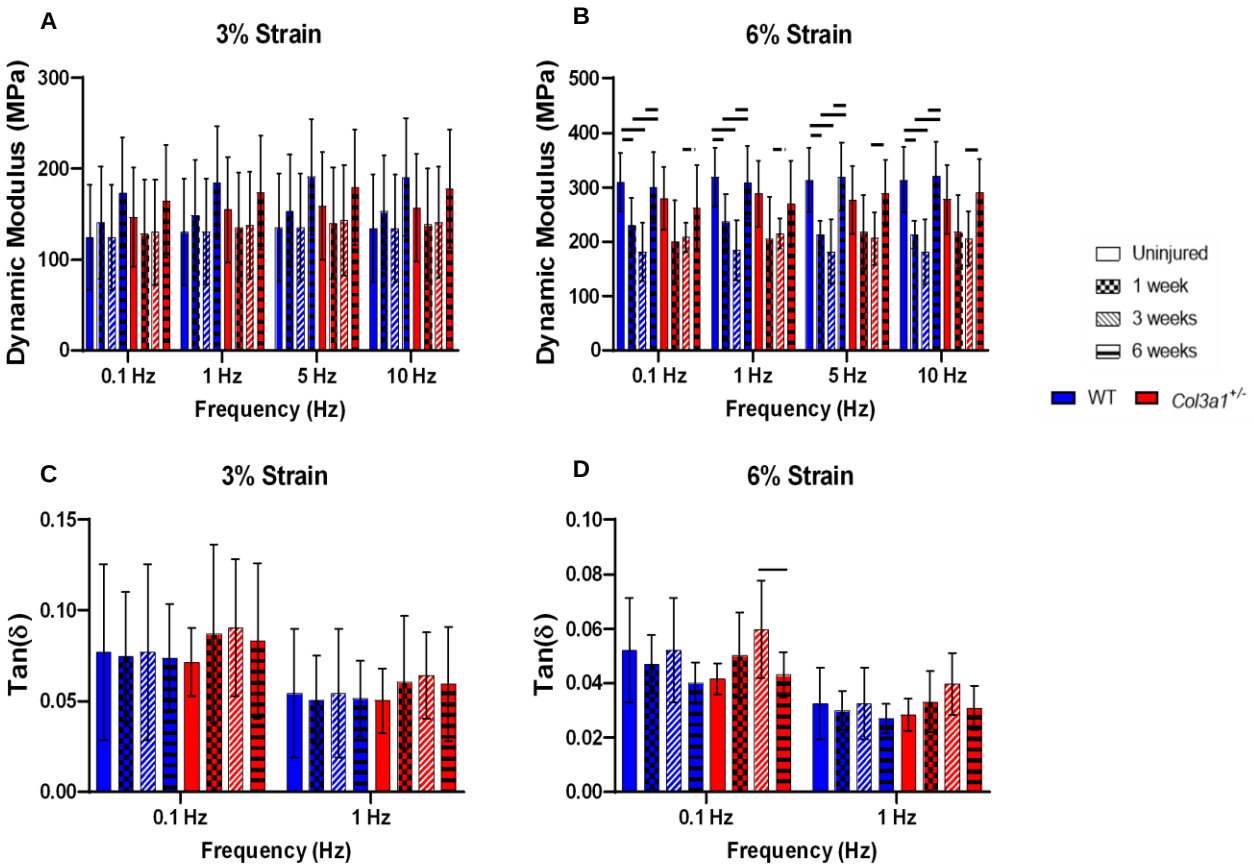

Figure 3.13: Dynamic Modulus and Tan Delta. WT tendons had reduced dynamic modulus values at 6% strain post-injury, and Col3-deficient tendons were unaffected by injury in both dynamic modulus and tanδ. Solid lines denotes significance of p≤0.05. n=7-10 tendons/genotype/timepoint.

3.3.8 Col3-deficient tendons had faster and more drastic collagen fiber realignment in response to load than WT tendons

Post- injury, *Col3a1*$^{+/-}$ tendons realigned faster than WT tendons and to a greater degree at both 1- and 6-weeks (**Fig. 3.14B,D**). No differences were seen in realignment in uninjured tendons (**Fig. 3.14A**). At 3-weeks post-injury, WT tendons realigned through 3% strain to a greater degree than *Col3a1*$^{+/-}$ tendons(**Fig. 3.14C**).

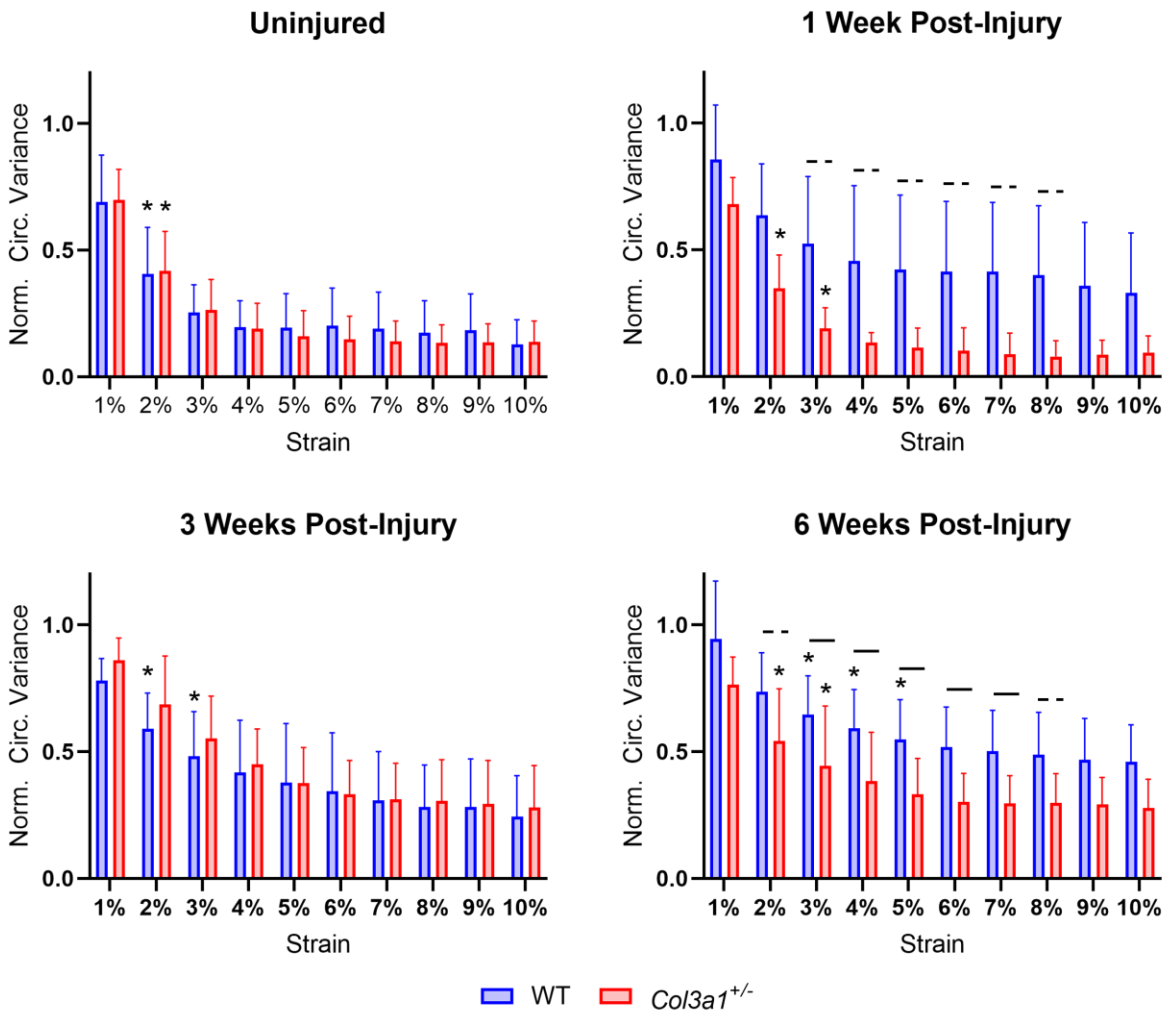

Figure 3.14: Collagen Fiber Realignment
Col3-deficient tendons realigned fasted and to a greater extent than WT tendons at 1- and 6-weeks post-injury. Solid line denotes significance of p≤0.05 and dotted line denotes a trend of p≤0.10. * denotes significant difference from the prior strain level. n=7-10 tendons/genotype/timepoint.

3.4 – Discussion

While the composition of healthy tendon is primarily Col1, Col3 is a main component of the open weave provisional matrix following injury.[5] In skin, a reduction in Col3 decreased the amount of granulation tissue post-injury, increased activation and contraction of myofibroblasts, and ultimately resulted in increased scar tissue deposition,[1] highlighting the importance of Col3 deposition early post-injury and resultant effects on the healing environment. The current study evaluated how Col3 expression alters injured matrix composition and organization and affects tendon mechanical and structural properties.

Col3 gene expression was decreased in *Col3a1*$^{+/-}$ tendons at 1- and 3-weeks post-injury, indicating dampened elevation in Col3 expression early post-injury. Col3 deposition was decreased at early healing time points, but the absolute difference between staining intensity measurements reduced with healing, likely as remodeling occurred and the matrix transitioned to a higher proportion of Col1:Col3 ratio. By 6-weeks post-injury, Col3 staining was not significantly decreased from WT ($p<.15$), which potentially explains the lack of mechanical differences seen at this time-point. Col3 expression in *Col3a1*$^{+/-}$ tendons returned to uninjured levels by 3-weeks post-injury, while prolonged elevated expression was seen in WT. This data supports the hypothesis that altered Col3 gene expression and corresponding matrix deposition post-injury in *Col3a1*$^{+/-}$ tendons results in changes in tendon functional properties. In this study, these changes were more pronounced at 1- and 3-weeks post-injury, and both genotypes returned to respective uninjured levels by 6-weeks post-injury. Due to *Col3a1*$^{-/-}$ mice being perinatally lethal, an inherent limitation of this mouse model, we were not surprised by these results.

While uninjured *Col3a1*$^{+/-}$ tendons only show a trending decrease in Col3 gene expression and no differences in Col3 localization or collagen alignment, failure stress and modulus were increased in WT compared to *Col3a1*$^{+/-}$ tendons. Alignment was no different in uninjured tendons, placing importance on structure not solely organization and composition. This indicates an effect

of decreased *Col3a1* expression on matrix development, homeostasis and structure, potentially through dysregulation of fibrillogenesis with Col3 deficiency, and poorer quality tissue in *Col3a1*$^{+/-}$ tendons. This is supported by previous work examining the relationship between fibril structure and tissue integrity in tendon.[23] High levels of *Col3a1* expression early in tendon development indicate a potential role in initial fibril assembly.[24] Other studies have shown that ECM architecture, organization, and stiffness regulate cellular proliferation and migration indicating that a Col3-rich matrix may influence tendon development and its healing environment,[6,25] placing emphasis on other characteristics not solely organization. Additionally, previous studies indicate that Scleraxis positive cells play a necessary role in initial wound deposition post-injury,[6] providing a potential mechanism for decreased tissue quality post-injury in Col3-deficient tendons and predicting the negative outcomes in long-term healing. Therefore, the abundance of Col3 in matrix will ultimately affect the structural and functional properties, due to physical differences in the matrix as well as alterations to compositional properties of the tendon. Additional support of this idea is that despite increased alignment at 6-weeks in *Col3a1*$^{+/-}$ tendons, mechanical properties are similar to uninjured levels, with no differences between genotypes, or slightly elevated WT value (modulus $p<0.1$). However, we would expect that increased alignment in Col3-deficient tendons compared to WT would lead to increases in mechanical properties. Therefore, no genotypic differences indicate that organization is unable to fully compensate for alterations in composition and structure in terms of mechanical properties. High retear rates seen clinically may be attributed to the decreased alignment seen in WT tendons, so while although mechanical properties returned to uninjured levels, the organization is not the same and therefore, repetitive loading may weaken the tissue overtime and lead to retears. Accumulating microdamage will affect long term functionality and mechanical behavior, as is seen in chronic tendinopathy overuse models. It is not surprising that composition and architecture play a large role in tendon functional properties, due to the nature of fibril engagement, cell-matrix interactions and resultant

mechanotransduction.[26] Fibril diameter distributions will be discussed in Chapter 4 and additionally support this notion. While increased alignment overtime leads to improved mechanical properties, this cannot explain all of the differences seen. As mentioned above, although mechanical properties have recovered to uninjured levels by 6-weeks post-injury in both genotypes, alignment of the matrix does not approach uninjured levels by 6-weeks in either measure. This indicates persistent scar tissue at this timepoint, as is evidenced in the clinic by high re-tear rates and reduced range of motion and functionality. However, alignment is naturally an important measure of tendon healing due to the characteristic highly aligned matrix of uninjured tendon. Further understanding these interactions will allow us to modulate the effects of Col3 on the matrix and cellular environment to optimize tendon healing and recovery post-injury.

Both FFT aspect ratio and fiber orientation analysis showed increased alignment in *Col3a1*$^{+/-}$ versus WT tendons post-injury. While not the only factor, there is evidence that increased alignment,[16,27] as well as altered fibrillogenesis,[20,23,28,29] likely contribute to increased mechanical properties, as was supported by this study. The lack of a decrease in mechanical properties post-injury in *Col3a1*$^{+/-}$ tendons is interesting although not surprising, due to the interconnected role of Col3 in dictating collagen-crosslinking, matrix alignment and fibroblast activation, and the use of a Haploinsufficient model versus a Null model. Although other studies have shown that in meniscus and cartilage,[2] disruption of matrix structure outweighs the fibril stiffening impacts, in our work we are seeing an opposite effect. This highlights the multifaceted role of Col3 and its unique contributions to various soft tissues. However, solely the preservation of quasistatic mechanical properties does not indicate better tissue quality or long-term healing outcomes. Although increased activation of myofibroblasts was also seen, potentially contributing to increased stiffness and contraction of the matrix, it has been shown that it is the density of myofibroblasts that contributes to improved tendon healing, not solely activation.[30] Therefore,

increased activation of myofibroblasts does not indicate that tissue quality is improved, even with increases in mechanical properties.

Work in both tendon[5,31] and skin[32] has shown that disrupted provisional matrix during the inflammatory phase affects cellular migration, and leads to an altered proliferative stage, with cell populations being affected. A transient inflammatory phase is known to be crucial for proper tendon healing,[5] and increased alignment and greater populations of larger diameter fibrils likely negatively impacts vulnerary cell infiltration in Col3-deficient tendons. This will disrupt the overall remodeling process later in healing. Therefore, although quasistatic mechanical properties are increased in Col3-defcient tendons compared to WT early in healing, later time-points are needed to examine remodeling effectiveness of the altered provisional matrix in order to parse out how an altered inflammatory and proliferative phase would affect long-term healing, and specifically if Col3 regulates healing. To further elucidate how matrix architecture evolves during tendon healing, we attempted to evaluate matrix structure utilizing CT Fire analysis for fiber width, length and straightness, however we did not see any differences in these parameters. We did see a reduced number of fibers analyzed (data not shown) between 1-week and 6-weeks post-injury, but this was likely due to the injury site decreasing over time, as the measurements were unable to be normalized for area.

In order to examine matrix engagement, we evaluated collagen realignment when tendons underwent a ramp-to-failure at a rate of 0.1% strain/sec. *Col3a1*$^{+/-}$ tendons realigned faster and to a greater degree 1- and 6-weeks post-injury than WT tendons. While material and structural properties do not differ at 6-weeks post-injury, collagen realignment is faster in *Col3a1*$^{+/-}$ compared to WT tendons at this timepoint. Increased alignment in these tendons allows for faster collagen fiber engagement when the tissue is loaded.[16] At a more micro-level, faster fiber realignment under loading conditions is likely correlated with increase inter-fibrillar interactions and matrix engagement. Unfortunately, we were unable to examine injured tendons utilizing AFM

to prove or disprove this assumption. Evaluating immunolabelling showed that while Col3 deposition is not different at 6-weeks post-injury, the matrix has begun remodeling and organizing into a more highly aligned matrix. This is likely due to increased myofibroblast activation. At 1-week, the mechanism is expected to be different, and due to the decreased amount of Col3 deposited at 1-week, leading to an increased proportion of more highly aligned Col1, and therefore the enhanced ability of fiber engagement and faster realignment under load. We expected that since fibers are more aligned at 1-week post-injury, they are easier to recruit when bearing load, and additionally, the matrix is potentially less dense with less overall fibers to recruit in *Col3a1*$^{+/-}$ tendons. Previous work in skin has shown decreased granulation tissue in the early healing phase,[1] yet in tendon, an increase in stiffness, stress and modulus at this timepoint is still seen. Potentially indicating that alignment, organization and quality of the matrix is more important than the amount of deposited matrix when evaluating mechanical properties in early healing. Additionally, stiffer fibers realign faster,[33] further supporting increases in quasistatic mechanical properties. At 3-weeks, while the tendons are stiffer, with higher failure loads, realignment is more gradual with load. In the toe region, WT tendons realign faster, with similar rates between genotypes once in the linear region. No differences in alignment are seen, potentially indicating a switch to importance of the architecture of the matrix over alignment, as was indicated in other soft tissues,[2] and highlighting a temporal response of Col3 to tendon healing. Matrix quality is not necessarily improved, but a shift to larger fibrils is likely, due to the impact of Col3 on fibrillogenesis. Previous work studying fibrillogenesis during development indicates that following fibril intermediate assembly, lateral and longitudinal growth occurs.[34] As fibrillogenesis progresses from early tendon into the proliferative phase, it is likely that lateral growth is ramping up around 3-weeks. More explanation surrounding fibril diameter distributions will be provided in Chapter 4. Even with an increase in matrix deposition in WT tendons compared to *Col3a1*$^{+/-}$ tendons, as is seen in increased cross-sectional area measurements, *Col3a1*$^{+/-}$ tendons still had increased

quasistatic properties at this time-point. This further supports findings from 1-week, which indicated that the amount of matrix deposited is not solely important for functional outcomes. However, this time-point indicates that alignment and matrix engagement may not play as much of a role in mechanical properties compared to composition and architecture. This conclusion supports the earlier statement that at 6-weeks post-injury, the importance of matrix architecture and quality may outweigh the importance of alignment, as despite increased alignment in *Col3a1*$^{+/-}$ tendons, mechanical properties do not differ.

Cross-linking analysis will be very important in a future study to further understand matrix engagement and fibril-fibril interactions, and how structure relates to function of the tendon and remodeling capability.[35] Matrix engagement and resultant realignment of collagen fibers with loading is potentially faster with more crosslinking, and there may also be more realignment overall due to molecular interactions within the matrix.[35] By realigning earlier, the fibers may have stiffer material properties at increasing strain levels.[36] There is also evidence that fibronectin is crucial for efficient load transferring between fibrils.[37] This could be a partial mechanism to explain faster and greater extent of realignment in *Col3a1*$^{+/-}$ tendons, due to increased fibronectin expression at 3-weeks compared to WT tendons, with downstream effects being seen at 6-week post-injury in realignment analysis. Additionally, increased connexin 43 may contribute to the enhanced ability of Col3-deficient tendons to respond to load[41].

Organization of the matrix plays a crucial role in viscoelastic properties, as the highly aligned collagen matrix contributes to the tendon's inherent viscoelastic properties.[38] Similar to quasistatic mechanical properties, WT dynamic modulus decreases post-injury, but more highly aligned *Col3a1*$^{+/-}$ tendons are unaffected by injury in viscoelastic properties. Complementary decreases in modulus and dynamic modulus at 1-week post injury in WT tendons may also be caused by increased in elasticity follow injury, due to the disorganized provisional matrix filling in the injury void and replacing the highly aligned uninjured matrix. This may explain the lack of a

decrease in these measures in *Col3a1*$^{+/-}$ tendons, as the matrix was shown to be more aligned when compared to WT. Stress relaxation, dynamic modulus and tanδ are no different between genotypes or across timepoints at 3% strain. As 3% strain is very early in the linear region, continued fiber engagement and variable uncrimping at this point in the loading curve may mask any potential differences in properties. Dynamic modulus increases from 3% to 6% strain, with corresponding decreases in tanδ as the tendon is strained.

Evaluating gene expression by category helped us to understand broadly the directional changes in related genes with Col3 deficiency. Overall patterns of expression were similar between genotypes, with a few clusters of genes that require explanation.

Cell cycle markers were particularly interesting, with an increased marker for proliferation (PCNA) seen in uninjured Col3-deficient tendons when compared to WT. This is consistent with previous work indicating increased proliferation with knockdown of Col3.[39] WNT signaling regulates cell fate determination, cell migration, and polarity, and is inhibited by Axin expression, which was downregulated in both genotypes following injury. This indicates that increased cellular activity post-injury would be expected during tendon healing. As PCNA was only minimally increased in Col3-deficient tendons post-injury, even with the baseline increased, this likely cannot compensate post-injury and may explain the reduction in open weave matrix deposited early post-injury in Col3-deficient tendons. Additionally, H2AFX expression promotes cell survival, and was downregulated early post-injury in *Col3a1*$^{+/-}$ tendons, and to a lesser degree in WT tendons 1-week post-injury but upregulated by 3-weeks post-injury. The expression of this subset of genes indicates cell cycle dysregulation in Col3-deficient tendons.

Decreases in cell marker gene expression further supports dysregulation of the cell cycle in *Col3a1*$^{+/-}$ tendons. In general, markers are upregulated to a greater degree in WT tendons from uninjured levels, with the exception of MPO expression at 3-weeks in *Col3a1*$^{+/-}$ tendons. MPO is a marker of inflammation and immune cell populations, including neutrophils,

monocytes and macrophages, and will need to be explored further as this spike is very drastic and may indicate high levels of immune cell activity at 3-weeks in *Col3a1*$^{+/-}$ tendons, which would be surprisingly since by this point in the healing process we would expect the inflammatory response to be declining. In contrast to the increased expression of MPO at 3-weeks, overall inflammatory markers didn't increase in expression in *Col3a1*$^{+/-}$ tendons to the same level as WT tendon expression, indicating dysregulation in the inflammatory response in *Col3a1*$^{+/-}$ tendons. This supports our hypothesis that with stiffer, more highly aligned provisional matrix, the inflammatory response would be dampened and result in long-term healing deficits. Immunofluorescence staining for macrophages also supports this data, which qualitatively showed differing populations of macrophages in the injury site across genotypes. In order to fully understand the inflammatory response, it is necessary to look at other markers, however, these results do indicate a dampened pro-inflammatory environment at 1-week post-injury in *Col3a1*$^{+/-}$ tendons, indicated by increased iNOS positive staining in WT tendons. Additionally, *Col3a1*$^{+/-}$ tendons shifted to a more robust anti-inflammatory response at 6-weeks indicated by increased CD206 positive staining. Further characterizing this population of macrophages will be crucial to better understanding the role of Col3 in inflammation in tendon healing.

Collagen and non-collagenous matrix gene expression was generally decreased in *Col3a1*$^{+/-}$ tendons, indicating decreased deposition of matrix post-injury. Decreased decorin, biglycan, and aggrecan during remodeling may predict poorer tissue quality long term with Col3 deficiency. Specifically, decorin and biglycan have previously been shown to increase elasticity of tissue, which may play a role in Col3-deficient tendons exhibiting increasing stiffness with decreased levels of these proteoglycans. Other proteoglycans may increase tissue contractility, and likely contribute to overall tissue remodeling, cell-ECM communication, fibrillogenesis regulation and matrix organization.[42] Further examination of proteoglycans is indicated utilizing

proteomics and immunohistochemistry to elucidate functional effects of altered expression with Col3-deficiency.

Interestingly, at 1-week post-injury, integrin-α11 was directionally increased in Col3-deficient tendons, while decreased in WT tendons. This is a potential mechanism for increased stiffness, stress and modulus at 1-week post-injury in Col3-deficient tendons compared to WT, as increased integrin expression may indicate increased matrix engagement, wound contraction and strength.[40]

Overall, changes in multiple parameters and at multiple timepoints in our mechanical testing data indicate that these differences are more impactful than solely seeing changes in one measure or timepoint. 3-weeks post-injury seems to be an important timepoint overall with the data shown. This could be due to the inherent nature of the healing process. At 1-week, there is less matrix overall, and by 6-weeks, remodeling is well underway. 3-weeks is an intermediate stage where remodeling is beginning, but the proliferative phase is still active, and cellular activity is high. This timepoint needs to be evaluated more closely in the future.

Increased alignment overall potentially preserves the quasistatic and viscoelastic mechanical properties, explaining why Col3-deficient tendons were unaffected by injury in these parameters. Early in healing, increased alignment in Col3-deficient tendons may contribute to increased realignment under load and result in increased modulus, stress and stiffness in these tendons compared to WT. Increased alignment is likely dampening the immune response, and while preventing an exuberant inflammatory response may be favorable early in healing, this may contribute to poorer outcomes long-term. At 1-week post-injury, organization of matrix is very important, potentially due to the poor quality of the provisional matrix that is deposited at this time.

Three weeks post-injury there is still activity from the proliferative phase, but also remodeling activity, making this a complex timepoint. Increased fibril diameter (see Chapter 4) in

Col3-deficient tendons likely leads to increases in mechanical properties. Additionally increased myofibroblast activation and realignment support increased fibril-fibril engagement and efficiency of load transfer. Alignment is not different at this time-point between genotypes, indicating that increased engagement and architecture is influencing the mechanical properties more than the organization. Similarly at 6-weeks post-injury, although there is an increase in alignment, as mentioned, fibril diameter growth has slowed, and this alteration in structure leads to decreased mechanical properties. In summary, early in tendon healing organization is important with a switch to architecture and structure at 3- and 6-weeks post-injury.

While comprehensive, this study is not without limitations. An inherent limitation of the model utilized is that it is a heterozygous Col3a1 knockdown model, as homozygous *Col3a1*$^{-/-}$ mice are perinatally lethal, and therefore unable to be studied in this context. This dampens the effects of Col3 knockdown. Additionally, evaluating matrix deposition with second harmonic imaging is difficult, as uninjured tendons require evaluation separately due to the highly aligned structure and necessary reduction in laser power. Additionally, we were unable to quantify integrated density measurements of these images due to the signal increasing with levels of deposited matrix overtime, with no way to parse out if alignment or quantity of collagen was impacting the signal. Lastly, this study aimed to limit variation in the subject population, and therefore utilized only female mice. As the first study in tendon to evaluate the role of Col3, this was a valid approach, however, future studies are necessary to examine sex differences on the influence of Col3 throughout matrix deposition and remodeling.

3.5 – References

1 Volk SW, Wang Y, Mauldin EA, Liechty KW, Adams SL. Diminished type III collagen promotes myofibroblast differentiation and increases scar deposition in cutaneous wound healing. Cells Tissues Organs 2011;194:25–37. https://doi.org/10.1159/000322399.

2 Wang C, Brisson BK, Terajima M, Li Q, Hoxha K, Han B, et al. Type III collagen is a key regulator of the collagen fibrillar structure and biomechanics of articular cartilage and meniscus. Matrix Biol 2020;85–86:47–67. https://doi.org/10.1016/j.matbio.2019.10.001.

3 Volk SW, Shah SR, Cohen AJ, Wang Y, Brisson BK, Vogel LK, et al. Type III collagen regulates osteoblastogenesis and the quantity of trabecular bone. Calcif Tissue Int 2014;94:621–31. https://doi.org/10.1007/s00223-014-9843-x.

4 Collagen in tendon, ligament, and bone healing. A current review - PubMed. n.d. URL: https://pubmed.ncbi.nlm.nih.gov/7671527/ (Accessed 4 August 2020).

5 Nichols AEC, Best KT, Loiselle AE. The cellular basis of fibrotic tendon healing: challenges and opportunities. Transl Res 2019:156–68. https://doi.org/10.1016/j.trsl.2019.02.002.

6 Dyment NA, Liu CF, Kazemi N, Aschbacher-Smith LE, Kenter K, Breidenbach AP, et al. The Paratenon Contributes to Scleraxis-Expressing Cells during Patellar Tendon Healing. PLoS One 2013;8:. https://doi.org/10.1371/journal.pone.0059944.

7 Varani J, Dame MK, Rittie L, Fligiel SEG, Kang S, Fisher GJ, et al. Decreased collagen production in chronologically aged skin: Roles of age-dependent alteration in fibroblast function and defective mechanical stimulation. Am J Pathol 2006;168:1861–8. https://doi.org/10.2353/ajpath.2006.051302.

8 Sunwoo JY, Eliasberg CD, Carballo CB, Rodeo SA. The role of the macrophage in tendinopathy and tendon healing. J Orthop Res 2020:1666–75. https://doi.org/10.1002/jor.24667.

9 Chamberlain CS, Clements AEB, Kink JA, Choi U, Baer GS, Halanski MA, et al. Extracellular Vesicle-Educated Macrophages Promote Early Achilles Tendon Healing. Stem Cells 2019;37:652–62. https://doi.org/10.1002/stem.2988.

10 Wang C, Zhang Y, Zhang G, Yu W, He Y. Adipose Stem Cell–Derived Exosomes Ameliorate Chronic Rotator Cuff Tendinopathy by Regulating Macrophage Polarization: From a Mouse Model to a Study in Human Tissue. Am J Sports Med 2021;49:2321–31. https://doi.org/10.1177/03635465211020010.

11 Cooper TK, Zhong Q, Krawczyk M, Tae HJ, Müller GA, Schubert R, et al. The Haploinsufficient Col3a1 Mouse as a Model for Vascular Ehlers-Danlos Syndrome. Vet Pathol 2010;47:1028–39. https://doi.org/10.1177/0300985810374842.

12 Leiphart RJ, Taylor BL, Weiss SN, Dyment NA SL. Collagen V Knockdown During Phases of Tendon Healing Differentially Impacts Gene Expression [Abstract]. Orthop Res Soc Annu Meet 2021.

13 Yamauchi M, Sricholpech M. Lysine post-translational modifications of collagen. Essays Biochem 2012;52:113–33. https://doi.org/10.1042/BSE0520113.

14 Favata M. Bioengineering PhD Thesis. University of Pennsylvania; 2006; 2006.

15 Lin TW, Cardenas L, Glaser DL, Soslowsky LJ. Tendon healing in interleukin-4 and interleukin-6 knockout mice. J Biomech 2006;39:61–9. https://doi.org/10.1016/J.JBIOMECH.2004.11.009.

16 Lake SP, Miller KS, Elliott DM, Soslowsky LJ. Effect of fiber distribution and realignment on the nonlinear and inhomogeneous mechanical properties of human supraspinatus tendon under longitudinal tensile loading. J Orthop Res 2009;27:1596–602. https://doi.org/10.1002/jor.20938.

17 Miller KS, Connizzo BK, Feeney E, Soslowsky LJ. Characterizing local collagen fiber re-alignment and crimp behavior throughout mechanical testing in a mature mouse supraspinatus tendon model. J Biomech 2012;45:2061–5. https://doi.org/10.1016/j.jbiomech.2012.06.006.

18 Zar J. Biostatistical Analysis, 5th Edition. Pearson; 2010.

19 Beason DP, Kuntz AF, Hsu JE, Miller KS, Soslowsky LJ. Development and evaluation of multiple tendon injury models in the mouse. J Biomech 2012;45:1550–3. https://doi.org/10.1016/j.jbiomech.2012.02.022.

20 Johnston JM, Connizzo BK, Shetye SS, Robinson KA, Huegel J, Rodriguez AB, et al. Collagen V haploinsufficiency in a murine model of classic Ehlers–Danlos syndrome is associated with deficient structural and mechanical healing in tendons. J Orthop Res 2017;35:2707–15. https://doi.org/10.1002/jor.23571.

21 Franco-Barraza J, Raghavan KS, Luong T, Cukierman E. Engineering clinically-relevant human fibroblastic cell-derived extracellular matrices. Methods Cell Biol., vol. 156. Academic Press Inc.; 2020. p. 109–60.

22 Bredfeldt JS, Liu Y, Pehlke CA, Conklin MW, Szulczewski JM, Inman DR, et al. Computational segmentation of collagen fibers from second-harmonic generation images of breast cancer. J Biomed Opt 2014;19:016007. https://doi.org/10.1117/1.jbo.19.1.016007.

23 Izu Y, Ansorge HL, Zhang G, Soslowsky LJ, Bonaldo P, Chu ML, et al. Dysfunctional tendon collagen fibrillogenesis in collagen VI null mice. Matrix Biol 2011;30:53–61. https://doi.org/10.1016/j.matbio.2010.10.001.

24 Connizzo BK, Yannascoli SM, Soslowsky LJ. Structure-function relationships of postnatal tendon development: A parallel to healing. Matrix Biol 2013:106–16. https://doi.org/10.1016/j.matbio.2013.01.007.

25 Freedman BR, Gordon JA, Bhatt PR, Pardes AM, Thomas SJ, Sarver JJ, et al. Nonsurgical treatment and early return to activity leads to improved Achilles tendon fatigue mechanics and functional outcomes during early healing in an animal model. J Orthop Res 2016;34:2172–80. https://doi.org/10.1002/jor.23253.

26 Kjaer M, Magnusson P, Krogsgaard M, Moller JB, Olesen J, Heinemeier K, et al. Extracellular matrix adaptation of tendon and skeletal muscle to exercise. J Anat 2006;208:445–50. https://doi.org/10.1111/j.1469-7580.2006.00549.x.

27 Marturano JE, Arena JD, Schiller ZA, Georgakoudi I, Kuo CK. Characterization of mechanical and biochemical properties of developing embryonic tendon. Proc Natl Acad Sci U S A 2013;110:6370–5. https://doi.org/10.1073/pnas.1300135110.

28 Beach ZM, Bonilla KA, Dekhne MS, Sun M, Adams TH, Adams SM, et al. Biglycan has a major role in maintenance of mature tendon mechanics. J Orthop Res 2022;40:2546–56. https://doi.org/10.1002/jor.25299.

29 Sun M, Connizzo BK, Adams SM, Freedman BR, Wenstrup RJ, Soslowsky LJ, et al. Targeted deletion of collagen V in tendons and ligaments results in a classic Ehlers-Danlos syndrome joint phenotype. Am J Pathol 2015;185:1436–47. https://doi.org/10.1016/j.ajpath.2015.01.031.

30 Best KT, Korcari A, Mora KE, Nichols AE, Muscat SN, Knapp E, et al. Scleraxis-lineage cell depletion improves tendon healing and disrupts adult tendon homeostasis. Elife 2021;10:. https://doi.org/10.7554/eLife.62203.

31 Paredes J, Marvin JC, Vaughn B, Andarawis-Puri N. Innate tissue properties drive improved tendon healing in MRL/MpJ and harness cues that enhance behavior of canonical healing cells. FASEB J 2020;34:8341–56. https://doi.org/10.1096/fj.201902825RR.

32 Landén NX, Li D, Ståhle M. Transition from inflammation to proliferation: a critical step during wound healing. Cell Mol Life Sci 2016:3861–85. https://doi.org/10.1007/s00018-016-2268-0.

33 Robinson KA, Sun M, Barnum CE, Weiss SN, Huegel J, Shetye SS, et al. Decorin and biglycan are necessary for maintaining collagen fibril structure, fiber realignment, and mechanical properties of mature tendons. Matrix Biol 2017;64:81–93. https://doi.org/10.1016/j.matbio.2017.08.004.

34 Zhang G, Young BB, Ezura Y, Favata M, Soslowsky LJ, Chakravarti S, et al. Development of tendon structure and function: Regulation of collagen fibrillogenesis. Journal of Musculoskeletal Neuronal Interactions. 2005. URL: https://pubmed.ncbi.nlm.nih.gov/15788867/

35 Connizzo BK, Sarver JJ, Birk DE, Soslowsky LJ. Effect of age and proteoglycan deficiency on collagen fiber re-alignment and mechanical properties in mouse supraspinatus tendon. J Biomech Eng 2013;135:. https://doi.org/10.1115/1.4023234.

36 Eekhoff JD, Fang F, Lake SP. Multiscale mechanical effects of native collagen cross-linking in tendon. Connect Tissue Res 2018:410–22. https://doi.org/10.1080/03008207.2018.1449837.

37 Fessel G, Snedeker JG. Evidence against proteoglycan mediated collagen fibril load transmission and dynamic viscoelasticity in tendon. Matrix Biol 2009;28:503–10. https://doi.org/10.1016/j.matbio.2009.08.002.

38 Wang JH-C, Guo Q, Li B. Tendon Biomechanics and Mechanobiology-A Minireview of Basic Concepts and Recent Advancements. J Hand Ther 2012;25:133–41. https://doi.org/10.1016/j.jht.2011.07.004.

39 Brisson BK, Mauldin EA, Lei W, Vogel LK, Power AM, Lo A, et al. Type III collagen directs stromal organization and limits metastasis in a murine model of breast cancer. Am J Pathol 2015;185:1471–86. https://doi.org/10.1016/j.ajpath.2015.01.029.

40 Schulz JN, Zeltz C, Sørensen IW, Barczyk M, Carracedo S, Hallinger R, et al. Reduced granulation tissue and wound strength in the absence of α11β1 integrin. J Invest Dermatol 2015;135:1435–44. https://doi.org/10.1038/jid.2015.24.

41 Shen H, Schwartz AG, Civitelli R, Thomopoulos S. Connexin 43 Is Necessary for Murine Tendon Enthesis Formation and Response to Loading. J Bone Miner Res. 2020 Aug;35(8):1494-1503. doi: 10.1002/jbmr.4018.

42 Chen D, Smith LR, Khandekar G, Patel P, Yu CK, Zhang K, Chen CS, Han L, Wells RG. Distinct effects of different matrix proteoglycans on collagen fibrillogenesis and cell-mediated collagen reorganization. Sci Rep. 2020 Nov 4;10(1):19065. doi: 10.1038/s41598-020-76107-0. PMID: 33149218; PMCID: PMC7642422.

CHAPTER 4: Collagen III Deficiency Following Injury in Female Murine Tendons Affects Fibril Structural and Mechanical Properties

4.1 – Introduction

Tendon transmits high tensile forces from muscle to bone due to its characteristically highly aligned, hierarchical structure. Tendon is organized into fascicles, which are made up of fibers, composed of individual collagen fibrils.[1] This arrangement allows for a high resistance to tensile loading and unique structural properties due to transfer of load down these different length scales. Previous studies have indicated that matrix nanostructure and behavior influence the overall functionality of the tendon.[2]

Cell-ECM interactions also play a role in overall mechanical strength of the tendon, indicating ECM composition, not solely organization, will affect function.[3] Fibril diameter has been implicated in influencing both elastic and viscoelastic properties of the overall tendon.[4] Additionally, individual fibril mechanical behavior and collagen cross-linking will dictate fibril sliding and deformation, ultimately affecting the alignment of the injury matrix and the response to load.[3] One method to evaluate fibril sliding and deformation, is through evaluation of the D-period that is characteristic of tendons due to the unique arrangement of fibrillar molecules.[5] The molecules are aligned in a quarter-staggered

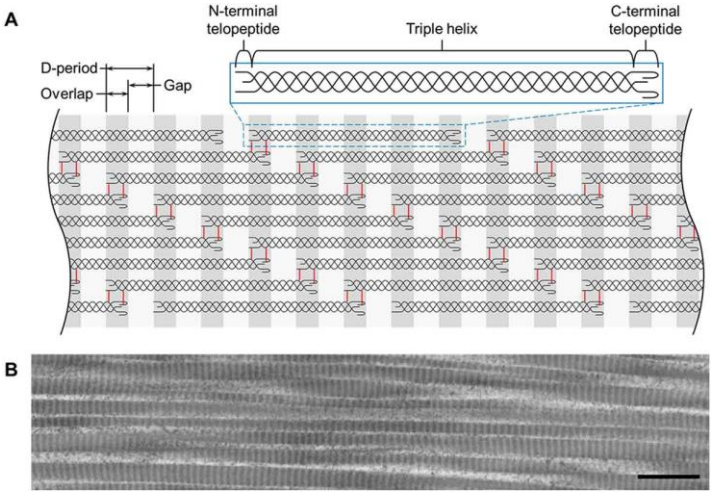

Fig. 4.1: Molecular and fibrillar structure of collagen. (A) Collagen molecules form a triple helix with an N-terminal telopeptide and a longer C-terminal telopeptide with a hairpin turn in both α1 chains.6 The molecules are aligned in a quarter-staggered arrangement with distinctive overlap and gap regions and a D-period of ~67 nm. Intermolecular cross-links (shown in red) stabilize the collagen fibril. (B) Collagen fibrils in mouse SST imaged using transmission electron microscopy exhibit the characteristic D-period as represented in (A) (scale bar = 500 nm). Reprinted with permission from Eekhoff *et al.* 2017.

arrangement, and the gap and overlap regions create the D-period (**Fig. 4.1**).[5–7] Unique cross-linking arrangement helps organize the fibrils and dictate interfibrillar interactions that ultimately influence whole tissue mechanics.

Previous work described in Chapter 3 evaluated cellular activity, gene expression and fiber alignment following patellar tendon injury surgery. The role of Col3 in influencing these measures, and resultant effect on overall tendon response to load was discussed. However, this study aims to expand upon the evaluation of the matrix organization and composition to evaluate matrix structure and behavior at the fibril level. Interfibrillar interactions are implicated in overall resistance to load and allow for unique tendon properties and ability to withstand repetitive loading. These interactions are influenced by fibril structure, adhesion molecules and the overall composition of matrix.

As discussed, Col3 is upregulated post-injury and fills the injury void in the days following tendon injury.[8] Col3 frequently co-assembles with Col1 in fibrous tissue matrices[9] influencing Col1 fibril growth and development. Therefore, as a main component of the healing matrix and its influence on Col1, we expect it is a key player in overall matrix behavior.

Width, length and cross-linking of collagen fibrils has been shown to influence overall tendon stresses and deformation.[12] As collagen matrix is loaded in tension, the rotation and reorientation of the collagen fascicles and fibers helps to preserve length and avoid premature stretching of the fibrils.[13–15] Sliding between fiber and fibrils will contribute to strain transfer and avoid shear stresses that can ultimately lead to molecular deformation and early failure.[12,16,17]

Cross-link type and distribution also contribute to shear loading and influences fibril sliding. Macroscale tendon mechanical properties are determined by internal shear loading paradigms as well, with shear transfer of load affecting overall failure properties. Shear loading will be dramatically affected by cross-linking composition and resultant fibril sliding and increased enzymatic cross-linking increased fibril stiffness and fibril sliding.[7] However, after

initial molecular alignment, the cross-links will resist sliding between collagen molecules and therefore stiffen the fibril.[7] Col3-deficiency was shown to increase immature and mature cross-linking in meniscus,[18] and numerous studies have shown that increasing cross-linking density did increase overall tendon mechanics.[7,19,20] An increase in mature cross-linking was a negative predictor of fibril deformation, while predicting increased sliding.[19] Additionally, reduced cross-linking was associated with a reduction in stiffness of the fibrils.[20] Our previous work, outlined in Chapter 3, showed decreased in mechanical stiffness in WT tendons, and this could be attributed to a reduced amount of cross-linking compared to Col3-deficient tendons. While we measured whole tendon stiffness, individual collagen fibril stiffness, and fiber stiffness is directionally the same, although attenuated as length scale decreases.[22] Future qualitative and quantitative characterization of cross-linking would be necessary to understand if this mechanism is resulting in increased stiffness.

Due to the role of Col3 in influencing fibril structure, organization and engagement, through fibrillogenesis, cross-linking formation and integrin engagement, fibril structure and behavior are important to evaluate to understand whole tissue mechanics. Therefore, the **objective of this study was to evaluate the structure-function relationship at the collagen fibril level through evaluation of fibril diameters and fibril response to load.** *We hypothesized that due to differences in collagen fibril diameter distributions, fibril behavior will differ between genotypes. Col3-deficiency will increase cell-matrix engagement and fibril-fibril interactions due to the unique structure and organization of the deposited matrix.*

4.2 – Methods

4.2.1 Animal Model and Study Design

This study was approved by the University of Pennsylvania Institutional Animal Care and Use Committee. Female wild-type (WT) BALB/c littermates and heterozygous ***Col3a1***$^{+/-}$ mice at 90 days of age (n=38) were used. Uninjured (n=22) and injured (n=16) groups were randomly

assigned, with injured mice undergoing bilateral patellar tendon defect injury surgery. Injured animals at 3- or 6 weeks post-injury, and uninjured age-matched (110 days of age) animals were euthanized using carbon dioxide. Right limbs of a subset of mice were utilized for TEM (n=4/genotype/timepoint). Uninjured mice were assigned to the AFM assay, with both limbs being utilized, and assigned to different strain levels.

4.2.2 Surgical Induction of Patellar Tendon Defect

Previously explained in *Section 3.3.2.* Briefly, using aseptic technique, the patellar tendon was initially exposed through a medial incision on the flexed knee, isolate with medial and lateral incisions and a 0.75 mm biopsy punch was used to create a full-thickness, partial width defect (~60%) in the midsubstance of the patellar tendon. Mice were administered Buprenorphine SR (0.1mg/kg) prior to surgery, returned to cage activity following completion, and were monitored for 5 days post-surgery with no adverse effects seen.

4.2.3 Matrix Structural Analyses

***Tendon Fibril Structure*.** Tendons will be analyzed using transmission electron microscopy (TEM) as described. Patellar tendons from 90 day-old mice (n=4 mice/genotype/timepoint) were harvested then underwent fixation in Karnovsky's fixative (4% paraformaldehyde, 2.5% glutaraldehyde, 0.1 M sodium cacodylate and 8 mM $CaCl_2$) for 4 hours, and then post-fixed in 1% osmium tetroxide to aid in infiltration. Tendons then underwent dehydration with an ethanol

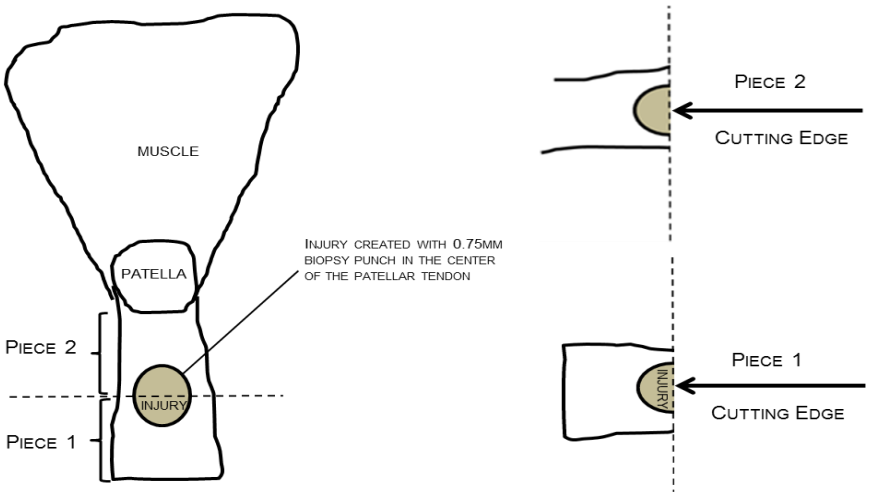

Figure 4.2: TEM Embedding proximal and distal halves of the patellar tendon for fibril diameter imaging.

series followed by infiltration with propylene oxide and Epon (EPON 812, DDSA, NMA, DMP-30). Tendons were then cut in half through the injury site and embedded in Epon with the injured cross section facing the front of the mold (**Fig. 4.2**).

Ultra-thin cross sections were obtained using a Leica Ultramicrotome and collected onto copper grids. Grids were stained using Uranyless and Phosphotungstic Acid to visualize the collagen fibrils. Imaging was completed on a JEOL 1400 transmission electron microscope (JEOL Ltd., Tokyo, Japan) fitted with a Gatan Orius widefield side mount CC Digital camera (Gatan Inc., Pleasanton, CA). 15 images per sample were collected at 60,000X magnification, with an average of 500 fibrils assessed per image. Four samples were analyzed per group. Fibril structure was defined including diameter (along the minor axis of the fibril), diameter distribution and regularity of cross-sectional profiles from the central portion of the uninjured PT or across the central wound. Images were randomly chosen in a masked manner and fibril diameter was measured utilizing a custom MATLAB (Natick, MA) code that thresholds the image and outlines the fibrils for measurement.

4.2.4 Matrix Functional Analyses

Collagen Fibril Deformation and Sliding. Fibril deformation and sliding will be quantified using atomic force microscopy and a flash-freeze testing protocol.[23-25] Patella-patellar tendon-tibia complexes were dissected from the knee joint, and excess soft tissue removed. Cross-sectional area was measured using a custom laser device.[26] The tibia was potted in a custom 3D-printed pot using PMMA. The patella was gripped with a custom grip and loaded into the Instron 5543. Gauge length was measured using imaging techniques prior to testing for strain calculations. The tendon then underwent a testing protocol consisting of preconditioning, a 60sec hold, and then ramp to 1% or 10% strain at a rate of 0.1%/s. Tendons were then flash frozen, cut from the grip, and embedded in chilled OCT and immediately submerged in methyl butane chilled with dry ice to avoid thawing. Blocks were then sectioned 20µm to obtain 5 slides with 3-4 sections per slide. For fibril deformation and sliding, imaging of 2 µm × 2 µm regions was performed in air by tapping mode imaging using NCHV-A probes (nominal spring constant $k \approx 42$N/m, radius $R \approx 10$ nm) and a Dimension Icon AFM as described.[27-29] PTs were scanned within the midsubstance, and at 4-6 sections through the tendon depth. 5-6 tendons were assessed per genotype at both strain levels. Custom software was used to measure the D-period length for multiple fibrils in a single image.[29] Mean and variance are obtained from D-period distributions. A change in fibril D-period variance from one strain to the next is indicative of strain heterogeneity between fibrils, or fibril sliding.[29]

4.2.5 Statistics

Two-way ANOVAs with post-hoc Bonferroni tests were used to assess the effects of genotype (collagen III expression), strain level (1% or 10%), and their interaction on fiber d-period average and variance. Collagen fibril diameter distributions were compared by genotype using Kolmogorov-Smirnov tests. Significance was set at $p \leq 0.05$.

4.3 – Results

4.3.1 Fibril diameter distributions differed between genotypes and across injury time-points

Fibril morphology was qualitatively no different between genotypes, with fibrils exhibiting normal circular cross-sectional shape in uninjured and injured tendons (**Fig. 4.3**). Uninjured *Col3a1*$^{+/-}$ tendons had a broader fibril diameter distribution than WT tendons, with an increased population of larger fibrils (**Fig. 4.4A**). Post-injury both genotypes showed a drastic shift to smaller diameter fibrils but had a small subpopulation of larger diameter fibrils in the injury site.

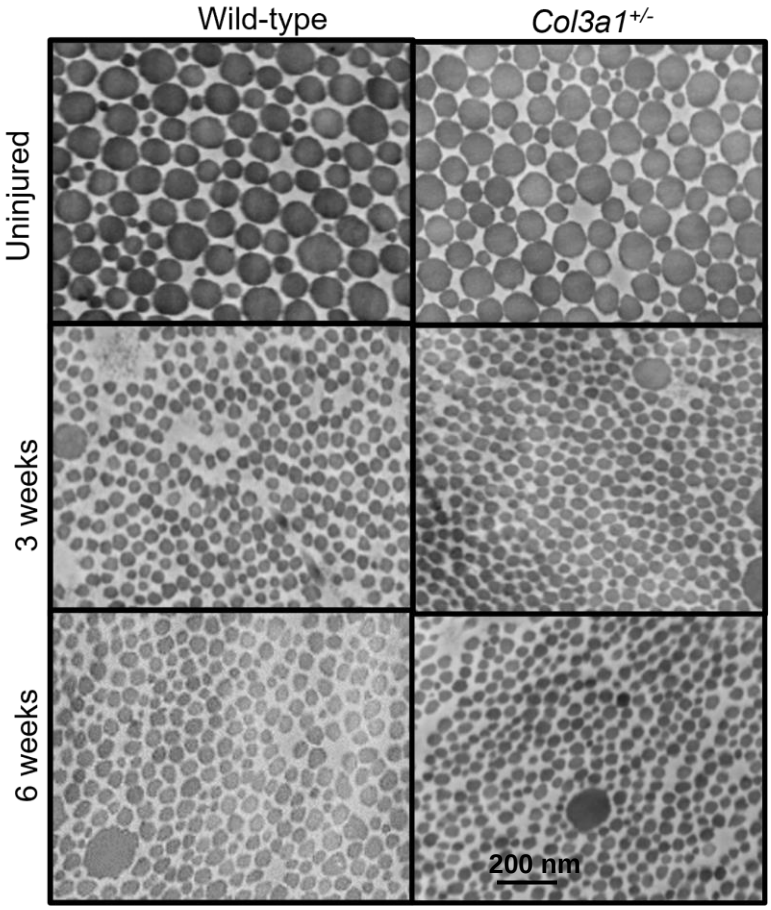

	Wild Type	*Col3a1*$^{+/-}$
Mean	117.6 nm	111.1 nm
Median (Q_2)	123.4 nm	115.5 nm
IQR (Q_3-Q_1)	73.5 nm	65.1 nm

	Wild Type	*Col3a1*$^{+/-}$
Mean	48.1 nm	50.3 nm
Median (Q_2)	42.6 nm	44.2 nm
IQR (Q_3-Q_1)	13.5 nm	14.7 nm

	Wild Type	*Col3a1*$^{+/-}$
Mean	53.3 nm	49.1 nm
Median (Q_2)	48.6 nm	43.4 nm
IQR (Q_3-Q_1)	16.3 nm	18.2 nm

Figure 4.3: Representative Images of Tendon in Cross-section
Qualitatively no differences can be seen in fibril morphology across genotypes within injury time-point. A drastic shift to smaller fibrils is seen within each genotype following injury. A subpopulation of larger fibrils is seen at both time-points following injury within each genotype. 15 images per sample were analyzed, with an average of 500 fibrils assessed per image. n=4 tendons/group.

Additionally, 3-weeks post-injury *Col3a1*$^{+/-}$ tendons had a greater population of larger fibrils (**Fig. 4.4B**). Interestingly, *Col3a1*$^{+/-}$ tendons 6-weeks post-injury had an increased population of smaller diameter fibrils when compared to WT, and a flattened distribution when compared to 3-week post-injured *Col3a1*$^{+/-}$ tendons. While WT fibril diameters increased from 3- to 6-weeks post-injury, 6-week *Col3a1*$^{+/-}$ tendons had a slightly flatter and broader distribution of fibril diameters from 3-weeks, with a peak in a similar range.

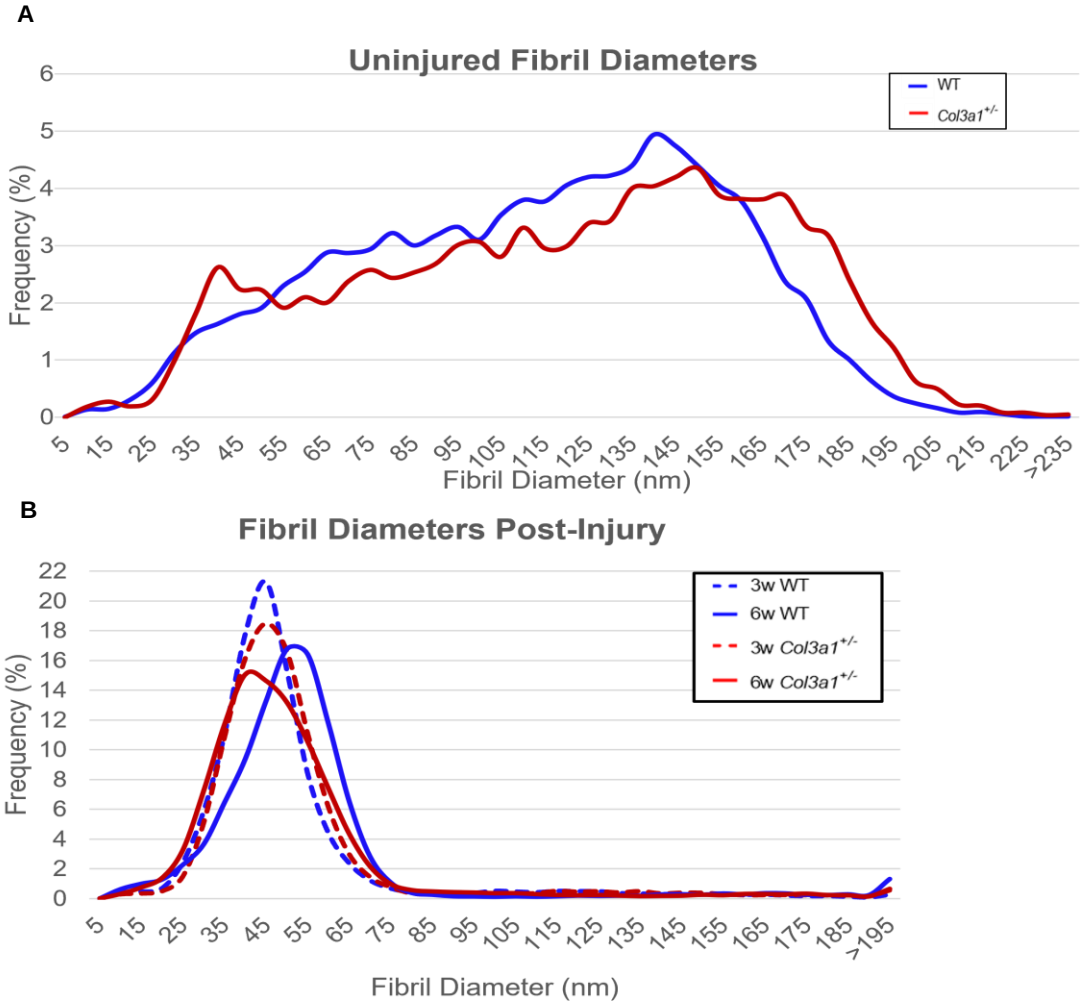

Figure 4.4: Fibril Diameter Distributions
(A) Uninjured Col3-deficient tendons had a larger population of larger diameter fibrils. **(B)** Post-injury Col3-deficient tendons had an increased population of larger fibrils at 3-weeks and smaller fibrils at 6-weeks. n=4 tendons/group.

4.3.2 Fibril sliding is increased in Col3a1$^{+/-}$ tendons at 1% strain compared to WT tendons, with sliding decreasing with increased strain.

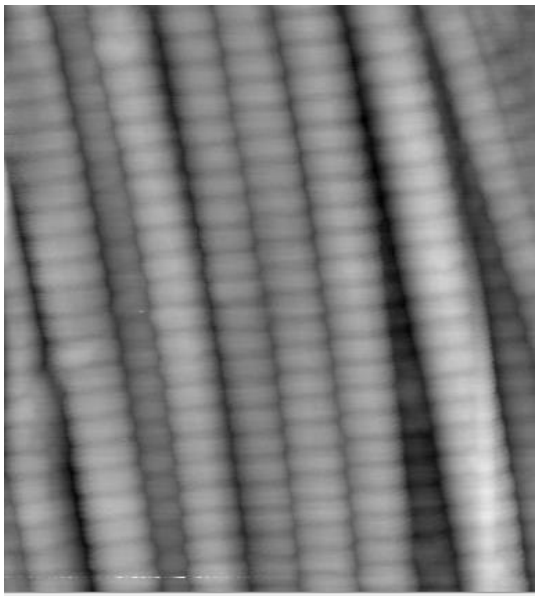

Figure 4.5: Sample scan of collagen fibrils using Atomic Force Microscopy

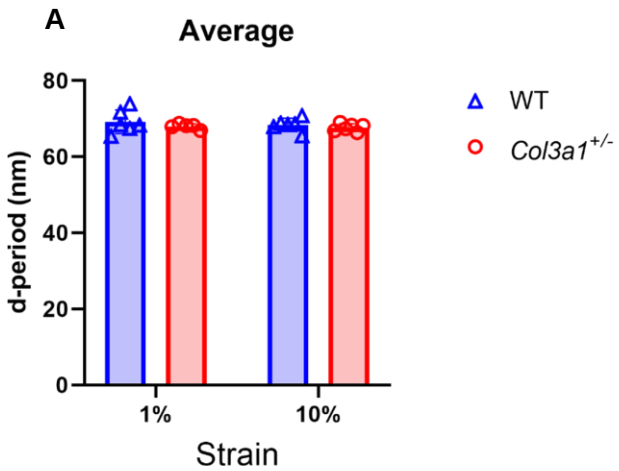

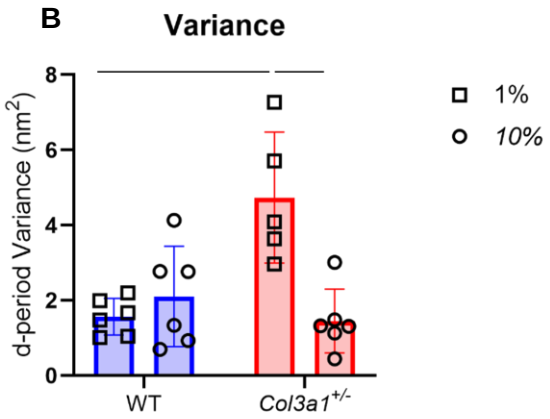

Figure 4.6: AFM Imaging Results
(A) No differences in d-period average were seen between genotypes or across strain. (B) Variance was increased in Col3-deficient tendons at 1% strain compared to Col3-deficient tendons at 10% strain and WT tendons at 1% strain. Statistical significance of p≤0.05 is denoted by solid lines. n=5-6 tendons/group.

Atomic Force Microscopy was used to quantify average d-period and fibril sliding with loading in uninjured tendons. No qualitative differences could be seen between genotypes (**Fig. 4.5**). D-period averages were similar in both genotypes and at both strain levels (**Fig. 4.6A**). Variance of the d-period in WT tendons did not differ with increased strain (**Fig. 4.6B**). D-period variance in *Col3a1*$^{+/-}$ tendons loaded to 1% strain was increased compared to tendons loaded to 10% strain (**Fig. 4.6B**). Additionally, when loaded to 1% strain, *Col3a1*$^{+/-}$ tendons exhibited more sliding than WT tendons, as indicated by increased d-period variance. Lastly, an interaction between genotype

and strain level indicated that variance of the d-period in *Col3a1*$^{+/-}$ tendons responded differently to loading than WT tendons.

4.4 – Discussion

ECM microstructure is known to play a key role in matrix behavior, strain transmission and response to load.[30] Col3-deficiency resulted in increased collagen fibril diameters in uninjured adult tendons, supporting our original hypothesis. An increased population of larger fibrils 3-weeks post-injury in *Col3a1*$^{+/-}$ tendons likely influenced increases in mechanical properties when compared to WT, as material and structural properties were increased in *Col3a1*$^{+/-}$ tendons at this time-point (see Chapter 3). Larger fibril diameters can withstand larger loads and are able to compensate for injury, as seen by the lack of a decrease in mechanical properties post-injury in Col3-deficient tendons (see Chapter 3). Increasing stiffness with increasing fibril diameter is supported by our work, as increased fibril diameters increase tendon macroscale stiffness. Interestingly, by 6-weeks post-injury, the *Col3a1*$^{+/-}$ tendon fibril diameter population remains similar to 3-weeks, while 6-week WT fibril diameter population shifts to larger fibrils. This may indicate that WT fibrils continue fibrillogenesis later post-injury, while *Col3a1*$^{+/-}$ fibrils lateralize earlier in the healing process due to dysregulation of fibrillogenesis from Col3 deficiency. Fibrillogenesis begins with assembly of intermediate molecules, progresses with nucleation, or beginning of growth, and finishes with longitudinal and lateral growth.[31–33] By 6-weeks, WT tendons surpass *Col3a1*$^{+/-}$ tendons in fibril diameter growth, and this may explain why genotypic differences in mechanics are no longer seen by 6-weeks post-injury (Data presented in Chapter 3). This same behavior was not seen in uninjured tendons, where material properties are decreased from WT levels, indicating that in uninjured, healthy tendon matrix, developmental fibrillogenesis may be different than healing matrix formation. While development is a good starting point for understanding matrix deposition and growth, these processes occur in a healthy environment, without the influence of inflammatory factors

and healing processes. Healing matrix likely behaves differently than the homeostatic tendon, as the cellular environment is much more active, compared to a relatively hypocellular matrix. Therefore, it is not surprising that fibril development would differ in an injury environment. Cell-matrix interactions, matrix quality and organization likely play a larger role during healing, as both genotypes had very highly aligned uninjured matrix.

While fibril structure is important individually, organization and fibril-fibril interactions also need to be examined and the compounding changes that may be seen with alterations in organization and structure. This includes the relationship between stiffness, fibril diameter and cross-linking. Evaluating matrix behavior under load via Atomic Force Microscopy helps to elucidate the functional implications of the altered matrix composition and structure of *Col3a1*$^{+/-}$ tendons and fibril mechanics. Increased variance at 1% strain in *Col3a1*$^{+/-}$ animals compared to 10% strain indicates increased sliding with lower strain. This behavior is different from WT tendons, where sliding occurs at more moderate strain levels[21], although these levels were not examined in this current body of work. Work in meniscus has indicated that Col3 abundance affects fibril cross-link types and may influence mechanical strength of matrix.[18]

Additionally, shear forces have been shown to be very important in influencing the strength of the matrix in tendon loading, with importance decreasing with increased alignment and load.[7,20,21] Cross-links hold together the triple helices in tendon, and as it is known that Col3 deficiency alters assembly of these helices, it can be argued that Col3 will directly and indirectly affect cross-linking in the matrix. After initial molecular alignment, the cross-links will resist sliding between collagen molecules and therefore stiffen the fibril.[7] Our findings support this idea, as we only saw fibril sliding when tendons were loaded to 1% strain, and not at the higher strain value. However, cross-link evaluation and characterization was beyond the scope of this study, but cross-linking analysis in the future will further elucidate the contribution of fibril mechanics to overall tissue response to load.

Statistical analysis of WT compared to *Col3a1*$^{+/-}$ tendons across strain levels revealed that there was an interaction between genotype and strain level, indicating that strain is affecting genotypes differently. A higher amount of fibril sliding occurs in *Col3a1*$^{+/-}$ tendons, as indicated by the increased d-period variance. While FFT and OrientationJ are not sensitive enough to capture any differences in alignment in uninjured tendons between genotypes, this is a possibility for a mechanism for the increased sliding in *Col3a1*$^{+/-}$ tendons. If the fibrils are more highly aligned, less activation energy is needed to engage the fibrils, and sliding will occur. This notion is supported by faster realignment in tendons during the mechanical testing protocol, as was discussed in Chapter 3. Increase cell-matrix interactions would also contribute to increased sliding and can be attributed to increased levels of connexin 43 likely present in Col3-deficient tendons, as indicated by increased expression of Gja1. Additionally, more organization in the toe region, which corresponds to 1% strain, will result in more sliding[27,28] due to less consistent collagen even if it is overall more organized. Other studies have shown that rat tail tendons, which are known to be very highly organized, have more sliding than a less organized matrix.[7] All of this previous work supports our findings that *Col3a1*$^{+/-}$ tendons exhibit more sliding at 1% strain than 10% strain, and their increased alignment leads to increased sliding compared to WT tendons. Although it was expected that with this drastic difference in variance that we would see differences in d-period average, as this is not a normal distribution, it makes sense that the mean would not be affected across groups.

Fibril sliding also plays a role in supra fiber-length scales, influencing both viscoelastic and quasistatic mechanical properties.[12,20,21] Diminished fibril sliding at higher loads leads to a loss of a viscous response and an increase in tissue modulus. Unfortunately, inherent constraints in our AFM protocol did not allow us to effectively perform imaging on injured tissue, but hopefully this can be completed in the future to further understand the mechanical response to load of newly deposited matrix and fibrils. Mechanical properties of WT and *Col3a1*$^{+/-}$ tendons

at 6-weeks post-injury may indicate reduced sliding at this time-point when compared to earlier time-points, with increased dynamic modulus and tissue modulus values (Data presented in Chapter 3). Additionally, *Col3a1*$^{+/-}$ tendons had a damped viscoelastic response and increased modulus compared to WT at 1- and 3-weeks post-injury, potentially indicating diminished fibril sliding at these injury time-points as well.

While matrix organization, architecture and fibril-fibril interactions are crucial to understanding tendon response to load, a more nuanced understanding is necessary. Future work can include examining proteoglycans, GAGs and other matrix components to further understand their contribution to mechanotransduction and load dissipation throughout ECM.

4.5 – References

1 Alshomer F, Chaves C, Kalaskar DM. Advances in Tendon and Ligament Tissue Engineering: Materials Perspective. J Mater 2018;2018:1–17. https://doi.org/10.1155/2018/9868151.

2 Robinson KA, Sun M, Barnum CE, Weiss SN, Huegel J, Shetye SS, et al. Decorin and biglycan are necessary for maintaining collagen fibril structure, fiber realignment, and mechanical properties of mature tendons. Matrix Biol 2017;64:81–93. https://doi.org/10.1016/j.matbio.2017.08.004.

3 Eekhoff JD, Fang F, Lake SP. Multiscale mechanical effects of native collagen cross-linking in tendon. Connect Tissue Res 2018:410–22. https://doi.org/10.1080/03008207.2018.1449837.

4 Darrieutort-Laffite C, Beach ZM, Weiss SN, Eekhoff JD, Soslowsky LJ. Knockdown of biglycan reveals an important role in maintenance of structural and mechanical properties during tendon aging. J Orthop Res 2023. https://doi.org/10.1002/jor.25536.

5 Ricard-Blum S. The Collagen Family. Cold Spring Harb Perspect Biol 2011;3:1–19. https://doi.org/10.1101/cshperspect.a004978.

6 Kwansa AL, De Vita R, Freeman JW. Mechanical recruitment of N- and C-crosslinks in collagen type I. Matrix Biol 2014;34:161–9. https://doi.org/10.1016/j.matbio.2013.10.012.

7 Eekhoff JD, Fang F, Lake SP. Multiscale mechanical effects of native collagen cross-linking in tendon. Connect Tissue Res 2018:410–22. https://doi.org/10.1080/03008207.2018.1449837.

8 Nichols AEC, Best KT, Loiselle AE. The cellular basis of fibrotic tendon healing: challenges and opportunities. Transl Res 2019:156–68. https://doi.org/10.1016/j.trsl.2019.02.002.

9 Niederreither K, D'Souza R, Metsäranta M, Eberspaecher H, Toman PD, Vuorio E, et al. Coordinate patterns of expression of type I and III collagens during mouse development. Matrix Biol 1995;14:705–13. https://doi.org/10.1016/S0945-053X(05)80013-7.

10 Tiger CF, Fougerousse F, Grundström G, Velling T, Gullberg D. α11β1 integrin is a receptor for interstitial collagens involved in cell migration and collagen reorganization on mesenchymal nonmuscle cells. Dev Biol 2001;237:116–29. https://doi.org/10.1006/dbio.2001.0363.

11 Schulz JN, Zeltz C, Sørensen IW, Barczyk M, Carracedo S, Hallinger R, et al. Reduced granulation tissue and wound strength in the absence of α11β1 integrin. J Invest Dermatol 2015;135:1435–44. https://doi.org/10.1038/jid.2015.24.

12 Tang Y, Ballarini R, Buehler MJ, Eppell SJ. Deformation micromechanisms of collagen fibrils under uniaxial tension. J R Soc Interface 2010;7:839–50. https://doi.org/10.1098/rsif.2009.0390.

13 Thorpe CT, Klemt C, Riley GP, Birch HL, Clegg PD, Screen HRC. Helical sub-structures in energy-storing tendons provide a possible mechanism for efficient energy storage and return. Acta Biomater 2013;9:7948–56. https://doi.org/10.1016/j.actbio.2013.05.004.

14 Lake SP, Miller KS, Elliott DM, Soslowsky LJ. Effect of fiber distribution and realignment on the nonlinear and inhomogeneous mechanical properties of human supraspinatus tendon under longitudinal tensile loading. J Orthop Res 2009;27:1596–602. https://doi.org/10.1002/jor.20938.

15 Shearer T, Thorpe CT, Screen HRC. The relative compliance of energy-storing tendons may be due to the helical fibril arrangement of their fascicles. J R Soc Interface 2017;14:. https://doi.org/10.1098/rsif.2017.0261.

16 Fang F, Lake SP. Multiscale strain analysis of tendon subjected to shear and compression demonstrates strain attenuation, fiber sliding, and reorganization. J Orthop Res 2015;33:1704–12. https://doi.org/10.1002/jor.22955.

17 Gautieri A, Pate MI, Vesentini S, Redaelli A, Buehler MJ. Hydration and distance dependence of intermolecular shearing between collagen molecules in a model microfibril. J Biomech 2012;45:2079–83. https://doi.org/10.1016/j.jbiomech.2012.05.047.

18 Wang C, Brisson BK, Terajima M, Li Q, Hoxha K, Han B, et al. Type III collagen is a key regulator of the collagen fibrillar structure and biomechanics of articular cartilage and meniscus. Matrix Biol 2020;85–86:47–67. https://doi.org/10.1016/j.matbio.2019.10.001.

19 Connizzo BK, Adams SM, Adams TH, Jawad AF, Birk DE, Soslowsky LJ. Multiscale regression modeling in mouse supraspinatus tendons reveals that dynamic processes act as mediators in structure-function relationships. J Biomech 2016;49:1649–57. https://doi.org/10.1016/j.jbiomech.2016.03.053.

20 Puxkandl R, Zizak I, Paris O, Keckes J, Tesch W, Bernstorff S, et al. Viscoelastic properties of collagen: Synchrotron radiation investigations and structural model. Philos Trans R Soc B Biol Sci 2002;357:191–7. https://doi.org/10.1098/rstb.2001.1033.

21 Connizzo BK, Sarver JJ, Han L, Soslowsky LJ. In situ fibril stretch and sliding is location-dependent in mouse supraspinatus tendons. J Biomech. 2014 Dec 18;47(16):3794-8. doi: 10.1016/j.jbiomech.2014.10.029. Epub 2014 Oct 31. PMID: 25468300; PMCID: PMC4261030.

22 Sasaki N, Odajima S. Elongation mechanism of collagen fibrils and force-strain relations of tendon at each level of structural hierarchy. J Biomech 1996;29:1131–6. https://doi.org/10.1016/0021-9290(96)00024-3.

23 Miller KS, Connizzo BK, Soslowsky LJ. Collagen fiber re-alignment in a neonatal developmental mouse supraspinatus tendon model. Ann Biomed Eng 2012;40:1102–10. https://doi.org/10.1007/s10439-011-0490-3.

24 Connizzo BK, Han L, Birk DE, Soslowsky LJ. Collagen V-heterozygous and-null supraspinatus tendons exhibit altered dynamic mechanical behaviour at multiple hierarchical scales. Interface Focus 2016;6:. https://doi.org/10.1098/rsfs.2015.0043.

25 Miller KS, Connizzo BK, Feeney E, Soslowsky LJ. Characterizing local collagen fiber re-alignment and crimp behavior throughout mechanical testing in a mature mouse supraspinatus tendon model. J Biomech 2012;45:2061–5. https://doi.org/10.1016/J.JBIOMECH.2012.06.006.

26 Favata M. Bioengineering PhD Thesis. University of Pennsylvania; 2006; 2006.

27 Rigozzi S, Müller R, Stemmer A, Snedeker JG. Tendon glycosaminoglycan proteoglycan sidechains promote collagen fibril sliding-AFM observations at the nanoscale. J Biomech 2013;46:813–8. https://doi.org/10.1016/j.jbiomech.2012.11.017.

28 Rigozzi S, Stemmer A, Müller R, Snedeker JG. Mechanical response of individual collagen fibrils in loaded tendon as measured by atomic force microscopy. J Struct Biol 2011;176:9–15. https://doi.org/10.1016/j.jsb.2011.07.002.

29 Buckley MR, Sarver JJ, Freedman BR, Soslowsky LJ. The dynamics of collagen uncrimping and lateral contraction in tendon and the effect of ionic concentration. J Biomech 2013;46:2242–9. https://doi.org/10.1016/j.jbiomech.2013.06.029.

30 Roeder BA, Kokini K, Voytik-Harbin SL. Fibril microstructure affects strain transmission within collagen extracellular matrices. J Biomech Eng 2009;131:. https://doi.org/10.1115/1.3005331.

31 Birk DE, Mayne R. Localization of collagen types I, III and V during tendon development. Changes in collagen types I and III are correlated with changes in fibril diameter. Eur J Cell Biol 1997;72:352–61.

32 Birk DE. Type V collagen: Heterotypic type I/V collagen interactions in the regulation of fibril assembly. Micron 2001:223–37. https://doi.org/10.1016/S0968-4328(00)00043-3.

33 Birk DE, Trelstad RL. Extracellular compartments in tendon morphogenesis: Collagen fibril, bundle, and macroaggregate formation. J Cell Biol 1986;103:231–40. https://doi.org/10.1083/jcb.103.1.231.

CHAPTER 5: Collagen III Deficiency Alters Mechanical Properties and Decreases Regulation of Fibrillogenesis Following Injury in Female Adolescent Murine Tendons

5.1 – Introduction

Col3-rich matrix influences migration, proliferation and differentiation of tendon progenitor cells, indicating that it plays a crucial role in the development and growth of tendons. Col3 is present at high levels throughout postnatal tendon development, however, the contribution to ECM organization is unknown. Throughout development of the tendon, Col3 modulates fibrillogenesis both directly and indirectly.[1,2] Col3 colocalizes with Col1, dictating the lateral growth of the fibrils, while indirectly influencing the nucleation site of new fibrils through these interactions.

This study will elucidate differences in stiffness, organization and density of a Col3-deficient matrix during adolescence (P30) to evaluate differences in healing in a developing matrix. This will provide insight into compensatory mechanisms of a more biologically active, younger mouse, and explore if this results in better healing outcomes than in an adult mouse.

Col3 is essential in homeostasis and healing of other collagen I (Col1)-rich tissues[3-5] due to its role regulating fibrillogenesis, ECM organization and remodeling, and the formation of cross-links and scar tissue. A previous study[6] showed increased fibril diameter with a reduction of Col3 throughout development, however, this could be the result of increased Col1 fibrils, or dysregulation of fibrillogenesis, and therefore needs to be examined further. During development, mice are known to heal more rapidly, with a more regenerative response than skeletally mature mice, we hope to elucidate differences by comparing to previous work in an adult mouse model. This study will lay groundwork for future studies investigating more time-

point throughout development, as well as investigating aged mice, who are on the other end of the spectrum, with a decreased in Col3 seen with aging.[7]

Previous work in adult mice, described in Chapter 3, has shown that matrix is more highly aligned post-injury with a reduction of Col3. We anticipate that this same phenotype would be true in adolescent mice and allow for preservation of mechanical properties. Additionally, due to overcompensation and hypersecretion of matrix in these animals and a naturally higher level of Col3, we anticipate that fibrillogenesis will be less affected by Col3-deficiency.

Utilizing a conventional Col3 heterozygous (*Col3a1*$^{+/-}$) mouse model[8], we will elucidate the role of Col3 in driving matrix structure and function. **The objective of this study was to define the role of Col3 in both tendon homeostasis and in response to injury, regulating collagen fibril deposition and resultant alterations in tendon mechanics in an adolescent female mouse model.** As we believe that Col3 is crucial to early tendon healing to allow for the properly regulated healing environment needed to tissue debridement and shaping the matrix for new deposited of healthy tendon, increased levels earlier on in healing is a considered a more regenerative phenotype. *We hypothesized that a reduction in Col3 would result in a more robust, stiffer provisional matrix early in tendon healing, with smaller diameter fibrils when compared to wild-type tendons.* This innovative approach addresses the regulatory roles of Col3 in a young animal and allows us to broaden our understanding of its influence in the developing matrix, when Col3 content is known to be higher than later stages of life. Tendon injuries occur at all stages of life, with the adolescent population making up a significant proportion due to their active lifestyle. To better evaluate potential solutions to suboptimal healing, it is necessary to understand that different age groups may benefit from different therapies, due to the inherent differences in the matrix composition and structure as the tissue is still developing.

5.2 – Methods

5.2.1 Animal Model and Study Design

This study was approved by the University of Pennsylvania Institutional Animal Care and Use Committee. Female wild-type (WT) Balb/cJ and heterozygous *Col3a1*$^{+/-}$ mice at 30 days of age (n=48) were used (IACUC approved). Uninjured (n=24) and injured (n=24) groups were randomly assigned, with injured mice undergoing bilateral patellar tendon defect injury surgery,[9-11] with sacrifice 1-week post-injury in the early proliferative phase of healing. Uninjured animals were age-matched to account for developmental changes and were euthanized at 37 days of age. Right limbs of a subset of mice were utilized for TEM and gene expression (n=4/genotype/timepoint/assay). Left limbs of all mice were utilized for mechanical testing (n=12/genotype/timepoint).

5.2.2 Surgical Induction of Patellar Tendon Defect

Previously explained in *Section 3.2.2.* Briefly, using aseptic technique, the patellar tendon was initially exposed through a medial incision on the flexed knee, isolate with medial and lateral incisions and a 0.75 mm biopsy punch was used to create a full-thickness, partial width defect (~60%) in the midsubstance of the patellar tendon. Mice were administered Buprenorphine SR (0.1mg/kg) prior to surgery, returned to cage activity following completion, and were monitored for 5 days post-surgery with no adverse effects seen.

5.2.3 Real-time PCR of Col3a1 Expression

Immediately following sacrifice, patellar tendons were excised and placed in RNA Later. Samples were stored at 4°C for 24 hours, and then transferred to -20°C freezer for longer term storage. Patellar tendons were thawed in RNA Later when RNA extraction began. RNA was extracted utilizing a Zymo Quick-RNA Microprep kit, and then cDNA was prepared from

template RNA (Thermo high-Capacity cDNA RT). cDNA was pre-amplified with Taqman probes for target genes (Fluidigm Preamp Master Mix) and PCR performed with Taqman probes for *Col3a1* and GAPDH for a housekeeper.

5.2.4 Matrix Functional Analyses

Biomechanical Testing*.** Previously described in *Section 3.2.4*. Briefly with the altered testing protocol. ***Sample Preparation. Patella-patellar tendon-tibia complexes were prepared for mechanical testing (n=12/group).[12,13] Excess soft tissue is removed, and cross-sectional area was measured using a custom laser device.[14] The tibia was potted using PMMA in a custom 3D-printed pot, which holds the bone at a 35° angle, to test the tendon at a physiologically relevant angle. ***Mechanical testing****.* Specimens will be tested utilizing the following protocol on an Instron 5848, as described:[13,15-17] preload to 0.2 N, 2) 10 cycles of preconditioning to 1.5% strain at 0.25 Hz, 3) return to gauge length and 4) ramp to failure at 0.05%/s.

5.2.5 Matrix Structural Analyses

***Tendon Fibril Structure*.** Method previously described in *Section 4.2.3*. Tendons for TEM (n=4/group) were fixed *in situ*, processed and embedded into Resin blocks. These blocks were sectioned at ~100 µm thickness, collected onto copper grids and stained for imaging with the JEOL 1400 transmission electron microscope (JEOL Ltd., Tokyo, Japan) fitted with a Gatan Orius widefield side mount CC Digital camera (Gatan Inc., Pleasanton, CA). 60 images per sample were collected at 60,000X magnification from the central portion of the uninjured PT or across the central wound. Images were randomly chosen in a masked manner and fibril diameter was measured utilizing a custom MATLAB (Natick, MA) code that thresholds the image and outlines the fibrils for measurement.

5.2.6 Statistics

Two-way repeated measures ANOVAs with post-hoc Bonferroni tests were used to assess the effects of genotype, injury and their interaction on *Col3a1* gene expression and quasistatic mechanical properties. Collagen fibril diameter distributions were compared by genotype using Kolmogorov-Smirnov tests. Significance was set at p≤0.05 (solid lines) and trends at p≤0.1 (dotted lines).

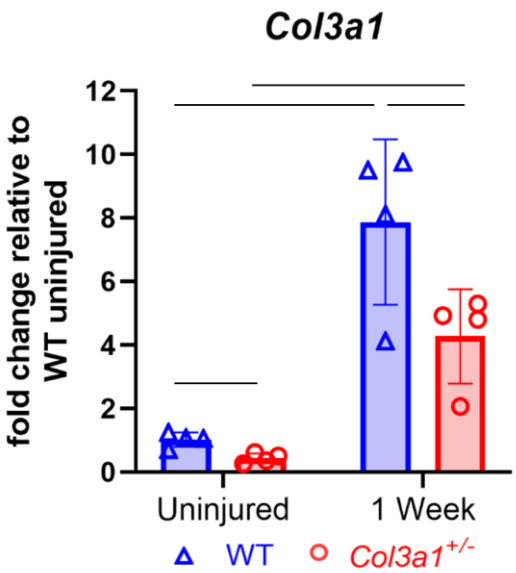

Figure 5.1: *Col3a1* Gene Expression. *Col3a1* expression increases post-injury in both genotypes. Expression is significantly increased in uninjured and 1-week WT tendons compared to Col3-deficient tendons. Solid lines denote statistical significance of p≤0.05. n=4 samples/genotype/timepoint.

5.3 – Results

5.3.1 Col3a1 expression was increased post-injury in both genotypes, and increased in both uninjured and injured WT compared to Col3-deficient tendons

Col3a1 gene expression increases post-injury in both WT and *Col3a1*$^{+/-}$ tendons (**Fig. 5.1**). Additionally, *Col3a1* expression is decreased in uninjured *Col3a1*$^{+/-}$ tendons compared to WT and a decrease is seen at 1-week post-injury. Adult tendons showed no differences in uninjured *Col3a1* expression (Chapter 3).

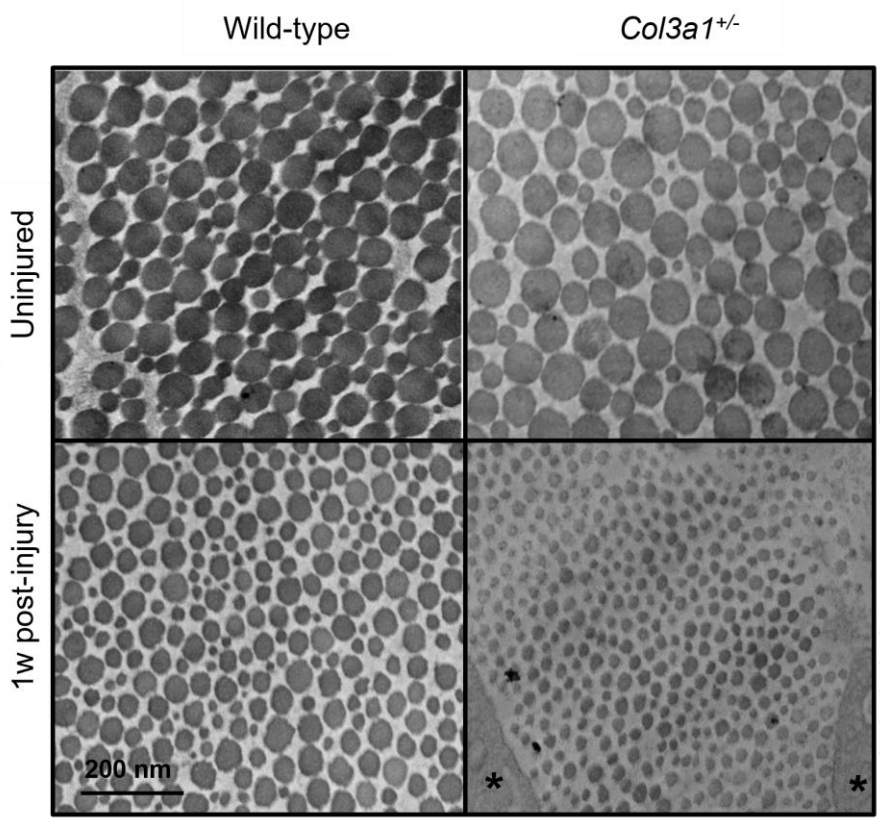

	Wild-type	*Col3a1*$^{+/-}$
Mean	92.9 nm	89.2 nm
Median (Q_2)	96.9 nm	92.8 nm
IQR (Q_3-Q_1)	47.0 nm	44.5 nm

	Wild-type	*Col3a1*$^{+/-}$
Mean	56.3 nm	50.1 nm
Median (Q_2)	52.6 nm	40.5 nm
IQR (Q_3-Q_1)	37.5 nm	26.5 nm

Figure 5.2: Representative Images of Collagen Fibrils from Tendon in Cross-Section
Fibril morphology is not qualitatively different between genotypes. A shift to smaller diameter fibrils can be seen post-injury in both genotypes. * denotes cellular region that was not quantified. n=4 tendons/group.

5.3.2 Fibril diameter distributions were altered in uninjured and 1-week injured Col3-deficient tendons

Normal circular cross-sectional profiles were seen in uninjured and injured tendons, with no qualitative differences noticed between genotypes (**Fig. 5.2**). Distinctly different distributions for WT and *Col3a1*$^{+/-}$ fibrils post-injury were seen, with *Col3a1*$^{+/-}$ tendons having a larger population of smaller and larger fibrils, and WT tendons having a less pronounced peak and more flat distribution (**Fig. 5.2, 5.3**). Fibril diameter analysis showed a shift to smaller diameter fibrils post-injury in both genotypes (**Fig. 5.3**).

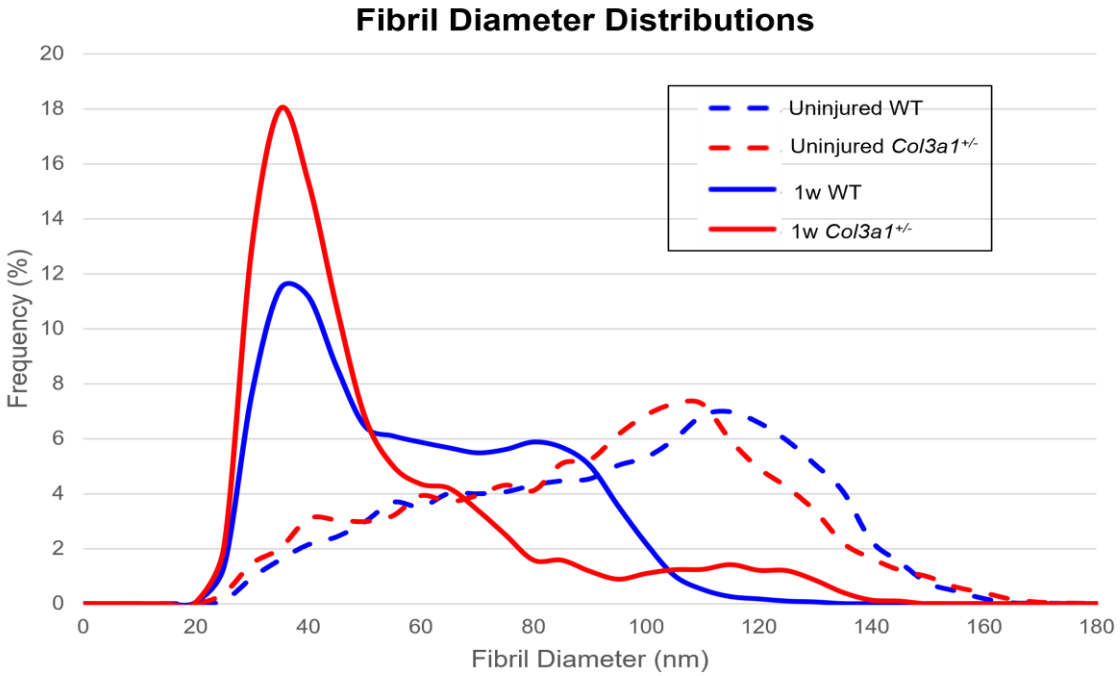

Figure 5.3: Fibril Diameter Distributions
Uninjured WT tendons had an increased population of larger fibrils when compared to *Col3a1*$^{+/-}$ tendons. n=4 tendons/group.

5.3.3 Failure load and stiffness were increased in Col3-deficient tendons compared to WT post-injury

Gauge length was no different between genotypes or following injury. Following injury, tendon cross-sectional area was increased in both WT and *Col3a1*$^{+/-}$ tendons, with *Col3a1*$^{+/-}$ tendons having a larger area than WT tendons (trend) (**Fig. 5.4B**). WT failure load and modulus (trend) decreased 1-week post-injury, with no effect of injury seen in *Col3a1*$^{+/-}$ tendons (**Fig. 5.5**). Failure stress (**Fig. 5.5C**) was decreased in both genotypes 1w following injury. Failure load and stiffness were increased 1-week post-injury in *Col3a1*$^{+/-}$ tendons compared to WT, with no other genotypic differences seen (**Fig. 5.5**).

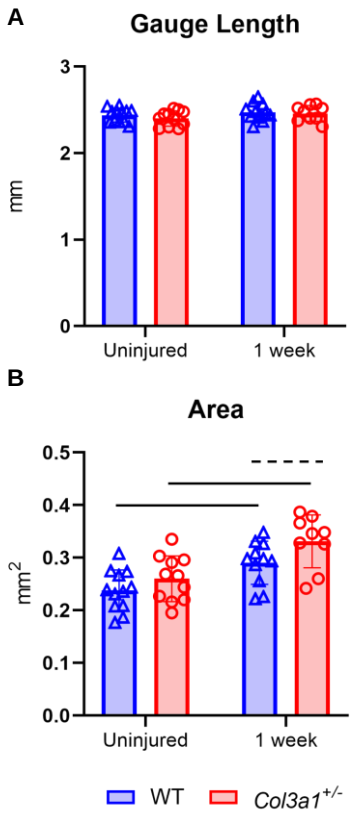

Figure 5.4. Tendon gauge length and cross-sectional area
(A) No changes were seen in gauge length in uninjured or injured tendons. (B) Area was increased post-injury in both genotypes when compared to uninjured tendons. Statistical significance of p≤0.05 is denoted by solid lines. Dashed lines indicate trends of p≤0.10. n=9-11 tendons/group.

5.4 – Discussion

This study shows that Col3 deficiency alters both mechanical properties and matrix structure 1-week post-injury in an adolescent murine patellar tendon injury model. *Col3a1* expression increased post-injury in both WT and *Col3a1*$^{+/-}$ tendons. This was expected due to characteristic increased expression of Col3 following tendon injury and predominantly Col3 provisional matrix being deposited in the injury void.[18,19] Additionally, compared to WT, *Col3a1* expression was decreased in uninjured and 1-week post-injury *Col3a1*$^{+/-}$ tendons. This is consistent with an increased deposition of provisional matrix, secondary to increased activation of fibroblasts in *Col3a1*$^{+/-}$ tendons. This is supported by previous work indicating that a reduction in Col3 increased myofibroblast activation.[5] A trending increase in cross-sectional area in *Col3a1*$^{+/-}$ tendons compared to WT tendons post-injury provides potential support for this idea, and further examination of later time-points is warranted as myofibroblast activation continues to increase later in tendon healing and fibroblasts proliferate through the proliferation phase. Data in adult tendons (Chapter 3) show an increase in area at 3-weeks post-injury, supporting the idea that matrix is continually laid down through the proliferative phase of tendon healing. Unlike adult mice, adolescent mice are known to have increased collagen deposition following injury, as well as a more robust healing

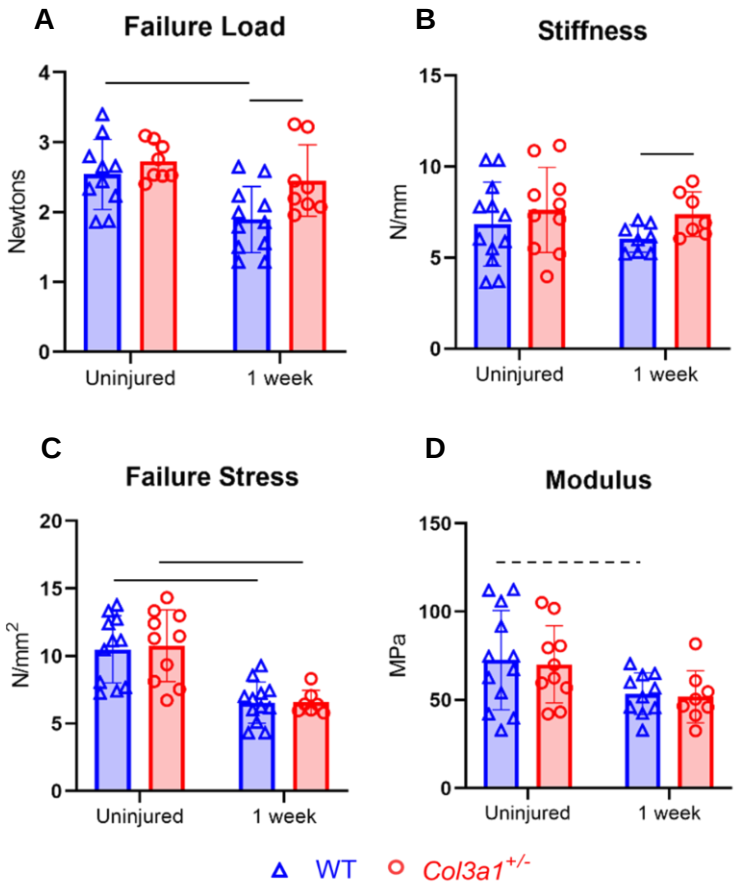

Figure 5.5. Quasistatic Mechanical Properties
Failure load and stiffness was increased in *Col3a1*$^{+/-}$ tendons 1w post-injury compared to WT. Failure stress was decreased in both genotypes following injury. Statistical significance of $p \leq 0.05$ is denoted by solid lines. Dashed lines indicate trends of $p \leq 0.10$. n=9-11 tendons/group.

response and regenerative phenotype.[20] Both genotypes showed increased tendon cross-sectional area following injury as healing tissue is deposited into the wound site, with *Col3a1*$^{+/-}$ area increasing to a larger degree. Differences between genotypes in structural properties post-injury between genotypes, without changes in material properties indicates that the area changes post-injury are influencing overall functional behavior.

Increased matrix deposition likely influences the healing population of cells migrating into the wound site, as a dense matrix during the initial inflammatory phase of tendon healing will inhibit cellular migration.[19,21] Denser, aligned matrix early in healing will improve mechanical

properties, but will be detrimental to long term healing, as the proper inflammatory environment will be necessary to have proper tendon healing. Decreases in failure stress in both genotypes following injury is due to increases in area without concurrent increases in failure load, indicating poor quality tissue following injury in both genotypes as would be expected 1-week post-injury. Solely increased activation of myofibroblasts will not improve tendon healing, and likely the density of the cellular infiltrate will have the most impact.[22]

WT tendons also had decreases in load and modulus, whereas *Col3a1*$^{+/-}$ tendons did not show any other changes post-injury. The difference in mechanical response between genotypes indicates altered healing in WT tendons compared to *Col3a1*$^{+/-}$ tendons. Additionally, fibril diameter analysis showed a more densely packed provisional matrix with smaller fibrils following injury in *Col3a1*$^{+/-}$ tendons, further indicating a hypersecretory state of myofibroblasts for Col1 post-injury. WT tendons had an increased population of midsize fibrils, but along with smaller fibrils, *Col3a1*$^{+/-}$ tendons also had an increased population of larger fibrils present in the injury site. While this may be explained by increased lateralization of fibrils, as is predicted in *Col3a1*$^{+/-}$ tendons,[6] at such an early time-point it is more likely to be enhanced wound contraction and engagement of existing boundary fibrils that are being drawn into the injury site. This population can explain increased stiffness during mechanical testing, and further supports the hypothesis that the provisional matrix deposited in *Col3a1*$^{+/-}$ tendons will not support cellular activity. While *Col3a1*$^{+/-}$ tendons have increased failure load following injury compared to WT tendons at this time point, the poor quality of healing tissue quantified in this study supports the likelihood of an important role of Col3 in dictating cellular activity and healing potential. Previous work in skin does indicate that a reduction in Col3 will influence cell-matrix engagement, along with myofibroblast activity.[4] Data presented in Chapter 3 shows increased myofibroblast activation in Col3-deficient tendons post-injury, as well as increased fiber realignment during loading indicating increased cell-matrix engagement. Additionally, in Chapter 4, uninjured Col3-deficient

tendons exhibited greater fibril sliding, also supporting increased engagement. As the patellar tendon defect is inherently small compared to the overall width and length of the tendon, increased contraction could make a significant difference in mechanical properties and overall architecture of the injury matrix.

This dysregulation supports our hypothesis that Col3 presence decreases lateral growth during fibrillogenesis,[6] as these are likely fibrils present from development versus new deposition. However, this population of larger fibrils is small in comparison to the population of fibrils centered around 40nm. This indicates that the hypersecretory state of myofibroblasts and increased deposition immediately post-injury will influence tendon mechanics to a greater degree at this stage of healing.

Notably, the uninjured distributions were unexpected, as we would have thought a shift towards larger fibrils in *Col3a1*$^{+/-}$ tendons would be noticeable, and as was seen in adult mice (See **Chapter 4**). However, the opposite was true, with WT tendons having an increased population of larger fibrils, potentially indicating that during development, Col3 may play a more nuanced role in fibrillogenesis, with less influence on fibril diameter, and more impact on fibril nucleation.[1,2,23] As tendons mature, continued fibrillogenesis may be impacted by Col3 expression, as there is a shift to emphasis on continued growth versus new fibril deposition.

A limitation of this study was the inability to look at time-points past 1-week post tendon injury. To further elucidate differences between adult and adolescent tendon healing and the role of Col3, we will need to examine later time-points to understand how fibril growth continues into later stages of healing, along with alterations to the cellular population and activity.

5.5 – References

1 Birk DE, Mayne R. Localization of collagen types I, III and V during tendon development. Changes in collagen types I and III are correlated with changes in fibril diameter. Eur J Cell Biol 1997;72:352–61.

2 Birk DE, Zycband EI, Woodruff S, Winkelmann DA, Trelstad RL. Collagen fibrillogenesis in situ: Fibril segments become long fibrils as the developing tendon matures. Dev Dyn 1997;208:291–8. https://doi.org/10.1002/(SICI)1097-0177(199703)208:3<291::AID-AJA1>3.0.CO;2-D.

3 Volk SW, Shah SR, Cohen AJ, Wang Y, Brisson BK, Vogel LK, et al. Type III collagen regulates osteoblastogenesis and the quantity of trabecular bone. Calcif Tissue Int 2014;94:621–31. https://doi.org/10.1007/s00223-014-9843-x.

4 Volk SW, Wang Y, Mauldin EA, Liechty KW, Adams SL. Diminished type III collagen promotes myofibroblast differentiation and increases scar deposition in cutaneous wound healing. Cells Tissues Organs 2011;194:25–37. https://doi.org/10.1159/000322399.

5 Wang C, Brisson BK, Terajima M, Li Q, Hoxha K, Han B, et al. Type III collagen is a key regulator of the collagen fibrillar structure and biomechanics of articular cartilage and meniscus. Matrix Biol 2020;85–86:47–67. https://doi.org/10.1016/j.matbio.2019.10.001.

6 Liu X, Wu H, Byrne M, Krane S, Jaenisch R. Type III collagen is crucial for collagen I fibrillogenesis and for normal cardiovascular development. Proc Natl Acad Sci U S A 1997;94:1852–6. https://doi.org/10.1073/pnas.94.5.1852.

7 Varani J, Dame MK, Rittie L, Fligiel SEG, Kang S, Fisher GJ, et al. Decreased collagen production in chronologically aged skin: Roles of age-dependent alteration in fibroblast function and defective mechanical stimulation. Am J Pathol 2006;168:1861–8. https://doi.org/10.2353/ajpath.2006.051302.

8 Cooper TK, Zhong Q, Krawczyk M, Tae HJ, Müller GA, Schubert R, et al. The Haploinsufficient Col3a1 Mouse as a Model for Vascular Ehlers-Danlos Syndrome. Vet Pathol 2010;47:1028–39. https://doi.org/10.1177/0300985810374842.

9 Freedman BR, Rodriguez AB, Hillin CD, Weiss SN, Han B, Han L, et al. Tendon healing affects the multiscale mechanical, structural and compositional response of tendon to quasi-static tensile loading. J R Soc Interface 2018;15:. https://doi.org/10.1098/rsif.2017.0880.

10 Freedman BR, Rodriguez AB, Leiphart RJ, Newton JB, Ban E, Sarver JJ, et al. Dynamic Loading and Tendon Healing Affect Multiscale Tendon Properties and ECM Stress Transmission. Sci Rep 2018;8:1–13. https://doi.org/10.1038/s41598-018-29060-y.

11 Ansorge HL, Beredjiklian PK, Soslowsky LJ. CD44 deficiency improves healing tendon mechanics and increases matrix and cytokine expression in a mouse patellar tendon injury model. J Orthop Res 2009;27:1386–91. https://doi.org/10.1002/jor.20891.

12 Dunkman AA, Buckley MR, Mienaltowski MJ, Adams SM, Thomas SJ, Satchell L, et al. Decorin expression is important for age-related changes in tendon structure and mechanical properties. Matrix Biol 2013;32:3–13. https://doi.org/10.1016/j.matbio.2012.11.005.

13 Dunkman AA, Buckley MR, Mienaltowski MJ, Adams SM, Thomas SJ, Kumar A, et al. The injury response of aged tendons in the absence of biglycan and decorin. Matrix Biol 2014;35:232–8. https://doi.org/10.1016/j.matbio.2013.10.008.

14 Favata M. Bioengineering PhD Thesis. University of Pennsylvania; 2006; 2006.

15 Ansorge HL, Adams S, Birk DE, Soslowsky LJ. Mechanical, compositional, and structural properties of the post-natal mouse Achilles tendon. Ann Biomed Eng 2011;39:1904–13. https://doi.org/10.1007/s10439-011-0299-0.

16 Johnston JM, Connizzo BK, Shetye SS, Robinson KA, Huegel J, Rodriguez AB, et al. Collagen V haploinsufficiency in a murine model of classic Ehlers–Danlos syndrome is associated with deficient structural and mechanical healing in tendons. J Orthop Res 2017;35:2707–15. https://doi.org/10.1002/jor.23571.

17 Lin TW, Cardenas L, Glaser DL, Soslowsky LJ. Tendon healing in interleukin-4 and interleukin-6 knockout mice. J Biomech 2006;39:61–9. https://doi.org/10.1016/j.jbiomech.2004.11.009.

18 Nichols AEC, Best KT, Loiselle AE. The cellular basis of fibrotic tendon healing: challenges and opportunities. Transl Res 2019:156–68. https://doi.org/10.1016/j.trsl.2019.02.002.

19 Dyment NA, Liu CF, Kazemi N, Aschbacher-Smith LE, Kenter K, Breidenbach AP, et al. The Paratenon Contributes to Scleraxis-Expressing Cells during Patellar Tendon Healing. PLoS One 2013;8:. https://doi.org/10.1371/journal.pone.0059944.

20 Walia B, Li TM, Crosio G, Montero AM, Huang AH. Axin2-lineage cells contribute to neonatal tendon regeneration. Connect Tissue Res 2022;63:530–43. https://doi.org/10.1080/03008207.2022.2036732.

21 Freedman BR, Gordon JA, Bhatt PR, Pardes AM, Thomas SJ, Sarver JJ, et al. Nonsurgical treatment and early return to activity leads to improved Achilles tendon fatigue mechanics and functional outcomes during early healing in an animal model. J Orthop Res 2016;34:2172–80. https://doi.org/10.1002/jor.23253.

22 Best KT, Korcari A, Mora KE, Nichols AE, Muscat SN, Knapp E, et al. Scleraxis-lineage cell depletion improves tendon healing and disrupts adult tendon homeostasis. Elife 2021;10:. https://doi.org/10.7554/eLife.62203.

23 Birk DE, Trelstad RL. Extracellular compartments in tendon morphogenesis: Collagen fibril, bundle, and macroaggregate formation. J Cell Biol 1986;103:231–40. https://doi.org/10.1083/jcb.103.1.231.

CHAPTER 6: Overall Conclusions and Future Directions

6.1 – Chapter Conclusions

6.1.1 Chapter 2 Conclusions

Overall, this study indicates that increased *Col5a1* expression post-injury is necessary to re-establish matrix architecture, alignment and cellularity throughout tendon healing. Utilizing our well establish mouse patellar tendon injury model,[1,2] we were able to examine Col5-deficient tendons throughout healing to determine healing alterations when compared to WT mice.

Col5-deficient tendons demonstrated altered and decreased healing compared to WT tendons. The lack of resolution in cellularity by 6-weeks post-injury in Col5-deficient tendons influenced overall decreased mechanical properties. While WT tendons returned to uninjured levels, this was not seen in Col5-deficient tendons. This finding supports the important role of Col5 in tissue laxity, stiffness and maintaining the hierarchical structure of the tendon. This potentially can be attributed to dysregulated matrix deposition immediately post-injury, when *Col5a1* fails to increase in expression to initiate fibrillogenesis and aid in matrix deposition. Col5 may play a role in fibroblast collagen deposition, and well as a regulatory role in the migration of healing cells to the wound site, explaining the different healing potential in a Haploinsufficient *c*EDS model.[3]

Altered cell-matrix engagement was also indicated, through delayed fiber realignment during mechanical loading, indicating a lack of efficiency in load transfer, and further implicating Col5 in fibril growth, interfibrillar interactions and overall matrix organization. Additionally, a goal of this work was to evaluate the response to Col5-deficiency in female tendons compared to previously studied male tendons.[4] This study indicated that structural properties of *Col5a1*$^{+/-}$ male tendons were affected by the reduction of Col5 to a greater degree than the structural properties of *Col5a1*$^{+/-}$ female tendons.

Future directions may include examining fibril diameter distribution in this mouse model to understand if a reduction in Col5 alters the diameter distribution and if this can explain the mechanical alterations and support the histological findings from this study. Additionally, we will examine the response to fatigue loading of these tendons to further understand how the dampened healing response of *Col5a1*$^{+/-}$ tendons responds to cyclic loading, as preservation of mechanical properties throughout repetitive loading is a characteristic quality of healthy tendon function.

6.1.2 Chapter 3 Conclusions

This study aimed to evaluate the role of Col3 in modulating matrix deposition and organization through tendon healing, utilizing a *Col3a1* Haploinsufficient female mouse model.[5] In order to study tendon healing, we utilized our highly reproducible patellar tendon injury surgery.[2,6] Throughout tendon remodeling and healing, elevated Col3 in later stages of recovery indicates increased scar tissue and reduced function. However, early in tendon healing, Col3 content is upregulated by 3-days post-injury, and Col3-rich provisional matrix fills the injury void.[7,8] This is a crucial component to encouraging cell migration, proliferation and the appropriate inflammatory response. Through this study, we evaluated how Col3-deficiency affected early and later stage matrix alignment, cellular populations and matrix deposition. We combined these assays with a focus on tendon mechanics to understand structural, compositional and functional relationships.

Col3 was downregulated post-injury with reduced localization to the injury site, confirming the appropriateness of our model. Increased activation of myofibroblasts and altered populations of macrophages in the injury site in Col3-deficient tendon indicates altered cellular activity post-injury. Additionally, a more highly aligned matrix was seen, potentially from a shift of the ratio of Col1:Col3 deposition into the injury void. The dampened proinflammatory response seen 1-week post-injury supported our hypothesis that lack of Col3 in the provisional

matrix would hinder migration of infiltrating vulnerary cells and dampen the initial inflammation. Proinflammatory interleukins returned to baseline by 3-weeks post-injury in Col3-deficient tendons, with a shift to upregulation of anti-inflammatory cytokines at 6-weeks, potentially influencing the predominance of characteristically anti-inflammatory macrophages phenotype by 6-weeks post-injury. The opposite was seen in WT tendons, indicating that an increased level of Col3 expression early in tendon healing leads to prolonged inflammation and a delay in anti-inflammatory cellular phenotype shift. Additionally, the downregulation of the proinflammatory alarmin IL-33 in Col3-deficient tendons further indicates that Col3 modulates the severity of the immune response through its influence on the provisional matrix structure and organization. This highlights a potential mechanism for increased retear rates following injury, where prolonged Col3 presence will result in inflammation dysregulation, and resultant fibrosis, disorganization and scarring. Lastly, our findings showed that the reduction in Col3 was able to preserve mechanical properties post-injury, raising an important point, that although matrix quality may not be improved, collagen fiber/fibril mechanics and response to load can still be functional. This is likely due to increased alignment and the ability to transfer load more effectively throughout testing. The increase in alignment was able to compensate for the decrease tissue quality and preserve mechanical properties early in tendon healing, however, long-term the environment will negatively impact function and degeneration.

In conclusion, early alterations to the tendon matrix negatively impact the inflammatory environment, affecting long-term healing. This ultimately leads to poorer outcomes and healing. Insufficient matrix production early on in healing sets the stage for decreased remodeling and a return to mechanical deficits later in healing, after an initial period of increased mechanical properties due to impacts in alignment and stiffness.

6.1.3 Chapter 4 Conclusions

ECM components are the part of the tissue that bears load, with composition, architecture and organization ultimately influencing tendon functional properties. This study evaluated fibril structure throughout healing and the influence on fibril structure on fibril mechanics and behavior.

Tendon interfibrillar interactions influence mechanical response and transfer of strain during loading.[10–12] While previous work examined this mechanism at the fiber level, utilizing alignment and fiber realignment analysis, this study evaluated tendon response at the fibril level. Matrix structure, not only organization plays a crucial role in behavior following loading. Due to tendon's unique structure and ability to bear repetitive load, the transfer of strain to conserve these properties is extremely physiologically important.[13] In this study, we showed fibril diameter differs between genotypes and post-injury. With a greater population of larger fibrils 3-weeks post-injury in Col3-deficient tendons, and a shift to a greater population of smaller fiber diameter at 6-weeks post-injury, we have shown that Col3 plays a differing role throughout healing in the regulation of fibrillogenesis. We saw a lack of fibril width growth in the later stage of healing in Col3-deficient tendons. This indicates earlier fibrillogenesis, and potentially more rapid in Col3-deficient tendons, slowing down in later healing. WT tendons continue to lateralize until at least 6-weeks. Due to the integration of Col3 within Col1 triple helices, and its tendency to be located on the lateral aspect of the fibrils, it was not surprising that lateral growth was affected post-injury with Col3 knockdown. Likely, fibrils in Col3-deficient tendons lateralize earlier post-injury, before reaching the maximum diameter, with Col3-expression impacting fibril nucleation. In normal tendon, the rate of fibril growth is slower, however continues for a longer period of time. The latest time-point is 6-weeks in this study, and WT tendons continue to lateralize until at least that time-point. Without Col3 present in the fibrils, unrestricted growth occurs immediately following injury, however, later healing relies on Col3 expression to continue growth.

Additionally, tissue quality is decreased with a reduction in Col3 by 6-weeks post-injury, indicating that while early lateralization may preserve mechanical properties in Col3-deficient tendons, the lack of continued growth is a detriment to the remodeling phase of healing.

Work examining fibril development has shown that mature fibril growth continues after the initial fibrils are deposited early in development. This idea following injury supports our data. Col3 is necessary for proper fibril initialization and early deposition, which can then continue lateralization into mature fibrils. While early fibril growth is rapid in Col3-deficient tendons, without proper development, long-term tissue quality is compromised. Lack of continued lateralization from 3 to 6-weeks post-injury in Col3-deficient tendons may predict a deficit in mature fibril development, supported by the reduction in mechanical properties at this time-point.

Additionally, this work showed differing responses to strain in Col3-deficient tendons at the fibril level. Increased sliding in the toe-region of tendon loading with Col3 knockdown indicates increased alignment and different interfibrillar interactions. D-period is determined primarily by Col1, indicating that Col3 expression dictates Col1 structure and function. Dysregulated cross-linking is likely influencing this behavior and can likely explain the increased stiffness during failure testing seen in Chapter 3. This also supports the increased, and rapid, fiber realignment when under increased strain (Chapter 3). This measure may be an early indicator of tissue quality compromise. Altered microscale mechanics will influence macroscale mechanics throughout healing, potentially contributing to decreasing stiffness, modulus and failure load in the remodeling phase. In early tendon healing Col3-deficiency increased myofibroblast activation, encouraging matrix engagement, alignment and fibril sliding. However, by 6-weeks post-injury, this increase was no longer apparent, contributing to the mechanism behind reducing mechanical properties throughout healing.

Both fibril size, organization and response to load influenced histological properties of the tendons. Fibril size and inter-fibrillar reactions influenced structure and organization, leading to cellular migration alterations, as indicated by a decreased inflammatory response early in healing with increased alignment in the Col3-deficient matrix. Cell-matrix interactions contributed to the progression of the immune response, including macrophage phenotypic switch from pro to anti-inflammatory. Additionally stiffer matrix with larger fibril diameters predicted a decreased pro-inflammatory response, followed by a faster switch of macrophage phenotype to an anti-inflammatory state.

Fibrillogenesis affects cell-matrix interactions, and the disruption to this process will impact overall structure. Early fibrillogenesis includes the formation of fibril intermediates by fibroblasts and is heavily influenced by the composition of the initial compartment, and in this case, the reduction of Col3 in the initial matrix. Increased activation of fibroblasts may contribute to increased nucleation and growth early post-injury. These intermediates are then organized into fibers and begin linear growth. This is then followed by lateral growth and formation of mature fibrils.

Non-collagenous matrix genes in general were downregulated to a greater extent in Col3-deficient tendons than WT tendons at 6-weeks, which may predict decreased tissue quality following remodeling. Proteoglycans affect both early fibrillogenesis and remodeling of provisional matrix into mature aligned matrix, providing a potential mechanism for increased mechanical properties early due to alignment and increased fibril diameters, as well as the decreased tissue quality alter in healing, when remodeling becomes the main process.

This study supported our hypothesis that Col3-deficiency leads to dysregulated fibrillogenesis, which ultimately affects matrix organization, fibril structure and ECM engagement under load. This work coupled with the findings from Chapter 3 indicate that alterations at the

fibril levels affect whole tissue mechanics, and therefore, reiterate that it is necessary to study tendon mechanics at all hierarchical levels to understand the interplay between length scales.

6.1.4 Chapter 5 Conclusions

Col3 is present at high levels throughout postnatal tendon development, however, its role in matrix structure and organization is unknown. Col3-rich matrix plays a crucial role in the development and growth of tendons and is expected to be implicated in response to injury and functional outcomes. This study elucidated differences in stiffness, organization and density of a Col3-deficient matrix during adolescence (P30).

Increased mechanical properties of Col3-deficient tendons and greater number of small fibrils is likely due to overactivity of myofibroblasts 1-week post-injury, as was seen in P90 mice. At 30-days of age, tendon fibrillogenesis is generally at the end of the assembly phase and the middle of the lateral growth phase. Col3-deficiency during tendon healing led to increased nucleation, indicated by more small fibrils post-injury, but also increased population of larger fibrils because Col3 is known to prevent lateralization of fibrils. To better compare to the P90 data, looking at future timepoints would be useful, as we could understand if this pattern continues or if the population of larger fibrils increases as it did in P90 mice. As tendons mature, later fibrillogenesis may be impacted by Col3 expression, as we saw in Chapter 3.

No uninjured differences in mechanical properties were seen, however, there was a greater population of smaller fibrils in WT uninjured tendons. This was the opposite of what we saw in adult tendons, where Col3-deficient tendons had a greater population of larger fibrils than WT tendons, with no differences in mechanical properties. Structure is not affecting function in uninjured tissue. There is likely an effect of Col3 early in fibril development, which changes later in fibrillogenesis post-injury.

In conclusion, this work is the beginning of a possible developmental study. Young animals are known to be more biologically active and have a more robust response to injury,

likely with increased expression and deposition of Col3. Other studies have shown that healing wounds that are comparatively enriched in Col3 (such as those of the African spiny mouse) are distinct in their ability to heal in a scarless manner.[14,15] Evaluation of multiple ages in tendons healing becomes increasingly important as you move closer to a therapeutic phase and would need to apply to multiple populations of patients.

6.1.5 Overall Conclusions

Overall, this body of work attempts to explain the role of fibrillar collagen in tendon healing. Through utilizing genetic knockdown models,[3,5] we have been able to isolate both Col3 and Col5 to evaluate the differential healing response with a reduction in specific collagen expression. Although a small percentage of overall matrix, both Col3 and Col5 play important roles in development, homeostasis, and response to injury. Both collagens play a role in fibrillogenesis, and likely, this influences the extent that they effect matrix deposition and remodeling. Additionally, increased expression in the early stages of healing sets the framework for later collagen deposition and remodeling. Findings are summarized in **Figure 6.1**, asterisks highlighting similarities between the effects of Col5 and Col3-deficiency.

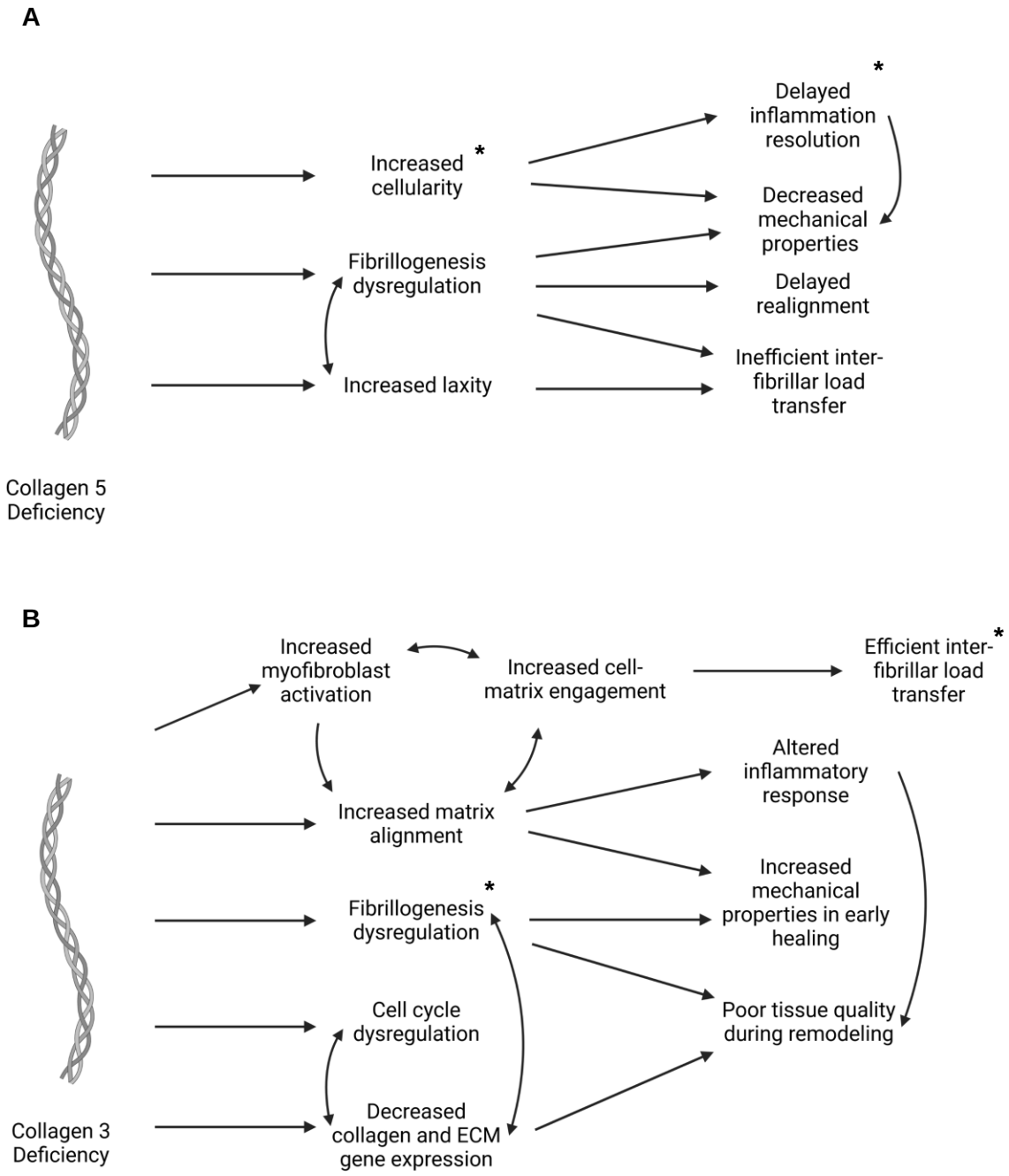

Figure 6.1: Summary of Structural and Functional Changes Related to Alterations in Fibrillar Collagen. * indicates similarities between Col3 and Col5.

Col5 alone influences the nucleation of new fibrils, and the location of newly deposited fibrils. Clinically this leads to increased joint laxity, tissue elasticity and poor healing. A shift to smaller, likely reduced stiffness fibrils supports these clinical findings. Additionally, whole tissue mechanics indicates reduced stiffness in Col5-deficient tendons, as we could expect.

Interestingly, our Col3-deficient tendons increased in stiffness post-injury compared to WT tendons. Fibril diameter increased with Col3-deficiency early in healing, and an increase in mechanical properties was seen. By later healing, this increased population was no longer apparent, and interestingly, mechanical properties showed decreased healing compared to WT. Deposited matrix post-injury sets the stage for future remodeling and long-term tendon healing. Increased gene expression immediately following injury is crucial for proper healing, as this influences composition of the new matrix. Additionally, the composition will dictate cell-ECM interactions, the cellular environment, and resolution of inflammation.

Col3-deficiency results in deposited matrix having less Col3 to remodel in general, and overcompensation of Col1 deposition. With a reduction in Col3, existing Col1 fibrils show greater alignment. Additionally, increased myofibroblast activity contributes to the aligned matrix, realignment properties and overall increase in mechanical properties, due to increased cell-matrix engagement and contraction.

Overall, it is apparent that both fibrillar collagens studied play a role in tendon healing, through modulation of fibrillogenesis, matrix organization and engagement. While Col5 seems to be necessary for matrix integrity throughout the time course studied, Col3 seems to play a larger role in fibrillogenesis early on, as well as playing a large role in influencing cellular populations during the inflammatory phase.

Long term healing is negatively impacted by a reduction in Col3 and Col5, and the initial increase following injury is crucial. As we saw, the reduced expression of both collagens in early tendon healing resulted in functional and structural changes.

6.2 – Future Directions

6.2.1 Examine matrix cross-linking and additional interfibrillar interactions in the conventional mouse model

ECM structure, organization and engagement was shown to influence whole tissue mechanical properties and functional improvements in a conventional *Col3a1* knockdown model.[5] One limitation from the previous work was the lack of cross-linking analysis on the matrix, and evaluation of integrin engagement and matrix localization. Completion of these assays could further our understanding of the impact of both matrix organization and structure to mechanical behavior. Additionally, evaluation of fibril mechanical behavior post-injury will advance our understanding of the healing matrix and elucidate specific outcomes of interfibrillar interactions directly related to the composition of the matrix. Additionally, our work showed interesting findings regarding cellular populations present in the injury site, and further evaluation is needed. Completing flow cytometry of injured tissue would better characterize the population of healing cells.

6.2.2 Evaluate the temporal response of Col3 throughout tendon healing

Currently we are utilizing a novel conditional Col3 knockdown model to understand the unique temporal role of Col3 throughout healing and more specifically, to rigorously analyze the targeted role of Col3 by evaluating the dose response in an otherwise normal matrix. Col3 is crucial during early wound healing, affecting matrix structure and function, likely influencing long-term healing.

Thus far, a novel inducible Col3 deficient (i.e., *Col3a1*$^{F/+}$, *Col3a1*$^{F/F}$) mouse model has been developed to determine the dose-dependent effects of Col3 by temporal targeting of Col3. Col3 knockdown has been established (**Fig. 6.2**). Skin samples analyzed 6-weeks post Tamoxifen administration show continued knockdown, justifying this as an appropriate model for our study and time-points.

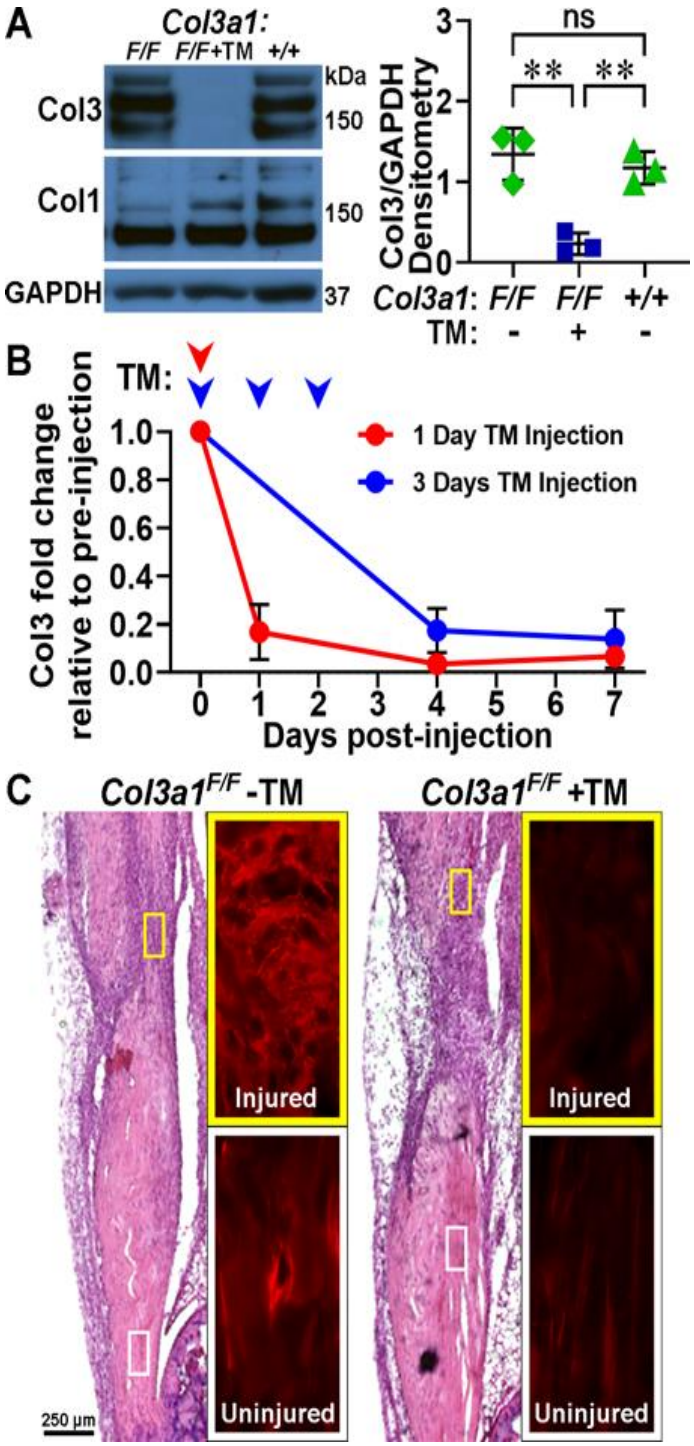

Figure 6.2: Efficient knockout of the floxed Col3 allele in the ERT2 conditional *Col3a1* knockout model. (**A/B**) Efficient reduction of Col3 protein in skin samples of TM-treated *Col3a1*$^{F/F}$ mice but not *Col3a1*$^{+/+}$ or untreated *Col3a1*$^{F/F}$ mice; **p<0.01. TM does not affect Col1 levels. (**B**) Time course showing one TM dose induces efficient knockdown of Col3 mRNA levels in *Col3a1*$^{F/F}$ mice (note injection done immediately after d0 tissue harvest; N=4/group). (**C**) H&E images of injured patellar tendons (7 days post injury) from *Col3a1*$^{F/F}$-TM (control) and *Col3a1*$^{F/F}$+TM mice. Immunofluorescent labelling of Col3 in injured and uninjured PT regions shows drastically decreased levels of Col3 (red) in TM treated animals. (**C**) Representative H&E stained sections of injured tendons (1 week post injury) in *Col3a1*$^{F/F}$ mice receiving vehicle (-TM; control) or TM. Insets show reduced Col3 immunofluorescence in injury site (yellow box) and flanking uninjured site (white box) in TM treated *Col3a1*$^{F/F}$ mice compared to control littermates.

In skin wounds, Col3 synthesis promotes cellular recruitment in early healing. In later healing, its presence protects against scar formation[16] by directing an open weave matrix microarchitecture that can be remodeled into a matrix more resembling unwounded skin than highly aligned scar matrix. However, and importantly, preferred collagen remodeling in tendon

repair diverges from skin wounds, relying on formation of a highly aligned matrix at later stages. Thus, while Col3 may orchestrate cellular activities and fate that are critical for an optimal reparative response post-injury at early stages in both tissues, its persistent expression in the remodeling phase may compromise the desired healing response in tendon.

Using this innovative approach, we will define the regulatory roles of Col3 throughout tendon healing at the time of injury, during the early proliferative phase, and during remodeling. In addition, by knockdown of Col3 in young, middle-aged, and old animals, we will evaluate the coordinate effects of aging on tendon healing with altered Col3. Understanding the role of Col3 throughout tendon healing will lead to clinically relevant insights to improve outcomes following tendon injury in patients of varying ages.

This study will provide insight into potential approaches to modulate Col3 expression and activity throughout healing. Determining the important, dynamic role throughout healing will allow future studies to capitalize on this knowledge to improve the infiltration of healing cells, increase vascularization early, and promote scarless healing. This will establish a necessary foundation for developing Col3-inspired therapies that optimize tendon healing and will ultimately have a profound impact on tendon healing, thereby decreasing healthcare expenditures and improving patient quality of life.

A summary of the existing aims is listed below:

Aim 1: To define the age-sensitive mechanistic role(s) of Col3 throughout tendon healing by knocking down Col3 at the time of tendon injury.

Hypothesis: The early, post-injury Col3-deficient matrix will fail to support recruitment and migration of tendon progenitor and immune cells, resulting in inferior tendon healing due to a lack of foundational cellular and structural components necessary for optimal healing. We also

hypothesize that Col3 deficiency will further compromise tendon healing in older mice, due to exacerbation of deficiencies in cell recruitment and activities.

Aim 1 Anticipated Results:

In Aim 1, we will investigate the age-sensitive mechanistic role of Col3 throughout tendon healing following knockdown at the time of injury, to examine its role in the inflammatory phase as well as compounding effects in later healing phases (**Fig.6.3**). Within days of injury, Col3 becomes a major driver of the provisional matrix filling the wound void.[17–19] Based on our data, a reduction in Col3 would result in a dose-dependent decrease in matrix mechanical properties with a concomitant loss of ECM porosity secondary to increased alignment and a shift to straighter, longer, and wider fibers of the initial wound scaffold in ERT2-*Col3a1*$^{F/+}$ and ERT2-*Col3a1*$^{F/F}$ mice.

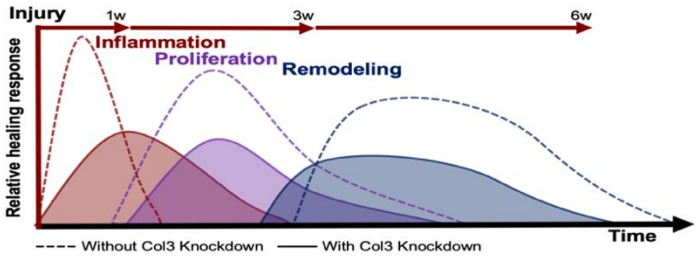

Figure 6.3: Aim 1 expected outcomes of Col3 loss at the time of injury (d0). Tendon healing will be assessed at 1-, 3- and 6w post injury and compared to healing without knockdown.

Aim 2: To elucidate the age-sensitive mechanistic role(s) of Col3 in directing reparative cell activities and prolonged effects of knocking down Col3 during the proliferative phase of tendon healing.

Hypothesis: Reduced Col3 expression in the early proliferative phase of tendon healing will result in a low density, but highly aligned matrix comprised of wider fibers uncharacteristic of early healing, impairing neovascularization and resolution of inflammation, as well as limiting infiltration of tendon fibroblasts that are necessary to produce and realign a collagen rich matrix.

Aim 2 Anticipated Results:

In Aim 2, we will investigate the age-sensitive mechanistic role of Col3 in directing reparative cell activities and prolonged implications by knocking down Col3 during the proliferative phase of tendon healing (**Fig. 6.4**). We anticipate that reducing Col3 expression early in the proliferative phase will impair deposition of a typically Col3-rich matrix, resulting in a matrix that is deficient in fibrillar collagen but stiffer and more aligned. As Col1 production begins, we also expect the loss of Col3 to result in abnormally shaped, larger fibrils.[20] Decreased matrix production by a paucity of fibroblasts is further compounded by an increase in protease activity anticipated in a Col3-deficient state.[21]

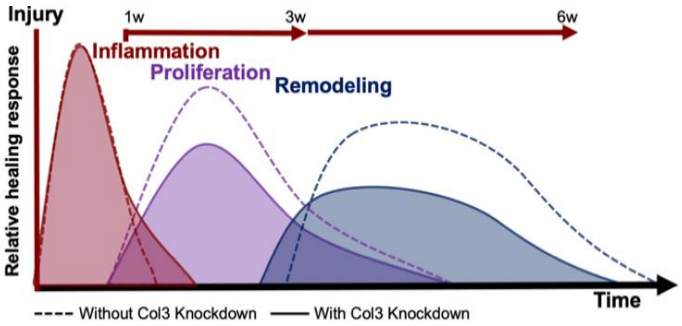

Figure 6.4: Aim 2 expected outcomes of Col3 loss at 1w post-injury. Tendon healing will be assessed at 3w and 6w post-injury and compared to healing without knockdown.

Aim 3 Anticipated Results:

In Aim 3, we will investigate the age-sensitive mechanistic role of Col3 in tendon repair by knocking down Col3 during the remodeling phase (**Fig. 6.5**). With this design, there are no effects on the inflammatory or proliferative phases.

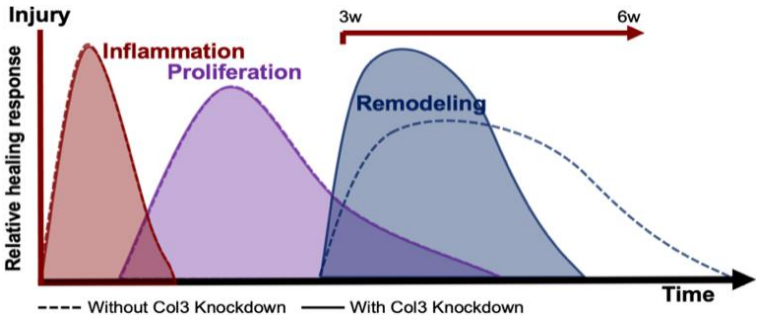

Figure 6.5: Aim 3 expected healing outcomes after Col3 loss at 3w post-injury. Tendon healing will be assessed at 6w post-injury and compared to healing without knockdown.

6.2.3 Col3 knockdown impacts on aged tendon

Aging impacts tendon health, with increased incidence of rupture with age, and patients presenting with chronic degeneration. The high frequency of tendon rupture across ages, and the high rate of long-term complications underscores the need to understand the tendon response to injury throughout aging and identify drivers of scarless tendon repair.[23,24] Our recent work has chosen 90- and 365-day old mice to correspond to young and aged adults, respectively. Our work, and that of others, has established the correlation between age and the decline in post-injury tendon mechanical properties.[25] While younger individuals heal better than aged patients, there are increased demands in this group, often leading to re-injury, particularly in athletes.[26] Elucidation of mechanisms that drive a robust healing response and subsequent remodeling toward a scarless state is essential for future development of a tailored therapeutic for improved tendon healing of all ages.

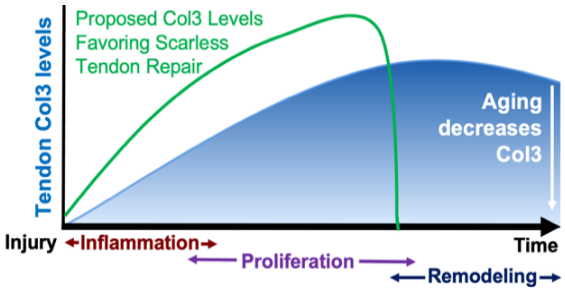

Figure 6.6: Col3 levels throughout physiologic tendon healing, the impact of age and proposed strategy to optimize healing through temporal Col3 regulation.

6.2.4 Sex differences in Col3 knockdown

Tendon biology and healing are affected by sex, with a differing healing response in females being attributed to decreased collagen synthesis[27–29] and altered expression of important inflammatory and repair factors.[30] Further, Col3 levels are increased by estrogen and decreased by hypoestrogenic states (i.e., menopause)[27] and *Col3*$^{+/-}$ aged male mice are predisposed to vascular lesions,[5] highlighting the need to study both sexes. Thus, the proposed studies will define the roles of Col3 in tendon healing of skeletally mature young, middle-aged

and old mice, and will examine both sexes, to determine mechanisms underlying age-related and sex-related differences in tendon biomechanical and biological properties and how this relates to Col3 levels.

6.2.5 Developmental effects of Col3 knockdown

Our findings indicated the P30 tendons healed differently than P90 tendons, potentially due to the overcompensation of Col3 expression post-injury in P30 tendons. Col3 plays a major role in tendon development, and healing matrix likely differs in composition, organization, and structure than in adult mice.

Deficiency of Col3 results in extreme phenotypes in other soft tissues of the body, indicating a role in proper development of tissue. Throughout tendon postnatal development, Col3 is highly expressed, however the role and importance has not been isolated. The alterations to the tendon matrix and cellular environment with a decreased expression of Col3 will provide valuable insight into the compensatory mechanisms and resultant long-term developmental phenotypes in tendon, where the matrix will be more aligned with a higher Col1:Col3 ratio. A previous study showed increased fibril diameter with a reduction of Col3 throughout development,[31] however, this could be the result of increased Col1 fibrils, or dysregulation of fibrillogenesis, and therefore needs to be examined further.

Therefore, evaluation of Col3-deficiency throughout development will allow us to study Col3-deficiency in a model that is closer to a regenerative model. This will allow us to evaluate whether Col3 plays a critical role in the increased regenerative phenotype seen in younger animals.

6.3 – References

1 Dunkman AA, Buckley MR, Mienaltowski MJ, Adams SM, Thomas SJ, Satchell L, et al. The tendon injury response is influenced by decorin and biglycan. Ann Biomed Eng 2014;42:619–30. https://doi.org/10.1007/s10439-013-0915-2.

2 Lin TW, Cardenas L, Glaser DL, Soslowsky LJ. Tendon healing in interleukin-4 and interleukin-6 knockout mice. J Biomech 2006;39:61–9. https://doi.org/10.1016/J.JBIOMECH.2004.11.009.

3 Wenstrup RJ, Florer JB, Davidson JM, Phillips CL, Pfeiffer BJ, Menezes DW, et al. Murine model of the Ehlers-Danlos syndrome: col5a1 haploinsufficiency disrupts collagen fibril assembly at multiple stages. J Biol Chem 2006;281:12888–95. https://doi.org/10.1074/jbc.M511528200.

4 Johnston JM, Connizzo BK, Shetye SS, Robinson KA, Huegel J, Rodriguez AB, et al. Collagen V haploinsufficiency in a murine model of classic Ehlers–Danlos syndrome is associated with deficient structural and mechanical healing in tendons. J Orthop Res 2017;35:2707–15. https://doi.org/10.1002/jor.23571.

5 Cooper TK, Zhong Q, Krawczyk M, Tae HJ, Müller GA, Schubert R, et al. The Haploinsufficient Col3a1 Mouse as a Model for Vascular Ehlers-Danlos Syndrome. Vet Pathol 2010;47:1028–39. https://doi.org/10.1177/0300985810374842.

6 Dunkman AA, Buckley MR, Mienaltowski MJ, Adams SM, Thomas SJ, Satchell L, et al. The tendon injury response is influenced by decorin and biglycan. Ann Biomed Eng 2014;42:619–30. https://doi.org/10.1007/s10439-013-0915-2.

7 Best KT, Korcari A, Mora KE, Nichols AEC, Muscat SN, Knapp E, et al. Scleraxis-lineage cell depletion improves tendon healing and disrupts adult tendon homeostasis. Elife 2021;10:1–64. https://doi.org/10.7554/eLife.62203.

8 Dyment NA, Liu CF, Kazemi N, Aschbacher-Smith LE, Kenter K, Breidenbach AP, et al. The Paratenon Contributes to Scleraxis-Expressing Cells during Patellar Tendon Healing. PLoS One 2013;8:. https://doi.org/10.1371/journal.pone.0059944.

9 Witherel CE, Sao K, Brisson BK, Han B, Volk SW, Petrie RJ, et al. Regulation of extracellular matrix assembly and structure by hybrid M1/M2 macrophages. Biomaterials 2021. https://doi.org/10.1016/j.biomaterials.2021.120667

10 Kwansa AL, De Vita R, Freeman JW. Mechanical recruitment of N- and C-crosslinks in collagen type I. Matrix Biol 2014;34:161–9. https://doi.org/10.1016/j.matbio.2013.10.012.

11 Eekhoff JD, Fang F, Lake SP. Multiscale mechanical effects of native collagen cross-linking in tendon. Connect Tissue Res 2018:410–22. https://doi.org/10.1080/03008207.2018.1449837.

12 Darrieutort-Laffite C, Beach ZM, Weiss SN, Eekhoff JD, Soslowsky LJ. Knockdown of biglycan reveals an important role in maintenance of structural and mechanical properties during tendon aging. J Orthop Res 2023. https://doi.org/10.1002/jor.25536.

13 Alshomer F, Chaves C, Kalaskar DM. Advances in Tendon and Ligament Tissue Engineering: Materials Perspective. J Mater 2018;2018:1–17. https://doi.org/10.1155/2018/9868151.

14 Seifert AW, Kiama SG, Seifert MG, Goheen JR, Palmer TM, Maden M. Skin shedding and tissue regeneration in African spiny mice (Acomys). Nature 2012;489:561–5. https://doi.org/10.1038/nature11499.

15 Xue M, Jackson CJ. Extracellular Matrix Reorganization During Wound Healing and Its Impact on Abnormal Scarring. Adv Wound Care 2015;4:119–36. https://doi.org/10.1089/wound.2013.0485.

16 Volk SW, Wang Y, Mauldin EA, Liechty KW, Adams SL. Diminished type III collagen promotes myofibroblast differentiation and increases scar deposition in cutaneous wound healing. Cells Tissues Organs 2011;194:25–37. https://doi.org/10.1159/000322399.

17 Lalley AL, Dyment NA, Kazemi N, Kenter K, Gooch C, Rowe DW, et al. Improved and biological outcomes in the MRL/MpJ murine strain following a full-length patellar tendon injury. J Orthop Res 2015;33:1693–703. https://doi.org/10.1002/jor.22928.

18 Maffulli N, Ewen SWB, Waterston SW, Reaper J, Barrass V. Tenocytes from ruptured and tendinopathic achilles tendons produce greater quantities of type III collagen than tenocytes from normal achilles tendons: An in vitro model of human tendon healing. Am J Sports Med 2000;28:499–505. https://doi.org/10.1177/03635465000280040901.

19 Liu SH, Yang R-S A-SR. Collagen in tendon, ligament, and bone healing. A current review 1995:265–278.

20 Liu X, Wu H, Byrne M, Krane S, Jaenisch R. Type III collagen is crucial for collagen I fibrillogenesis and for normal cardiovascular development. Proc Natl Acad Sci U S A 1997;94:1852–6. https://doi.org/10.1073/pnas.94.5.1852.

21 Briest W, Cooper TK, Tae HJ, Krawczyk M, McDonnell NB, Talan MI. Doxycycline ameliorates the susceptibility to aortic lesions in a mouse model for the vascular type of ehlers-danlos syndrome. J Pharmacol Exp Ther 2011;337:621–7. https://doi.org/10.1124/jpet.110.177782.

22 Schoenenberger AD, Foolen J, Moor P, Silvan U, Snedeker JG. Substrate fiber alignment mediates tendon cell response to inflammatory signaling. Acta Biomater 2018;71:306–17. https://doi.org/10.1016/j.actbio.2018.03.004.

23 Dressler MR, Butler DL, Wenstrup R, Awad HA, Smith F, Boivin GP. A potential mechanism for age-related declines in patellar tendon biomechanics. J Orthop Res 2002;20:1315–22. https://doi.org/10.1016/S0736-0266(02)00052-9.

24 Buckwalter JA, Heckman JD, Petrie DP. Aging of the north American population: New challenges for orthopaedics. J Bone Jt Surg - Ser A 2003;85:748–58. https://doi.org/10.2106/00004623-200304000-00024.

25 Dunkman AA, Buckley MR, Mienaltowski MJ, Adams SM, Thomas SJ, Kumar A, et al. The injury response of aged tendons in the absence of biglycan and decorin. Matrix Biol 2014;35:232–8. https://doi.org/10.1016/j.matbio.2013.10.008.

26 Lemme NJ, Li NY, DeFroda SF, Kleiner J, Owens BD. Epidemiology of Achilles Tendon Ruptures in the United States: Athletic and Nonathletic Injuries From 2012 to 2016. Orthop J Sport Med 2018;6:. https://doi.org/10.1177/2325967118808238.

27 Stevenson S, Thornton J. Effect of estrogens on skin aging and the potential role of SERMs. Clin Interv Aging 2007:283–97. https://doi.org/10.2147/cia.s798.

28 Yu WD, Panossian V, Hatch JD, Liu SH, Finerman GAM. Combined effects of estrogen and progesterone on the anterior cruciate ligament. Clin Orthop Relat Res 2001:268–81. https://doi.org/10.1097/00003086-200102000-00031.

29 Kjaer M, Magnusson P, Krogsgaard M, Moller JB, Olesen J, Heinemeier K, et al. Extracellular matrix adaptation of tendon and skeletal muscle to exercise. J Anat 2006;208:445–50. https://doi.org/10.1111/j.1469-7580.2006.00549.x.

30 Hart DA , Archambault JM, Kydd A, Reno C, Frank CB HW. Gender and neurogenic variables in tendon biology and repetitive motion disorders. Clin Orthop Relat Res 1998;351:44–56.

31 Birk DE, Mayne R. Localization of collagen types I, III and V during tendon development. Changes in collagen types I and III are correlated with changes in fibril diameter. Eur J Cell Biol 1997;72:352–61.

APPENDIX A: Protocols

Adapted for Soslowsky Lab from Volk and Dyment Laboratories at the University of Pennsylvania

Assay: Collagen 3/αSMA Immunofluorescent staining of mouse PT sections

Materials

- *Rinse:* 1X PBS and PBS-T (0.02% Tween 20)
- *Blocking buffer:* Odyssey PBS from LI-COR (4°C) + 5% Normal Donkey Serum (-20°C)
- *Antigen Retrieval:* Pepsin (4°C) 1mg/mL diluted in 0.01N HCl
- *1˚ antibodies* (centrifuge for 1 min and use supernatant):
    - Col3 made in goat (Southern Biotech: 1330-01)
    - αSMA conjugated:
- *2˚ antibody* (centrifuge for 1 min and use supernatant): Donkey anti-goat 647
- *Mounting medium:* 50% glycerol with 1/1000 Hoechst in 1X PBS (4˚C protected from light)
- Cover slips

Procedure

<u>Day 1</u>

1. Place slides in d-H2O to rehydrate.
2. Pap pen and label slides.
3. Pipette on 1mg/mL pepsin for 45 min @ 37°C.
4. Rinse with PBS+T 3x5 min at RT.
5. Incubate with blocking solution for 45 min at RT.

Protect from light from this point forward.

6. Incubate with 1˚ antibodies diluted (1:1000 Col3; 1:250 αSMA) in blocking buffer overnight at 4˚C.

<u>Day 2</u>

7. Rinse with PBS+T 3x5 min at RT.
8. Incubate with 2˚ antibody diluted (1:500 donkey anti-goat) in blocking solution for 1 h RT.
9. Rinse with PBS+T 3x 5 min at RT.
10. Coverslip with mounting medium.
11. Store at 4˚C protected from light and image within one week.

Optimizable parameters

- Permeabilization duration
- Blocking duration
- Antigen retrieval
- 1˚ antibody concentration and incubation duration
- 2˚ antibody concentration and incubation duration

Adapted for Soslowsky Lab from Volk and Dyment Laboratories at the University of Pennsylvania

Purpose: Ki67 Immunofluorescent staining of mouse PT sections

Materials

- *Rinse:* 1X PBS and PBS-T (0.02% Tween 20)
- *Blocking buffer:* Odyssey PBS from LI-COR (4°C) + 5% Normal goat Serum (-20°C) + 0.02% Tween 20 + 1% BSA
- *Antigen Retrieval:* ProK (1:1000 TE Buffer)
- *1˚ antibodies* (centrifuge for 1 min and use supernatant):
    - Ki67 made in Rabbit (ab16667)
- *2˚ antibody* (centrifuge for 1 min and use supernatant): goat anti-Rabbit 647
- *Mounting medium:* 50% glycerol with 1/1000 Hoechst in 1X PBS (4˚C protected from light)
- Cover slips

Procedure

<u>Day 1</u>

12. Place slides in d-H2O to rehydrate.
13. Pap pen and label slides.
14. Pipette on Prok dilution for 30 min @ 37°C.
15. Rinse with PBS+T 3x5 min at RT.
16. Incubate with blocking solution for 45 min at RT.
17. Incubate with 1˚ antibody diluted (1:100) in blocking buffer overnight at 4˚C.

<u>Day 2</u>

18. Rinse with PBS+T 3x5 min at RT.
19. Incubate with 2˚ antibody diluted (1:500 goat anti-rabbit) in blocking solution for 1 h RT.
20. Rinse with PBS+T 3x 5 min at RT.
21. Coverslip with mounting medium.
22. Store at 4˚C protected from light and image within one week.

Optimizable parameters

- Permeabilization duration
- Blocking duration
- Antigen retrieval
- 1˚ antibody concentration and incubation duration
- 2˚ antibody concentration and incubation duration

Soslowsky Lab Protocol

Purpose: F480, iNOS, CD206 Immunofluorescent staining of mouse PT sections

Materials

- *Rinse:* 1X PBS and PBS-T (0.02% Tween 20)
- *Blocking buffer:* Odyssey PBS from LI-COR (4°C) + 5% Normal Donkey Serum (-20°C) + 0.02% Tween 20 + 1% BSA
- *Antigen Retrieval:* ProK (1:1000 TE Buffer)
- *1˚ antibodies* (centrifuge for 1 min and use supernatant):
- *2˚ antibody* (centrifuge for 1 min and use supernatant):
- *Mounting medium:* 50% glycerol with 1/1000 Hoechst in 1X PBS (4˚C protected from light)
- Cover slips

Procedure

<u>Day 1</u>

23. Place slides in d-H2O to rehydrate.
24. Pap pen and label slides.
25. Pipette on Prok dilution for 30 min @ 37°C.
26. Rinse with PBS+T 3x5 min at RT.
27. Incubate with blocking solution for 45 min at RT.
28. Incubate with 1˚ antibody diluted in blocking buffer (1:25 F4/80, 1:50 iNOS, 1:50 CD206) in overnight at 4˚C.

<u>Day 2</u>

29. Rinse with PBS+T 3x5 min at RT.
30. Incubate with 2˚ antibody diluted (1:100 Donkey Anti-Rat AF 488 for F4-80, 1:100 Donkey Anti-Rabbit AF 555 for iNOS, 1:100 Donkey-Anti Goat AF 647 for CD206) in blocking solution for 1 h RT.
31. Rinse with PBS 3x 5 min at RT.
32. Coverslip with mounting medium.
33. Store at 4˚C protected from light and image within one week.

Optimizable parameters

- Permeabilization duration
- Blocking duration
- Antigen retrieval
- 1˚ antibody concentration and incubation duration
- 2˚ antibody concentration and incubation duration

Soslowsky Lab Patellar Tendon Dissection and Mechanical Testing Protocol Utilized for Mechanical Testing in Chapters 2,3 and 5.

Materials:

1x PBS
Dissection Tools (2 x Fine forceps, #3 Blade Holder, Microscissors)
Weigh boats (or any small container to hold specimens)
Plastic specimen bags (for extra tendons)
Gauze
Dissection Microscope (sign up on google calendar!)

Methods

Thaw Samples

1. Thaw samples in warm water approximately 30 minutes before dissection begins.
2. Label one weigh boat per sample.

Dissect Patellar Tendon

1. Find knee by palpation. Pick up skin over knee and cut with scalpel.
2. Pull skin apart using forceps to reveal knee, femur, and tibia.
    a. Patellar tendon will be bright white in uninjured samples and visible immediately.
3. Cut through excess skin on posterior side of limb to disconnect everything distal to the femur from the body of the mouse.
4. Cut off toes and make longitudinal incision down the top of the foot to easily deglove the foot.
5. Mark the borders of the patellar tendon using your scalpel blade. Do this by running your scalpel blade up from the insertion to midsubstance on each side of the patellar tendon.
6. Place scalpel blade at site of border (either border is fine, just use your steady hand) with blade facing proximally, then carefully slide the tip of the blade underneath the patellar tendon. Cut up (proximally), under the tendon and under the patella. Once blade has cleared patella and is running along femur, cut anteriorly through the quadriceps muscles.
7. Using forceps, grab distal end of quadriceps (connected to patella) and pull the patellar tendon towards the tibia to expose the knee joint. Insert tip of blade into knee cavity, then cut through the cruciate ligaments parallel to the tibial plateau to separate the tibia-tendon-patella complex from the femur.
8. Slide blade between tibia and Achilles tendon, cut proximally along tibia to separate calf muscles from tibia. Once calcaneous has been revealed, cut through ankle/distal tibia to remove foot. If preserving Achilles, wrap in hydrated gauze and store in proper location. Don't forget to label!
9. Rehydrate tendon in PBS (do this every 1-2 minutes for rest of dissection process, or keep tendon immersed in PBS pool during fine dissection)
10. Grip the fibula with forceps, break away from tibia.
11. Remove the muscle from the tibia using forceps. Clear bulk of excess tissue from sample.

Fine Dissection

12. Move to the dissection microscope.

13. Place tendon anterior side down on dissection mat. Using scalpel blade, cut through patella, removing proximal third of the bone and all of the quadriceps muscle.
14. Clear tibial plateau. Use forceps and microscissors to remove meniscus and knee ligaments. Ensure ACL and PCL are trimmed as close to plateau as possible to avoid interfering with Gismo.
15. Finish cleaning tibia.
16. Remove all soft tissue around the tendon insertion site and around the patella with forceps and microscissors.
17. If it is still present, clear soft tissue away from tendon. This tissue will appear to have bubbles in it. Below, a very white tendon will be clear. It is vital to remove as much of this as possible without damaging the tendon. If you find yourself picking at this tissue to clear it, but begin removing tendon fibers, stop immediately.
    a. **NOTE:** Steps 13-17 do not have to be performed in that order, although it is likely to be one of the most efficient orders of operation.
    b. **Some 'fiber-**like' tissue will need to be removed from both anterior and posterior side of tendon. As you are clearing, if you grab the thin tissue, and then rest of the tendon does not move, this is not a tendon fibril. Be very careful while removing this deep layer of tissue.

Area Measurement

Materials:

GisMO (Sign up on google calendar!)
Labview 2013
Kim Wipes
Fine Forceps

Method

1. Uncover GisMO and turn on box (~10 minutes ahead of time).
2. Open National Instruments Labview 2013. You will see this screen:

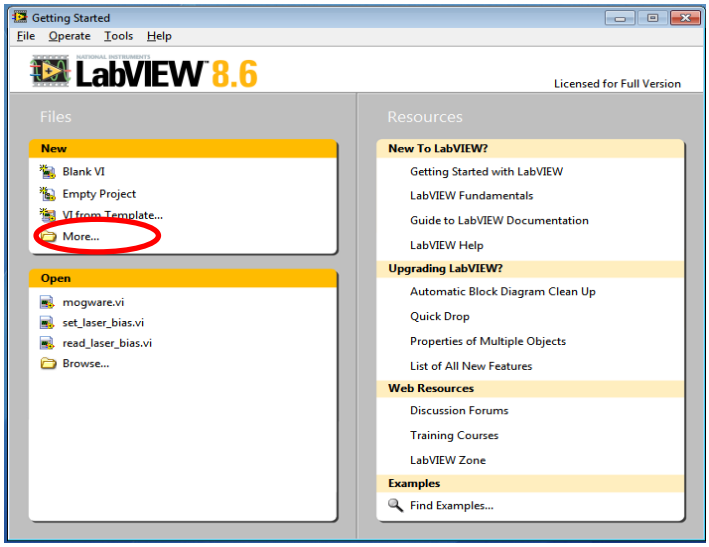

3. Open 'mogware.vi'.
4. Prepare tendon for measurement.

a. Dab tendon on Kim Wipe to remove excess liquid.
b. Place tibia posterior side up with tendon lying flat on stage.
c. Line laser up with the insertion site. This is the point closest to the tibial plateau in which the laser doesn't illuminate the bone (scan laser across tendon to validate).
d. Click 'Run (top left corner)', 'Start', 'zero' all 3 axes, 'Capture Mode'.

5. Turn the black wheel to scan across the tendon width. Watch computer screen to be sure you see the bump when crossing the tendon.
6. Turn the blue handle to move 0.5mm on the y-axis (should be approximately 2 full turns).
7. Repeat steps 5&6 until you reach the patella.
    a. Make sure your final pass is over the patella. Shape on Gismo thickness output will appear to be concave (as opposed to convex when going over the tendon) when tibia is hit.
8. Click 'Stop'.
9. Replace tendon in PBS.
10. Save file.
11. Click Capture mode Off.
12. Doublecheck file in Notepad to be sure all values were zeroed at start and that measurements were taken. You should see values increase during passes in the thickness column.
13. If finished, close software, log off computer, turn off laser, cover GisMO.

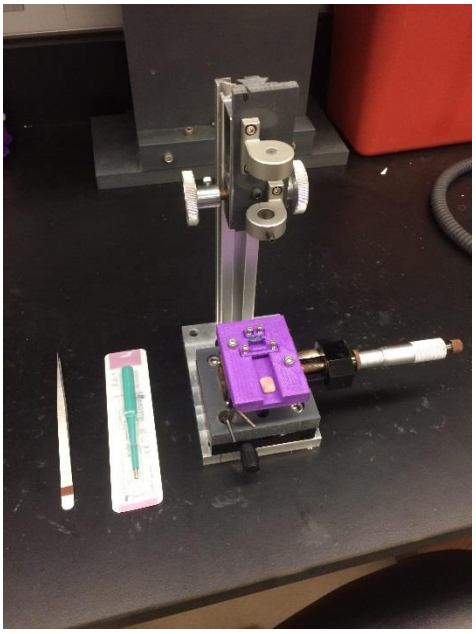

Tendon Stamping

Materials:

Fine forceps
2mm biopsy punch
Mouse tendon stamping apparatus

Method: (P30 tendons are not stamped)

1. Place tibia/tendon in channel in center of apparatus.
2. Using forceps, gently guide patella under the raised lip on the far side of the channel, with the anterior side of the tendon facing up.
3. Use hex key to tighten the two screws furthest from you. Gently tighten until patella is clamped below the 3D-printed bar. Be careful to not make any of the screws so tight that excessive force is applied to the tendon.
4. Place longer 3D-printed bar over tibia. This will span across the middle of the channel. Place small piece of wax (pink rectangle in picture) between underside of bar and anterior side of the tibia to avoid slippage during stamping.
5. Gently tighten screws over tibia, being careful to not stress tendon.
6. Insert biopsy punch in clamp above the patella. Use hex key to tighten.

7. Using the black and silver dials, center the biopsy punch above midsubstance of patellar tendon. If tendon is injured, center biopsy punch above injury.
    a. **Note:** Theoretically, injury should be in middle of tendon. This may not always be the case. Make sure biopsy punch is always centered above the injury itself so that it is isolated during testing.
8. Once centered, take note of which number is facing up on silver dial. This is your zero point. Use silver dial to translate biopsy punch 1.375mm to one side of tendon. Each tick mark on dial represents 0.01mm of translation. One full revolution is 0.5mm.
9. After 1.375mm of translation, gently bring biopsy punch down to stamp tendon.
10. Return to zero with biopsy punch, repeat steps 8 and 9 for opposite side of tendon.
11. Loosen tendon clamp and remove wax piece to slide tendon out of fixure. Rehydrate tendon. Dispose biopsy punch.
12. Return to dissection scope to ensure stamped tissue has been completely removed. If not, use scissors to fully remove the loose tissue.
13. Use GisMO to find cross-sectional area of stamped sample.

Stain Lines

Materials:

Verhoeff Stain (Recipe included)
Kimwipe/paper towel
Ruler
Rubber mat
Stain Line Suture
1x PBS
Dental wax

Verhoeff's stain recipe: Combine solution A:B:C in a 2:1:1 ratio. Only make enough to use that day in a small weigh boat. Do this about 30 minutes before you want to stain and put stain line suture in the solution to coat.

Methods:

1. Build your custom ruler setup out of wax pieces and your ruler.
2. Line up tendon on ruler setup with the ruler.
3. Dab away excess moisture from tendon on a Kim Wipe.
4. With suture, make stain lines on anterior side of tendon at the following points: tibial insertion, 1 mm proximal to tibial insertion, 2 mm proximal to tibial insertion, and patellar insertion.
5. Dab gently with Kim Wipe to blot excess stain.
6. Place tendon back in weigh boat with PBS to keep it hydrated.

Potting

Materials

Polymethyl methacrylate (PMMA). [Orthojet Powder and Liquid]
3D Printed Pots (Print from file in Resources folder of EDS or SLRP2 Grant, 1/sample)
Plastic specimen cup
Tongue depressors
1mL Syringe (no needle)
KimWipes

Method:

1. To prepare PMMA, mix powder and catalyst in plastic cup. Increase amount of powder until a paste-like thickness is achieved.
2. Pull up PMMA into the syringe. Wipe the tip of the syringe with a Kim Wipe.
3. Squirt some PMMA into the tibial hole of the pot and spread across entire surface of pot. Make sure this layer is uniform and not too tall (you'll need to be able to see insertion stain line during testing). This layer prevents the accumulation of bubbles in front of the tendon during mechanical testing.
4. Pot the tendon in the bone cement as it is hardening, ensuring that the tendon does not sink down into the PMMA. Since the specific 3D printed pot for patellar tendon testing pots the tibia at an angle, make sure that the tendon insertion site is the topmost point (posterior side of the tibia facing toward the center of the pot).
    a. **35 degree testing angle in pot**
    b. **Dremmel down PMMA and epiphysis to get more visibility of insertion site, apply thin layer of PMMA over top to avoid growth plate breakage. (not completed for Col5 tendons)**
5. Leave the sample submerged in PBS for ~30 minutes to cure.

Mechanical Testing Setup

Materials:

Instron 5848A (Sign up on google calendar!)
Computer with Wavemaker Runtime
Computer for Imaging
10N load cell
Tank
Screws, Grips, Pin
1x PBS
Torque wrench
Hex key (T-handle and regular)
Camera + Accessories (pictured below)
Cross Polarizer + Accessories (picture below)

Camera and Cross Polarizer Setup

Basler Scout

Lens

Camera Stand

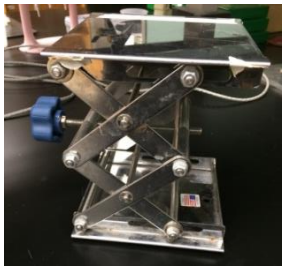

Light Box

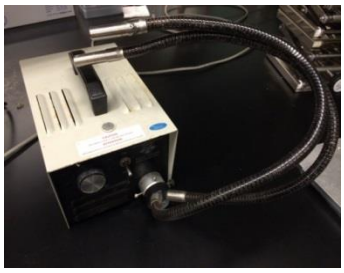

Rotating Cross Polarizer

Cross Polarizer

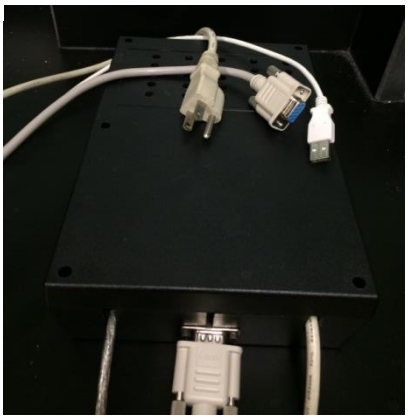

DAQ

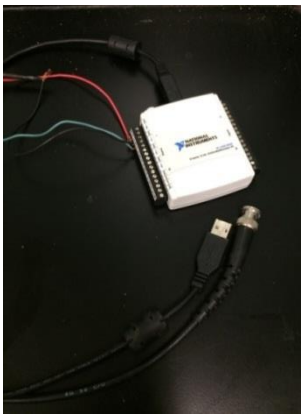

Set up Instron

1. Change Instron height to SLRP2/ColV mark.
2. Attach 10N load cell to crosshead.
    a. Make sure cord is unkinked after twisting it on.
    b. Plug into gray horizontal computer.
3. Add stage to the base. Use hex key wrench to screw in place (4 screws that are M-6s)
4. Attach tank to stage using two or four clamps (depending on size of stage).

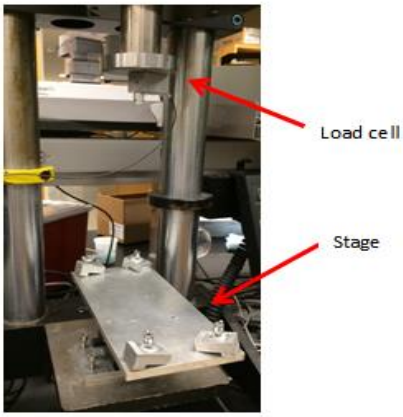

5. In this order:
    a. Turn on Instron machine (red button all the way on left of gray horizontal computer)
    b. Log on to computer that controls Instron (left computer)
    c. Start Console software
6. On Instron computer, open Wavemaker Runtime, then Editor (little blue and red on white background chart icon).

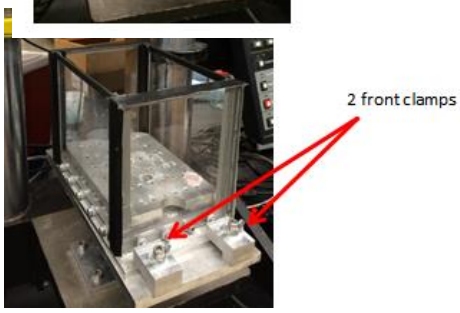

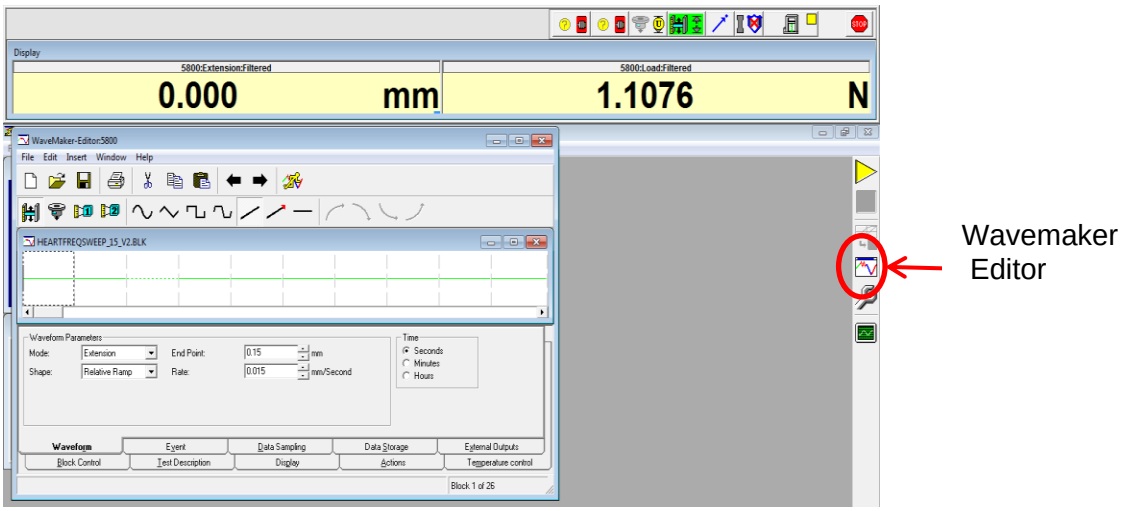

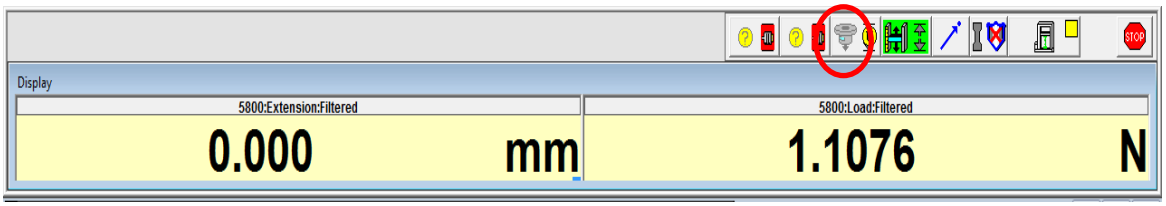

7. Calibrate the load cell. Right click on icon circled in red (above), then click:
    a. Calibration
    b. Calibration
    c. Next
    d. Next

e. Transducer details: Units in N (NOT kN)
f. Next
g. Start
h. Finish
i. Next.
j. Click most recent calibration file. Change the date in the filename. Save.

8. Check Load cell with low and high weights.

Set up Instron

1. Get 1.4L of PBS and pour into tank- enough to submerge the majority of heater.
2. Clamp tendon using the Honeymooner. First, fold gauze lengthwise and place in pot port. Place clamp in clamp port, and slide tendon pot into port with tendon stain lines facing down. Using forceps, glide tendon into clamp. Carefully tighten screws. Too tight will create stress concentrations around the patella; too loose will let the patella bone pull free during testing.
3. Attach the gray pot holder (1) into the tank

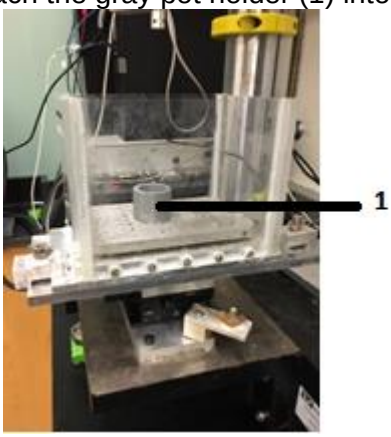

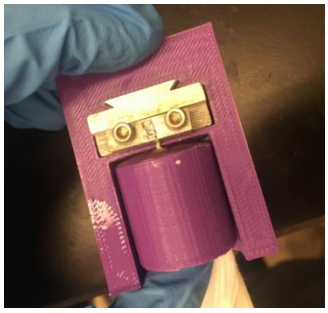

4. Place tendon pot + clamp into bottom gray grip, tighten bolt to pot. Be careful not to stress/stretch the tendon.
5. Attach jig with upper clamp under the load cell using the pin (push through to one click), then tighten the nut by hand. Do not pull down or push up on this as it exerts too much force on the load cell.
6. Connect top fixture that is gripping patella to the female piece connected to the load cell. Adjust tank stage as needed.

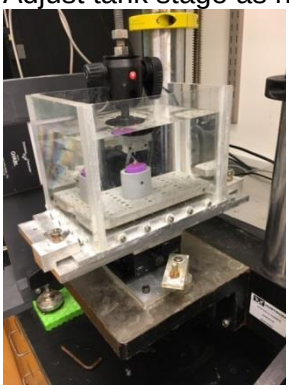

7. To set up…
    a. Make sure 2x teleconverter is attached to camera and lens
    b. Put extra elevating stand under camera and adjust height as needed.
    c. If Basler Ace, use Ethernet cable (in tangle of cords behind monitor)

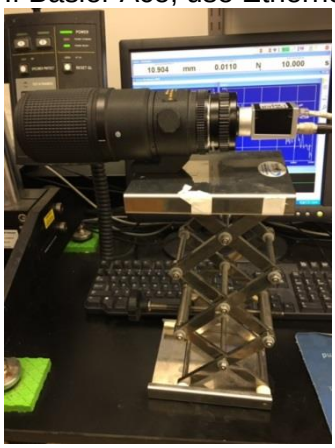

    d. If Basler Scout, use Firewire cable and C-clamp

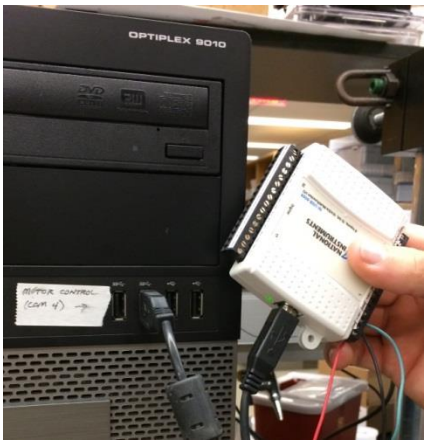

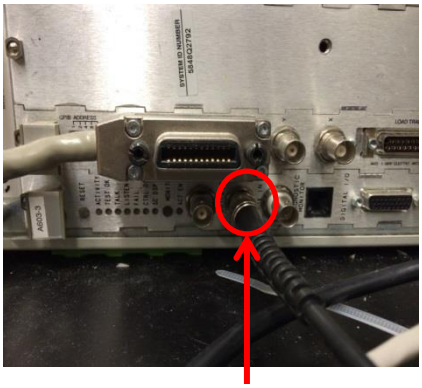

Output B on back

8. Plug in data acquisition device (DAQ) to the light gray computer under the black computer tower. Push and twist BNC cable until it plugs into output B (see picture for reference). Check that all wires are connected in the box. On imaging computer, plug USB cable into any port not reserved for motor control.
9. Plug USB cable from cross polarizer controller into marked USB port (White tape). Once connected, light will start blinking.
10. Plug controller into the wall outlet.

Start Imaging Software

1. On the imaging computer, open ‘Start’ menu and search for ‘Measurement’. Open Measurement and Automation Explorer (MAX).
2. In MAX, expand ‘Devices and Interfaces’ folder→NI-IMAQ dx devices → Camera
3. Turn on light and turn up intensity to setting of 7-10 (light box on shelf above monitor).
4. Adjust camera height, position, and focus to get tendon in field and focused.
    a. Right click on image -> viewer tools -> zoom to fit

5. Click grab to ensure image comes up (Focus not important)
6. Balance load cell (Right click load cell icon → 'Balance'), reset gauge length (button on Instron control panel).
7. 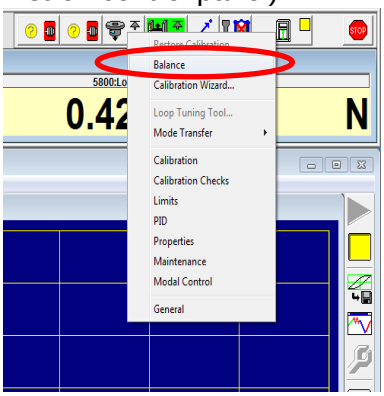

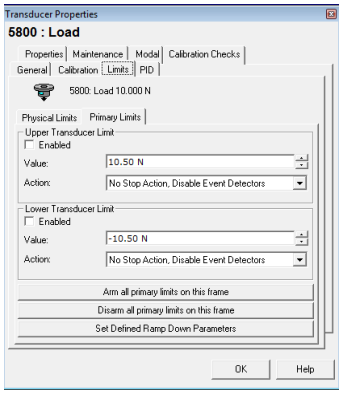

8. Change load readout to 5 decimal places (Right click, properties).
9. Make sure the tendon is aligned straight in all directions. Load tendon to 0.005N. Use jog up/down or fine adjust as well as black knobs below stage. Watch load on left monitor and tendon image in right monitor to get it perfectly straight. Unload tendon and let it 'settle'.
10. Load tendon to 0.02N, reset gauge length.
11. Use imaging computer to take pre-testing image once tendon is straight. Click 'Save image', select folder for this sample, title file "Sample ID pre-test". Click 'Save'. Unclick 'Grab'.
12. Unload tendon.
13. Click 'My system' (if you don't click this, CIMM Ware won't run).

Start Protocol

14. In Wavemaker Editor, choose protocol from protocols folder within your folder.
    a. **Col3_P90**
        i. **Preload: 0.02N**
        ii. **SR: 3,6%**
    b. **Col5_P120**
        i. **Preload: 0.005N**
        ii. **SR: 2,3,4%**
15. Click 'Data Storage' tab at bottom. Click box below 'Output Filename'. Create a folder for today's data and a subfolder for this sample and select that folder.
16. Select first block on left and click 'Apply Current Block to All Blocks' – multiple times to be safe.
17. Save. Click run button
18. Look at y-axis label on right side chart in Wavemaker Runtime. If says "Column 2" instead of "Load", restart the program.

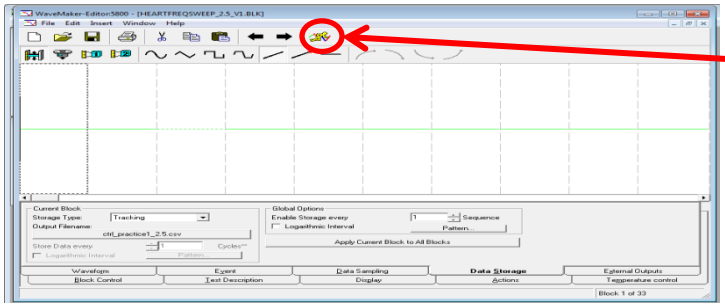

19. Open Labview 2013, top version under 2nd yellow bar on the left.
20. Open CIMM Ware – version 3.2.3
    a. Adjust threshold to = 1
    b. 'Sequence file which indicates which images to save' should be set to 'C:\McKay Software\Labview 2013\CIMMware\SequenceFiles\18fps_36fprev_18img_rev.txt'
21. Place crossed polarizer (in cabinet under 5848b) on the Instron base and clamp in place. Keep axle 2-3mm from wall of tank. Do NOT touch or bump the wheels of the polarizer. Plug in cord from toolbox to motor on left side of polarizer.
22. Position divot in polarizer wheel to the top of the wheel.
23. Click little folder icon (a in image below). Select desired folder for images. Click "Current Folder".
24. Retype sample name in Image Prefix (must leave ~ after the sample name or it won't work). (c)
25. Click 'Run' button (arrow on top left).
26. Refocus camera.
27. Click 'Zero angle' (red arrow on compass wheel should point to 360). (g)
28. Click 'Motor start'. Polarizer wheels should start spinning. (h)

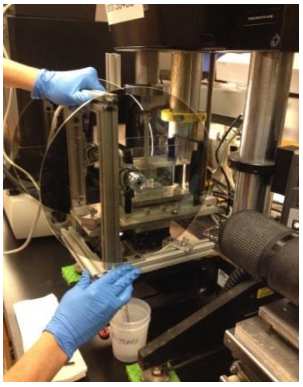

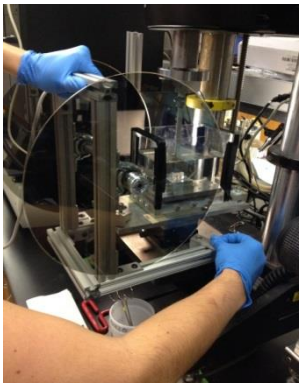

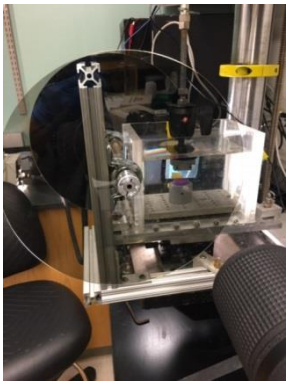

29. Balance load cell (Right click load cell icon → 'Balance')

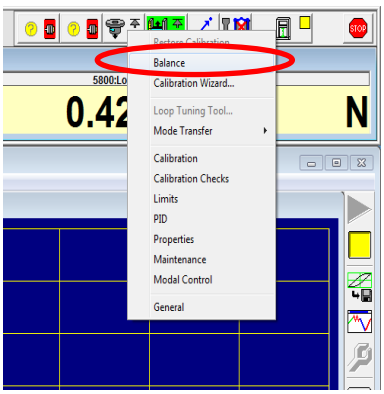

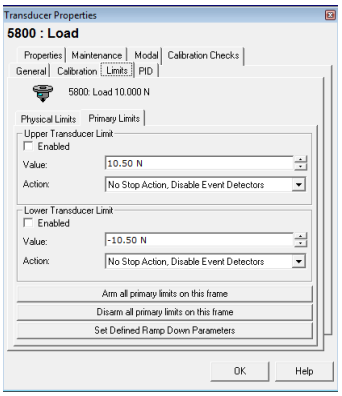

30. Set and enable limits.
31. Hit "Arm all primary limits on this frame"
32. Load tendon to 0.02 N (0.005 N for Col5).
33. Click "Yes" on left computer at exact same time as clicking "Zero Time" on right computer.

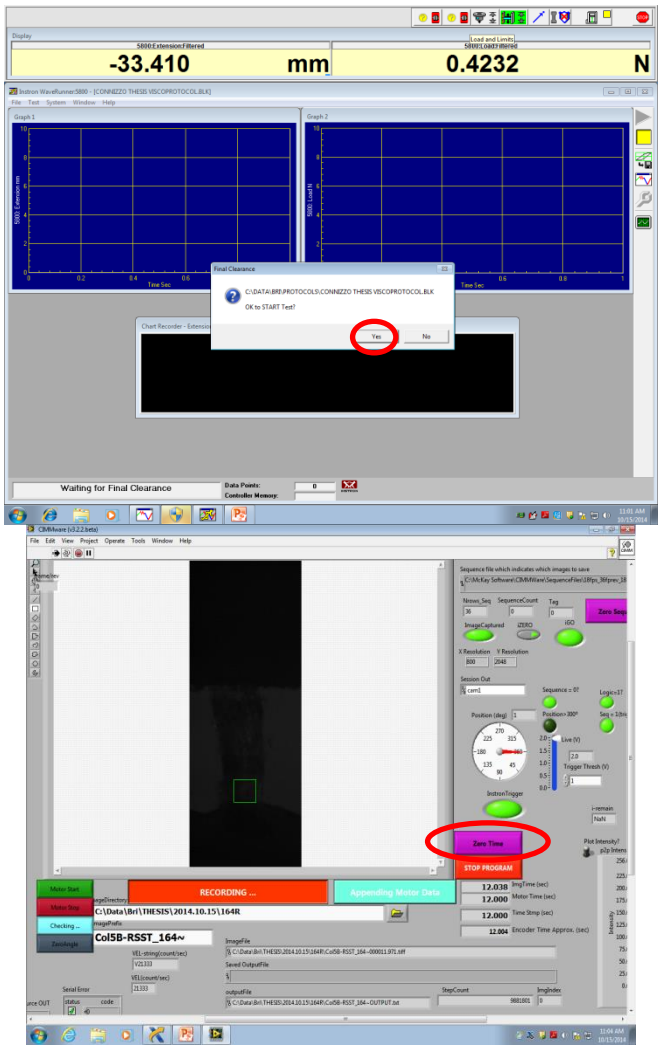

34. When test is complete, click stop button on imaging computer.
35. Turn off limits.
36. Hit ‘jog up’ and/or remove the whole upper grip/fixture apparatus from the load cell to make space for the ruler.

37. Go back to Cimmware. Open folder to which you want to save the waveplate image, click ‘current folder’. Name file “specimen number-wave~. Click ‘run’.
38. Tape wave plate to the outside of the far side of the tank (between tank and light source) with dots facing camera. Needs to be positioned with row of dots vertical (black tape tab facing up).
39. Replace polarizer. Put divot on cross-polarizer facing up.
40. Focus camera on one of the wave plate dots (may need to move camera up or down). **Do not change the lighting.**
41. Click ‘zero angle’.
42. Click ‘motor start’.
43. Change trigger to -1 when angle reading is just about to cross 360.
44. Capture 1 alignment map (until it reaches 180 degrees).
45. Stop program.

46. Remove polarizer. Minimize Cimmware.

47. In MAX, click ‘Grab’, focus camera, click ‘Save Image’ and name as “Sample ID_gauge”. Drag ‘save’ window down so live image visible, and keep mouse positioned over the save button to click once ruler in place.
48. Place ruler piece in tank positioned at location of tendon prior to tendon failure. Focus camera. Save. Unclick ‘grab’. Click ‘My system’.
49. Ready to set up next specimen.

Soslowsky Lab TEM Processing and Embedding Protocol, adapted from Birk Laboratory at the University of South Florida

Day 1:

SACRIFICE/ FIXATION

Karnovsky's Fixative- 2-4 hours on ice on shaker (can sit in buffer for up to 1 day)

Recipes:	For 80 ml use	For 40 ml use
- 1- 10 ml vial 25% Glutaraldehyde	8.0 ml	4.0 ml
- 2- 10 ml vial 16% Paraformaldehyde	20.0 ml	10.0 ml
- 0.2M Na Cacodylate Buffer	40.0 ml	20.0 ml
- 0.8M CaCl2	0.8 ml	0.4 ml
- deionized H2O	11.2 ml	5.6 ml

0.2M Sodium Cacodylate Buffer (EMS,Cat.#12300, FW.214.02)

For 250 ml, use 10.7 g Na Cacodylate

- Dissolve Na Cacodylate in 100ml dH2O
- Adjust pH to 7.4 with HCL
- Bring volume to 250ml (Use graduated cylinder) with dH2O

0.8M Calcium Chloride, Dihydrate (MW-147.02)

For 50 ml, use:

- CaCl2 5.88g
- dH2O 30ml
- Dissolve CaCl2 in dH2O
- Bring volume to 50ml (Use graduated cylinder) with dH2O

RINSE

0.1M Na Cacodylate buffer (pH = 7.4) [1:1 dH_2O + stock] - **5 min on ice**

Trim samples, remove all extra tissue, split injury ¾ way through, make two patellar cuts, remove tibia (this is harder to do later)

POST-FIXATION

1% OsO4 ***(highly toxic)*** in 0.1M Na Cacodylate buffer (pH=7.4) dilute from 2% OsO4 (suck dry)

- **1 hr on ice** (can stay in longer (15 min), but not shorter)

2% OsO4 Stock Solution

dH20 100ml

OsO4 2g

Fixative 1% OsO4 in 0.1M Na Cacodylate Buffer (pH =7.4)

Use equal parts 2% OsO4 and 0.2M Na Cacodylate buffer (pH=7.4)

While waiting, mix Epon (if needed)

Epon Recipe (ml) by volume		**Epon Recipe (g) by weight**	
EPON (812)	15.6ml	EPON (812)	18.1g
DDSA (softener)	5.4ml	DDSA (softener)	5.5g

NMA (hardener)	9.3ml	NMA (hardener)	10.9g
*DMP-30 (catalyst)	0.6ml	*DMP-30 (catalyst)	0.6ml

• Measure out the appropriate amount of each ingredient using a disposable syringe (30ml).
• Mix after measuring first three ingredients gently rocking for **15 min**. Add DMP and mix again thoroughly on rocker at room temp for approx **45 minutes**.
• Store in syringe tightly covered with parafilm. Date syringes and place in ziplock bags, in -20 freezer.

- Use 70% ETOH to clean sticky bottles

RINSE

0.1M Na Cacodylate buffer (pH = 7.4)- **5 min on ice**

DEHYDRATION

Dilute ETOH with dH2O (use EM grade ETOH). Samples should ALWAYS be wet

50% alc	**10 min on ice**
70% alc	**10 min on ice**
85% alc	**10 min on ice**
95% alc	**10 min start with cold alc and let it come to room temp**
100% alc	**10 min 3X's room temp**
Remove about half 100% alcohol and replace with prop oxide. approx. (1:1)	**10 min room temp**
Pure prop oxide	**10 min 2X'S room temp** (one extra untimed rinse)

***always under liquid once dehydrated, no air on tissue*

INFILTRATION

Prop oxide:epon 2:1 **2hrs or over night** [can do 2:1 for 2 hrs and then 1:1 overnight]

Day 2:

Take Epon out of the freezer 20-30 minutes before using to allow it to thaw and come to room temperature.

INFILTRATION

Prop oxide:epon	1:3	**next day on rotator (am)**
Pure epon		**overnight on rotator (pm)- 12-20 hours**

Print sample labels for blocks and place in mold

Day 3:

EMBEDDING

Mix fresh epon

Let epon bubbles rise to top of syringe **(15-20 min)**

Under stereomicroscope, fill mold blocks with epon and make sure there are no bubbles
Finish cuts in tissue (keep samples wet in a drop of epon)

Place samples in correct mold section
Top off mold sections with epon
Put flat in oven overnight (60ºC) ~24 hours

Day 4:
Remove blocks from oven
Check blocks with fingernail or blade to make sure consistency is right

Sectioning
Gross Trimming: Dremel rough surface and cut block face with razor blade to smooth
- Larger tissue- less border
- Smaller tissue- more border for structural support

Fine Trimming: Glass knife- 200-500 nm
- Thick sections: create even block face using microtome, important that the collagen fibers are perpendicular to block face
- Use fast stain to check progress/injury site
    - Put water on knife, use wooden spear to collect, put water on slide and then dry on slide warmer before quick stain

Ultrathin Sectioning: Diamond knife, 70-100 nm
- 0 .8 -1.0 cutting speed
- The specimen should be between 60-100nm, ideally around 90nm thick.
- 1mm x 1mm square face (can be longer but no wider)
- The following section colors relate to their thickness:
- 60 nm gray, 60-90 nm silver, 90-150 nm gold
- 150-190 nm purple, 190-240 nm blue, 240-280 nm green
- Isolate floating sections using the eyelash and pick up on the dull side of 150-200 mesh, naked (no support film) copper GRIDS. Number of sections will vary per grid, however, 4-6 centrally located is usually sufficient. At least 2 grids per specimen. SMA- 3-4 grids
- Rinse grids, line up 3
- Use diamond knife with dH2O in 'boat'. Boat full evenly looks silver (use syringe to get correct level)
    - Clean knife by rubbing Styrofoam over knife face
    - Knife parallel to block face
    - Use air gently on the knife, not a brush
- Collect 80, 90, 100 nm sections; can tell by reflection how thick
    - 20 good sections
    - Set up at 70nm then increase to 80, 90, 100 nm
- Use eyelash tool to group different thickness sections together using color reflection chart
- Collect ~4 sections on each of 5 grids, multiple thickness sections on each grid, collect on dull side of grid, use lens paper to get rid of extra water

- Chloroform helps flatten the sections, hold above them in the boat, don't touch the water
- Store in the grid box
- Scoops up the extras on a slide, save the thickest for injury location determination
- Fine trimming and Sectioning: https://www.youtube.com/watch?v=M3CMYAFrwUI&t=224s
- Sectioning: https://www.youtube.com/watch?v=zBKMRhQqBB4

Staining

Stain the best 3 sections, let dry overnight

- Uranyless - 20 minutes
    - Drop it over the vertical grid and stain for 20 minutes
    - Collect waste on KimWipe or paper towel and dispose of in labeled bag in bin under hood
    - Rinse off by submerging grids in dH2O
    - Using KimWipe or filter paper, gently touch edges of grids to get rid of dH2O and dispose of as above
- Phosphotungstic Acid (PTA)
    - 3.2 pH: pH matters!
        - Add NaOH if too low
    - Drop onto grids
    - 5-10 minute stain
    - Collect waste as described above
    - Rinse off by submerging grids in dH2O and dispose as above
    - Cover to protect and let dry overnight. Can image immediately once extra water is gone
    - Store in grid holder if not imaging immediately

Imaging

Imaging transverse sections from injury or midsubstance of tendon for analysis of fibril diameter. Images are taken at 60k scope magnification at 80kV, on JEOL 1010 transmission electron microscope.

<u>Image criteria</u>

Goal: to measure a significant number of fibrils to obtain data that represents specimens which allows for comparison (statistical significance) between experimental groups.

- Fibrils in cross section (no oblong fibrils)
- From center region of fiber (avoid edges)
    - Not from peripheral region of tendon
- Avoid cell and cell processes if possible
- Avoid processing (artificial) breaks in tendon structure
- Avoid folds, holes in section, and staining artifacts/dirt
- Do not image overlapping sections
- Collect from multiple fibers, sample area should be well represented
- Measurable fibrils should be at least 80/image*

    - In abnormal specimens (young, mutant or injured specimens) where tendon morphology is not typical or mature, imaging criteria are adjusted on a project to project basis.
- 15-20 images are taken per sample
- 10 representative images are chosen to be measured using the above criteria.

Injured tissue

    - Look for injury at low mag
    - Image in and adjacent to injury to get representative samples of all injured tissue*
    - 5 images measured directly in injury region (all small fibrils), 5 images measured wit a mix of large and small fibrils (move out in injury region), 5 images measured wit ~75% large fibrils and 25% small fibrils (injury edge)

Measuring

- Custom Matlab code is used to measure 15 images per sample

Soslowsky Lab Patellar Tendon Total RNA Preparation

RNA*later* ICE(ThermoFisher, AM7030), TRIzol (ThermoFisher, 15596018), RNase-free Pestles (Fisherbrand, 12-141-368), and Direct-zol RNA Microprep (Zymo, R2062)

1. At time of sacrifice, dissect PT by cutting below tibial plateau with bone crunchers and above patella through quadriceps muscle. Immediately freeze in liquid nitrogen and store at -80ºC.
2. At time of RNA isolation, immediately place tibial plateau-patellar tendon-patella complex in 1.5mL nuclease-free Eppendorf tube with 500 µL RNA*later* ICE. Dissect tendon while submerged in RNA*later* ICE:
    a. If isolating RNA from whole tissue, cut patellar tendon at tibial insertion and patella.
    b. If isolating regional RNA, cut patellar tendon at tibial insertion and 1mm proximal for insertion tissue. Cut at patella and use remaining tendon tissue for midsubstance tissue.
3. Wipe excess RNA*later* ICE off tissue and place in Eppendorf tube with 200 µL TRIzol (should be <u>ICE COLD</u>).
4. Using the pestle, mash tissue in Eppendorf tube for ~1 min. Close tube and vortex for >2 min.
5. Let samples incubate at RT for 5 min. <u>Potential stop point</u>: freeze at -80ºC.
    a. While the tissue sits in TRIzol, mix 5 µL DNase I and 35 µL DNA Digestion Buffer in RNase-free tube.
6. Add 40 µL chloroform (20% of TRIzol volume) and vortex tube for 15s. Let incubate at RT for 3 min.
7. Centrifuge samples at 4ºC and 12,000g for 10min.
8. Transfer clear supernatant phase (RNA containing) to new Eppendorf tube. Add equal volume 95-100% ethanol, and mix well by vortexing.
9. Transfer sample to Zymo-Spin IC Column in a collection tube and centrifuge for 15 sec at max speed (15-16k g). Transfer column to new collection tube and discard the flow through.
10. Add 400 µL RNA Wash Buffer to the column. Centrifuge for 15 sec at max speed. Discard the flow through.
11. Add DNase Digestion Buffer mix directly to column matrix. Let incubate at RT for 15 min.
12. Add 400 µL Direct-zol RNA PreWash to column. Centrifuge for 15 sec at max speed. Discard the flow through and repeat this step.
13. Add 700 µL RNA Wash Buffer to column. Centrifuge for 2 min at full speed.
14. Carefully transfer column to RNase-free Eppendorf tube. Add 15 µL of DNase/RNase-free water directly to column matrix. Centrifuge for 1 min at full speed to elute RNA.
15. Check RNA concentration and purity with NanoDrop (need 1.5 µL). Freeze rest of RNA at -80ºC.

Soslowsky Lab cDNA preparation and preamp for Fluidigm
Leiphart Thesis 2022

Objective: Convert template RNA samples to cDNA and preamplify for subsequent Fluidigm Dynamic Array analysis

Materials:
- Pipettes (1000µL, 200 µL, 20 µL, 2µL) and associated tips
- High-Capacity cDNA Reverse Transcription kit (Thermo, #4368814)
- RNase/DNase free water
- 96 well plates
- Plastic plate sealers
- Thermal cycler
- Preamp master mix (Fluidigm, #100-5580)
- Taqman probes for target genes
- Dilution reagent (Fluidigm, #100-8726)
- Ice

Procedure:
1. Thaw cDNA RT kit reagents on ice
2. Prepare cDNA RT master mix (MM, per sample):
    a. 2µL 10X RT Buffer
    b. 0.8µL 25X dNTP Mix
    c. 2µL 10X Random Primers
    d. 1µL Reverse Transcriptase (not included in NoRT MM)
    e. 4.2µL Nuclease-free water (for NoRT MM, becomes 5.2µL)
    f. 1.1x offset for pipetting error
3. Pipette 10µL of MM into each plate well allocated for samples
    a. Thaw RNA samples on ice during this step
4. Pipette 10µL of RNA sample into corresponding plate well
    a. Pipette up and down to ensure well-mixed
    b. If diluting RNA sample, add nuclease-free water to achieve 10µL (20µL total)
5. Seal plate, and centrifuge if air bubbles are present
6. Perform cDNA synthesis via thermal cycler with following protocol:
    a. 25ºC for 10min
    b. 37ºC for 120min
    c. 85ºC for 5min
    d. 4ºC indefinitely
7. POTENTIAL STOP: Plate can be stored at -20ºC indefinitely
8. Thaw preamp master mix and associated Taqman probes on ice
9. Prepare pooled assay mix:
    a. Determine volume needed
        i. 100µL minimum, or 1.25 x (# samples) x 1.1 (offset for pipetting error)
    b. Volume per Taqman probe: Total volume/100
    c. Volume of dilution reagent: Total volume – volume of Taqman probes
10. Prepare preamp master mix (MM, per sample):
    a. 1µL Preamp master mix
    b. 1.25µL pooled assay mix
    c. 1.5µL nuclease-free water
11. Pipette 3.75µL of MM into each plate well allocated for samples

12. Pipette 1.25µL of cDNA sample into corresponding plate well
    a. Pipette up and down to ensure well-mixed

13. Seal plate, and centrifuge if air bubbles are present
14. Perform preamplification via thermal cycler with following protocol:
    a. 95ºC for 2min
    b. 95ºC for 15sec
    c. 60ºC for 4min
    d. Repeat b + c until appropriate number of cycles are reached
    e. 4ºC indefinitely
15. Add 20µL dilution reagent to each sample well
16. Reseal and store at -20ºC

Soslowsky Lab AFM Protocol
Written by Dr. Jeremy Eekhoff, 2023

Tissue Preparation and potting
***follow PT dissection preparation protocol above**

Loading and Embedding

General Setup

1. Fill a cooler with dry ice and insert the following items into the cooler:
    a. Specimen cup with enough methylbutane to submerge an embedding mold
    b. Large piece of aluminum scrap and extra aluminum grip piece to serve as a chilled platform to keep sample frozen while removing grips later in protocol
    c. Scalpel blade holder with #11 blade
    d. Straight hemostat
2. Pre-chill a bottle of OCT upside down on ice.
3. Turn on the Instron 5848 and open Wavemaker Editor and Runtime.
4. Install a pot holder on an Instron base on top of an x-y stage, and threaded connecting rod with female dovetail fixture on the Instron actuator (Figure 2).
5. Set up the QPLI imaging system and open CimmwareLite3 (Figure 1).

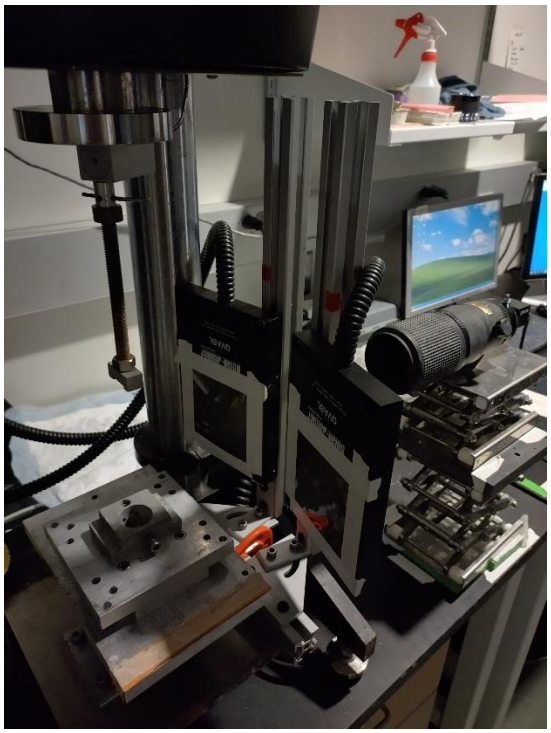

Figure 1

Run Test

1. Pre-label an OCT embedding mold with the sample name and insertion region direction, and put on dry ice in the cooler.

2. Edit the Wavemaker protocol (PT_AFM_1, PT_AFM_10, depending on target strain) to store data to a file named with the sample name.
3. Set up the image directory in CimmwareLite3 to save images to a folder named after the sample name.
4. Grip the sandpapered tendon in dovetailed aluminum grips, keeping the edge of the sandpaper flush with the edge of the grip. When finished with this step, put the forceps in the dry ice cooler to chill.
5. Install the potted sample with the attached grip into the pot holder on the Instron.
6. Gently slide the grip into the dovetail fixture, being careful to not apply any force to the tendon.
7. Cover the tendon in PBS to maintain hydration during pre-loading.
8. After balancing the load cell while the tendon is slack, apply a 0.02 N pre-load to the tendon and adjust the x-y stage so that the tendon is uniformly loaded.
9. Absorb the PBS surrounding the tendon with a kim wipe.
10. Adjust the QPLI camera so the tendon is centered in the field of view. Focus the camera on the tendon. (Figure 2)
11. Set the frame rate to 2fps in CimmwareLite3.
12. Run the Wavemaker protocol in Runtime. Click “Zero Time” in CimmwareLite3 at the same time the final confirmation in Wavemaker Runtime is clicked to synchronize times between images and Instron data.
13. Roughly 15 seconds before the end of the test, remove the aluminum pieces from the dry ice cooler and set up on the bench to use as a chilled platform. Place the pre-labeled embedding mold on the chilled aluminum platform. (Figure 3)

IMPORTANT NOTE: Steps 14-19 must be performed rapidly to avoid any thawing of the tendon once frozen. Only touch the tendon with pre-chilled instruments and materials.

14. When the tendon reaches its target strain, immediately freeze the tendon, the attached grip, and the pot using Rapid Freeze spray.
15. Cut the tendon from the humerus using the pre-chilled scalpel.
16. Remove the grip and attached tendon and place on the chilled aluminum platform.
17. Use a pre-chilled forceps to hold the tendon while cutting it off at the grip using the pre-chilled scalpel.
18. Transfer the tendon to the embedding mold on the chilled aluminum platform in the labeled orientation to keep track of insertion and midsubstance regions.
19. Fill the mold with pre-chilled OCT and flash freeze in methylbutane in the dry ice cooler.
20. Once frozen the embedded sample can be stored at -20° C if sectioning within 1 week, or stored at -80° C for longer-term storage.

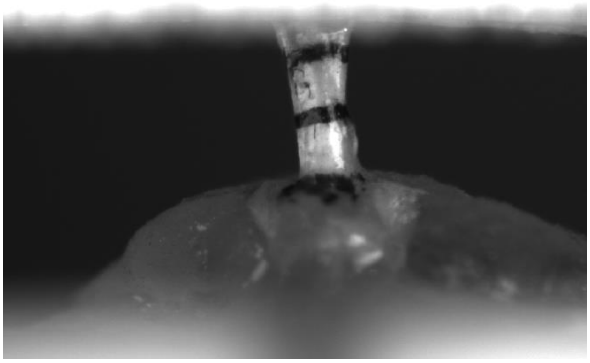

Figure 2

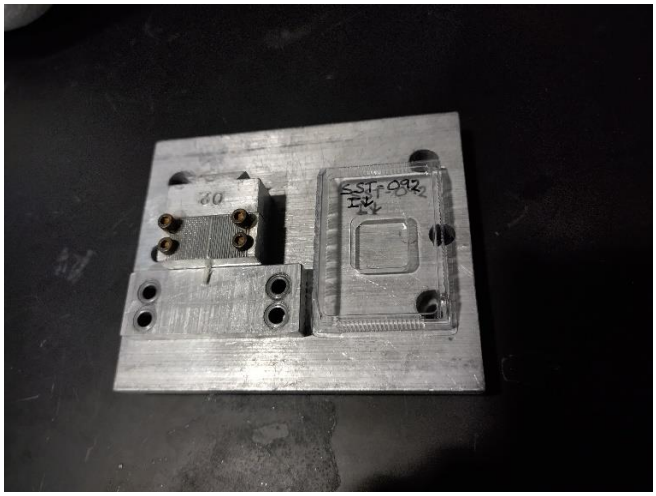

Figure 3

Sectioning and Fixation

1. Prior to sectioning, fill slide staining container with 4% formalin and chill in the fridge.
2. Set the cryostat temperature to approximately -22 to -25 degrees Celsius, which is optimal for sectioning tendon. During sectioning, if the block temperature goes up, close the lid for a minute or so to allow cool down.
3. Adhere the sample block to the metal sample holder by with a small amount of OCT and orient the top surface of the sample to be parallel with the surface of the metal sample holder.
4. Place the block on top of the cooling spot of the cryotome. Make sure the orientation of the sample is known (for example, insertion site down and midsubstance up) and be consistent across specimens.
5. Squeeze a small amount of OCT on top of the block in the direction of the longitudinal axis of the tendon. This will allow you to have OCT to section through the properly line up and adjust the angle of sectioning. Allow a few minutes for the OCT to fully cure.
6. Install a new blade and mount the sample onto the sample clamp. Adjust the clamp orientation so the surface of the sample is parallel with the metal plate behind the clamp.
7. Set the sectioning thickness to 20 µm. The trimming thickness can be set to 60-80 µm.
8. Bring the sample surface to the blade. Fine adjustment can be made by attempting to section with trimming thickness. Also fine adjust the orientation of the sample clamp to make sure sample surface is following the blade path.
9. Trim away the excess OCT until tendon can be seen. (Note: use two different regions of the blade for trimming and sectioning to achieve best quality)
10. Cut sections and apply charged glass slide to the sections. Make sure all sections are labelled clearly with the orientation and section number of the sample. The brightfield microscope can be used to examine the sections. Typical section cut parallel to the length of the tendon is shown in Figure 17. (Note: If planning to use the Bioscope Catalyst AFM for imaging, the sample should ALWAYS be put around the center ~15mm range diameter of the glass slide due to the AFM cannot reach outside this region, as shown in Figure 18)
11. Leave slides in cryostat. Always section all the way through the sample. It’s very difficult to obtain the appropriate orientation when trying to resection a sample.

12. Remove all slides from the cryostat and then place slides in the cold formalin for 5 minutes. Then remove from formalin.
13. Gently rinse the slides 3X with PBS, and be careful not to rinse away the sample.
14. Leave the slides on the slide rack in the hood overnight to dry.

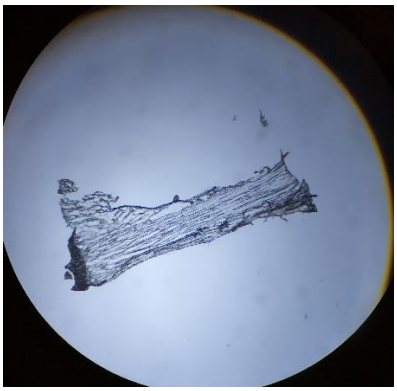

Figure 4

Figure 5

AFM Imaging

1. Switch on the AFM power and mount an appropriate probe onto the AIR holder (For example, NCHV-A). Install the holder onto the scanner head. (Note: setting the scanner head to upright position makes the installation of the holder easier).
2. Start the Nanoscope 8.15 program and choose the Tapping mode in Air (standard tapping) in the experiment select. After the experiment is loaded the laser should be on. Use the laser alignment station, align the laser and zero both deflections.
3. Initialize the stage. The stage initialization can ONLY be done after laser is properly aligned.
4. Perform auto tuning of the probe.
5. In the Nanoscope software, switch to Navigate and bring the scanner head down to make the probe tip close to the sample (approximately 0.5mm clearance).
6. Verify the SUM (at least >1, usually around 5-8) and both deflections to be approximately 0 (<0.1). Also verify that the amplitude shown on the E-box is appropriate. Usually an amplitude >500 mV is considered good. If it's lower than that it can be raised by increasing the drive amplitude in the "Check Parameters". Usually the drive amplitude should be much lower than the actual amplitude shown on the E-box. If a very high drive amplitude (>1000mV) is required to drive the probe to oscillate at ~500mV, recheck the tuning and/or consider replacing the probe. Click "Engage" and the AFM will automatically bring the scanner head down to the scan position.
7. Locate a region of the tissue to image by viewing the AFM tip and section in the eyepiece. Engage the tip and start scanning with the software. Typically, it is necessary to lower the amplitude setpoint to engage the tip with the sample and collect signal. It is recommended to start by imaging a larger area (6x6 μm) at a lower resolution (256x256) to more quickly find a location where distinct fibrils with clear d-periods are visible. It is worth the effort up-front to spend more time finding good locations to image, rather than having poor quality images that need to be re-done. A representative good image is shown in Figure 19.
8. When a good location to image is found, set the imaging parameters to acquire a 2x2 μm image at 1.5 Hz scan rate and 512x512 resolution. Click the box such that the image saves when the scan is completed.

9. Acquire 5 images per region (insertion and midsubstance) per sample, taking images throughout the entirety of the sample (ideally in different locations across 5 different sections, if section quality allows).

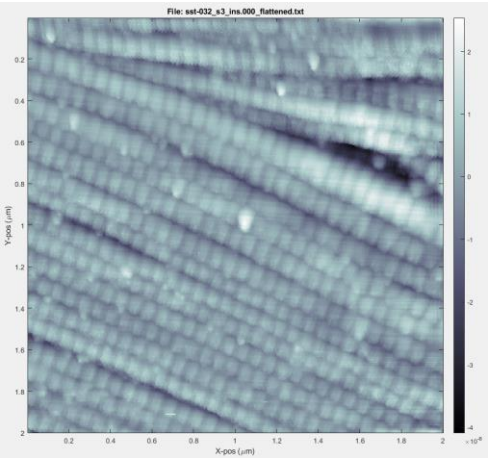

Figure 6